MÚ AV květen 2022

Paleooceán na Marsu

Mars – new findings with gravity and magnetic data using gravity aspects

Rukopis do Planetary and Space Sciences
v druhem recenznim kole 5/2022
obrazky vesmes Jan. Kostelecky

Highlights

Northern Martian Paleo-ocean

Isidis – volcano rather than a basin or mascon

Impact of Hellas likely stopped the Mars differentiation process

Gravity aspects confirmed asymmetry related to magnetic anomaly distribution

Gravitační a magnetické pole Marsu z družicových měření

Detailni globalní topografie povrchu Marsu z laserového výškoměru

Metoda gravitačních aspektů poprvé aplikována na Mars

Význačný přínos jednoho z gravitačních aspektů – úhlů napětí pro indikaci hypotetického severního paleooceánu

Abstrakt:

S novými daty a novou metodou nové výsledky o gravitačním a magnetickém poli Marsu. Mezi nimi indikace pro severní paleooceán na Marsu: rozsáhlá nížina, tlustá vrstva sedimentů, delty někdejších řek a fretted terén na přechodu mezi vysočinou na jihu a nížinou na severu, relativně klidné gravitační aspekty, velkoplošně učesané úhly napětí (analogie se Zemí pro místa paleojezer, říčních kaňonů, podzemní vody, nalezišť uhlovodíků, lemů impaktních kráterů...)

Gravitational aspects (descriptors)

Gravity aspect	Explanation
T	**Disturbing static gravitational potential**
Δ*g*	**Gravity anomaly or perturbation (various versions)**
Γ	**Marussi tensor (just 5 independent second derivatives of *T*)**
Tzz	**Element of the Marussi tensor (second derivative of *T* in the radial direction), usually most important**
Ij	**3 gravity invariants of the Γ (*I0, I1, I2*); preserved under any coordinate rotation**
I	**a ratio of *I1, I2*; when *I*~0, the causative body is ~2D; when *I* →1, causative body is 3D**
θ	**Strike angle is the main direction of Γ, under certain conditions**
vd	**Virtual deformation based on horizontal derivatives of *T* in latitudinal and longitudinal directions, expressing dilatation and pure sheer (compression)**

The gravity disturbances (anomalies) are in milligals [*mGal*], the second order derivatives in Eötvös [*E*]. Negative values are in blue colour, positive in red. Recall that 1*mGal* = 10-5 *ms*-2, 1*E* ≡ 1 Eötvös = 10-9 *s*-2 and that the invariants have units *I1* [*s*-4] and *I2* [*s*-6]. The strike angles are in degrees and *vd* are dimensionless.

We count azimuths from North to East (=90 deg E), South, West, and back to North (=360 deg E). We count longitudes from the main meridian (defined by astronomers) to East from 0 to 360 degrees (this differs from astronomers).

The strike angle θ [deg, 0] is expressed with respect to the local meridian; its red colour means its direction to the north and blue to the south of the east.

The strike angles are angles, not vectors. We plot them as short abscissae of the same length everywhere, in a regular network (5x5 arcmin). It does not mean that in the real world something like a regular net of tensions exist: geological and geophysical lineaments are never of a constant or identical length, and neither are they separated by uniform distances.

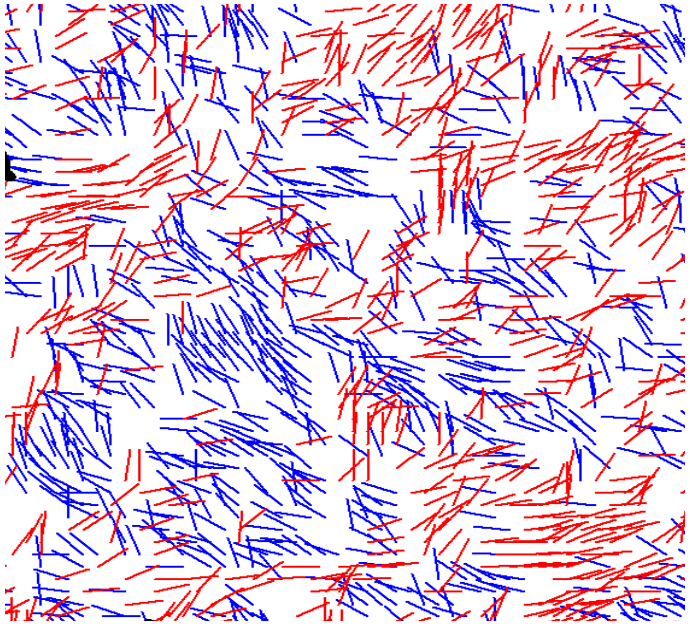

Comments:

Left
highly combed,
linearly

Right
dishevelled

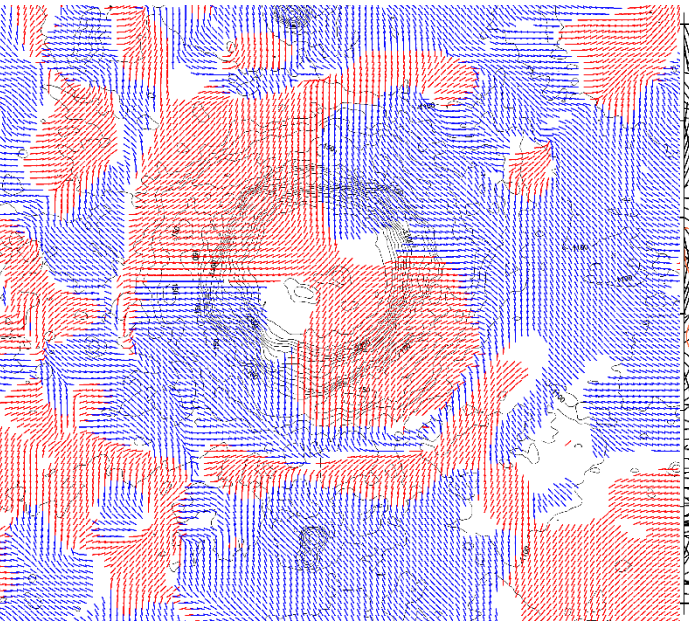

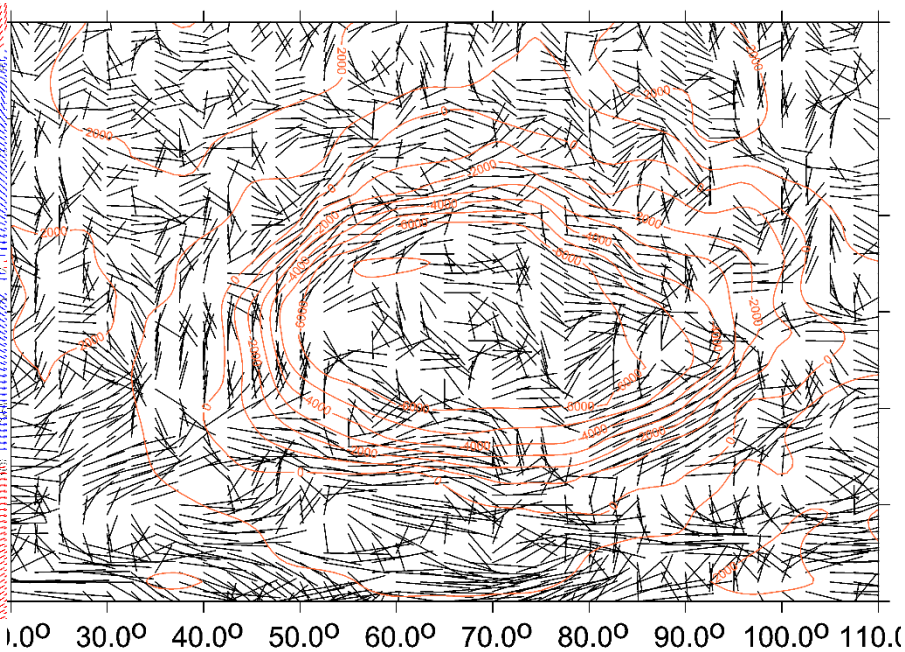

Left
combed,
creating a halo
around the crater
segments
in color

Right
halo
in black&white

the Moon/Copernicus

Hellas basin on Mars

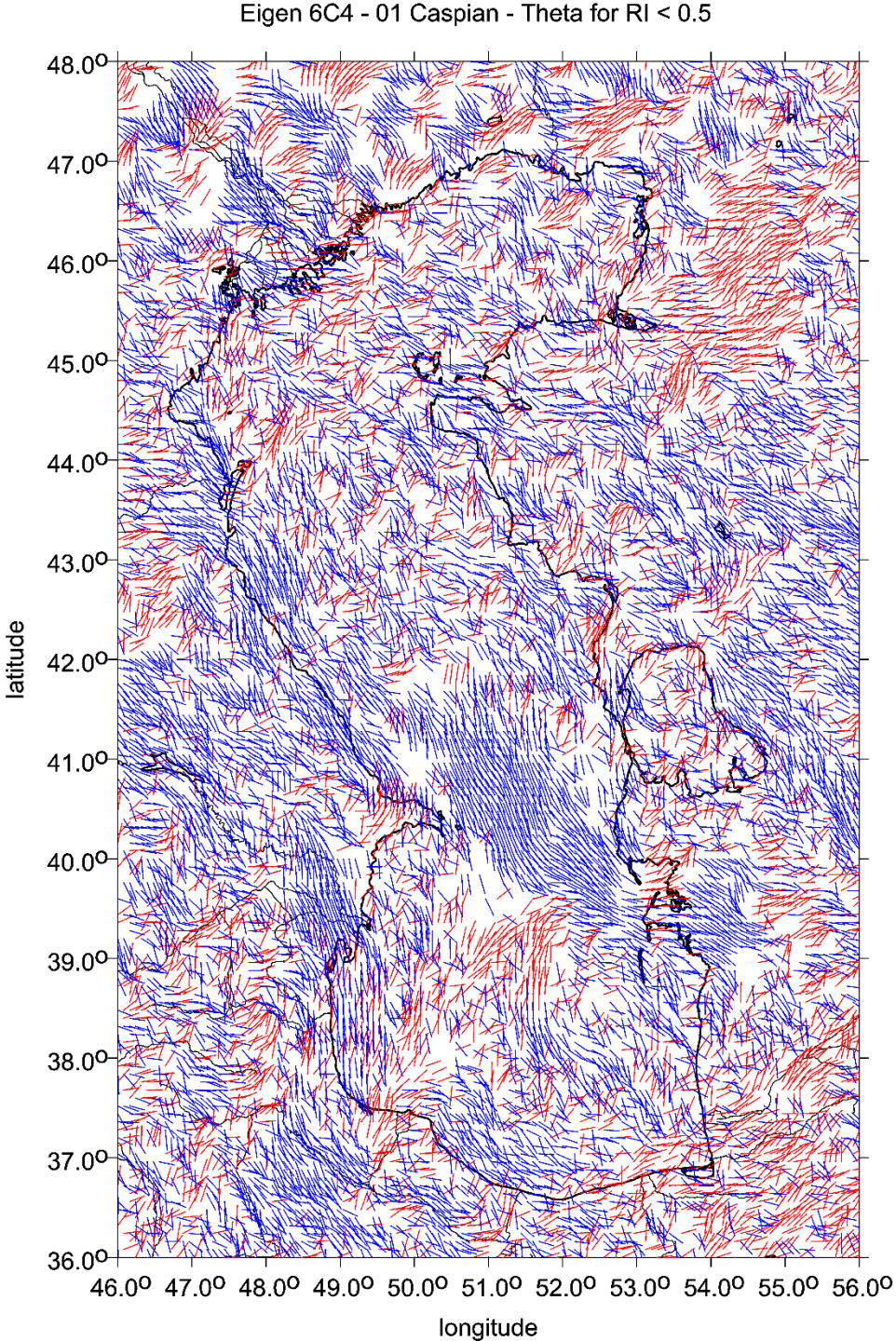
Eigen 6C4 - 01 Caspian - Theta for RI < 0.5
48.0°
47.0°
46.0°
45.0°
44.0°
43.0°
42.0°
41.0°
40.0°
39.0°
38.0°
37.0°
36.0°
latitude
46.0° 47.0° 48.0° 49.0° 50.0° 51.0° 52.0° 53.0° 54.0° 55.0° 56.0°
longitude

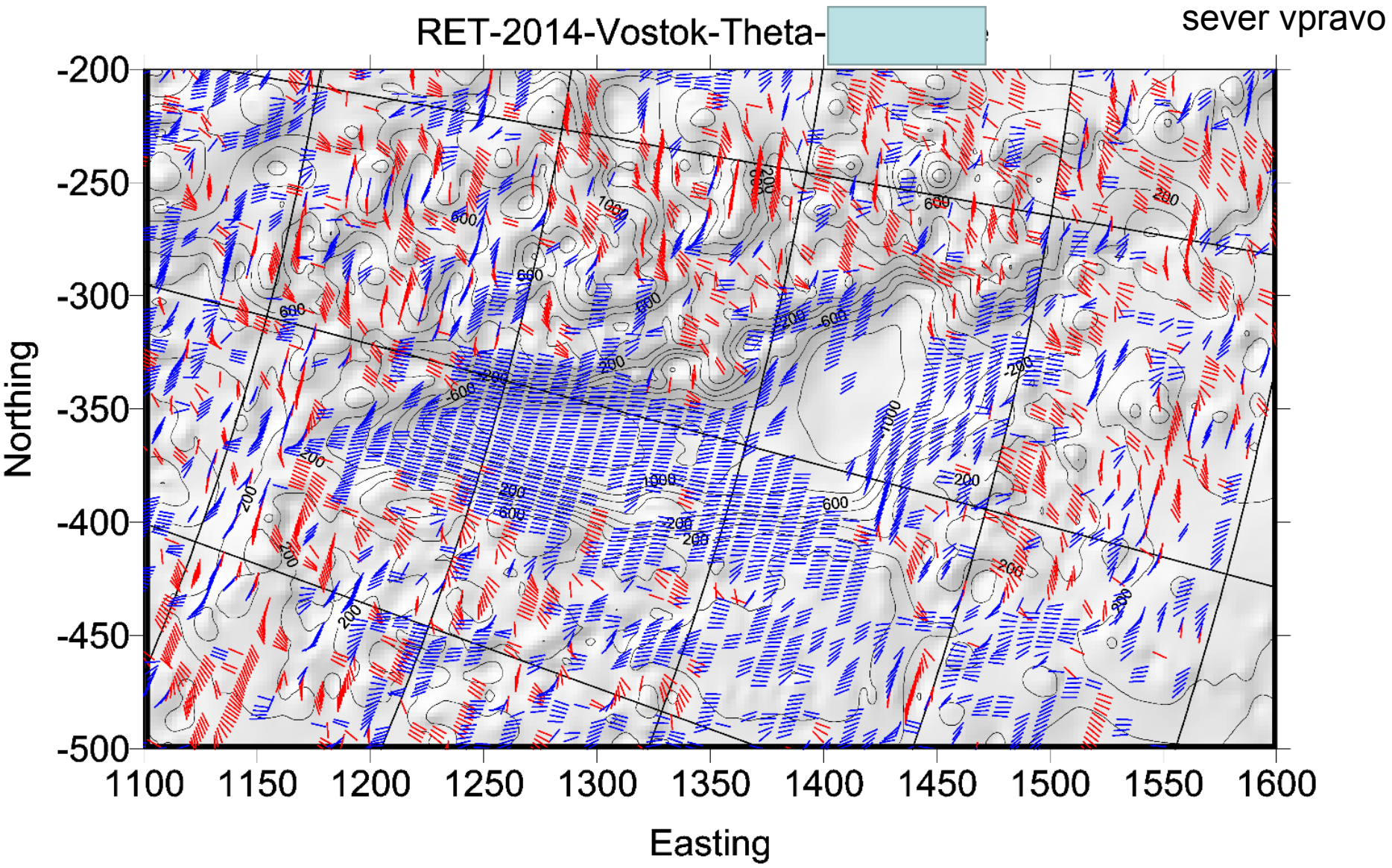
RET-2014-Vostok-Theta-
sever vpravo
Northing
Easting
-200
-250
-300
-350
-400
-450
-500
1100
1150
1200
1250
1300
1350
1400
1450
1500
1550
1600

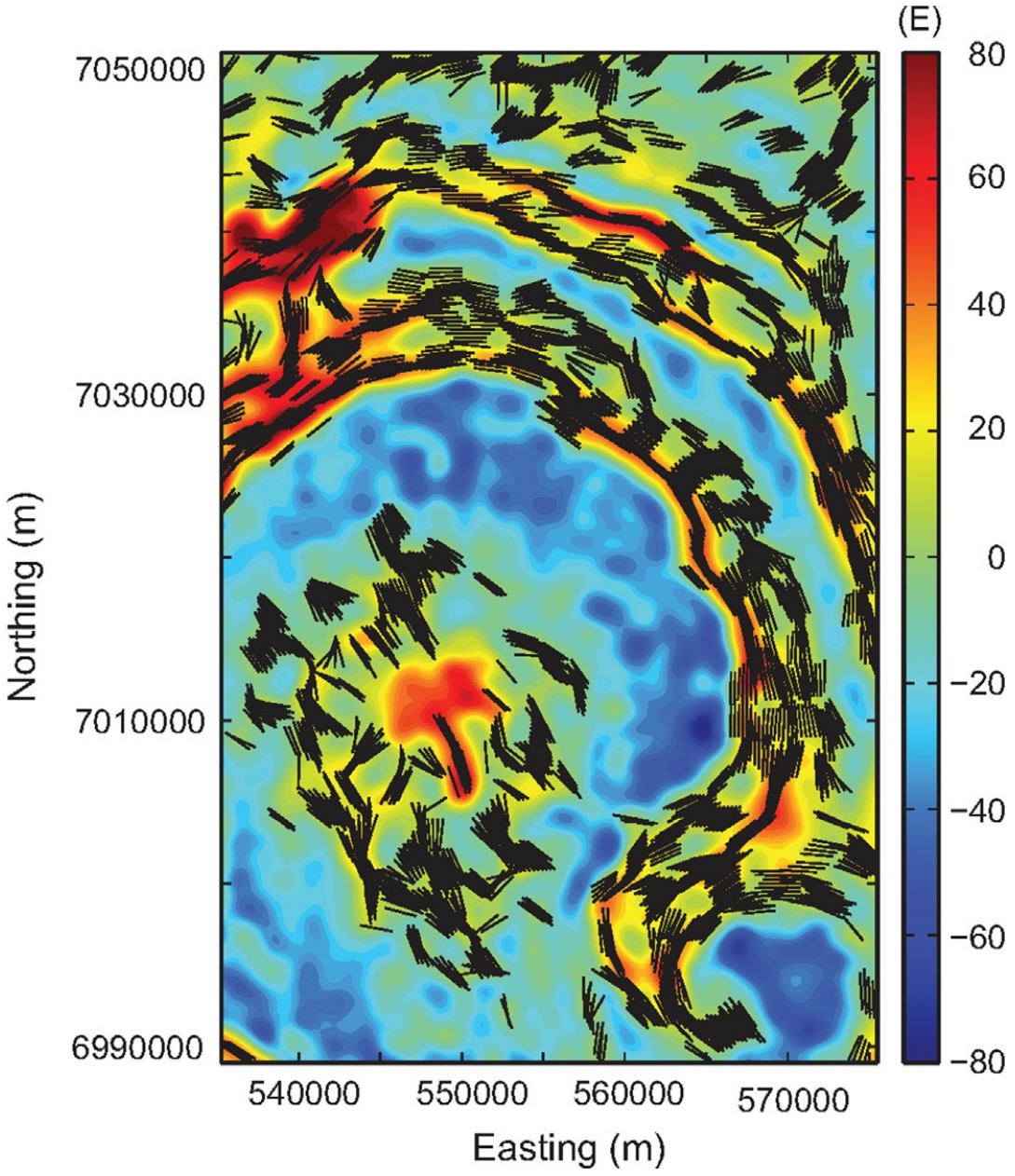

impact crater
Vredefort, South Africa

The strike angles follow rings of the impact structure Vredefort, South Africa. In the central part of the crater they are combed not around the crater but in one prevailing direction.

To draw this, **Beiki and Pedersen (2010**) used the detailed local airborne gradiometry data, which we have not available and the resolution of our data source (EIGEN 6C4) is not sufficient for this purpose.

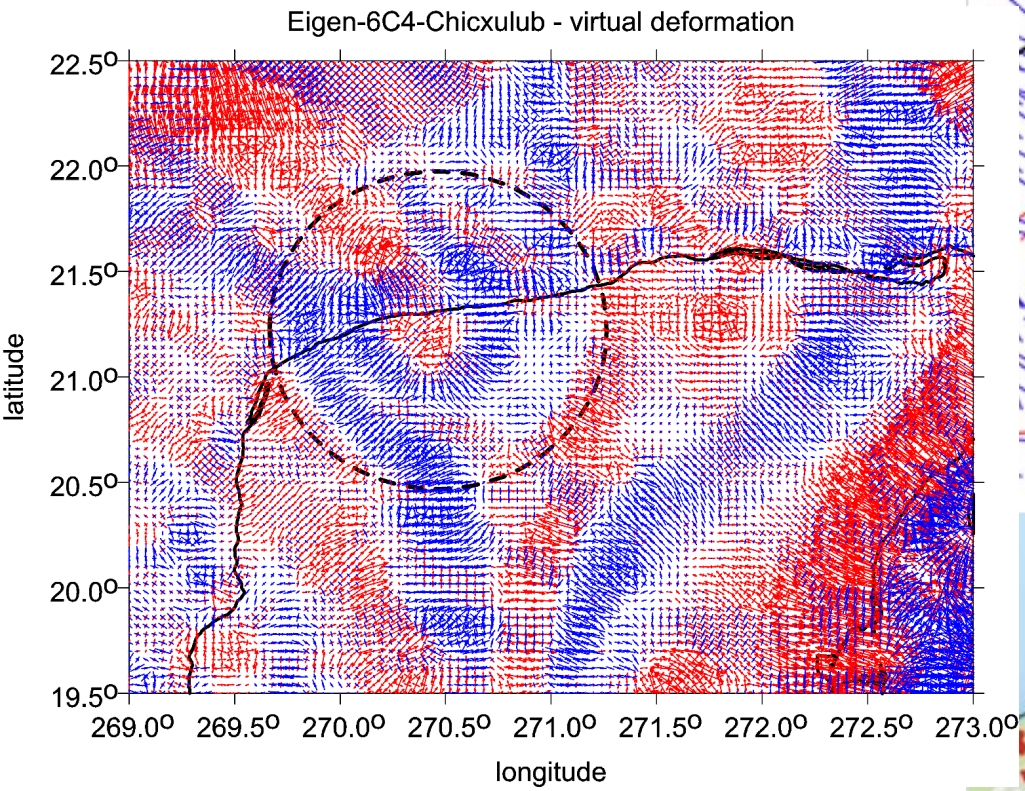
Eigen-6C4-Chicxulub - virtual deformation
22.5°
22.0°
21.5°
21.0°
20.5°
20.0°
19.5°
latitude
269.0°
269.5°
270.0°
270.5°
271.0°
271.5°
272.0°
272.5°
273.0°
longitude

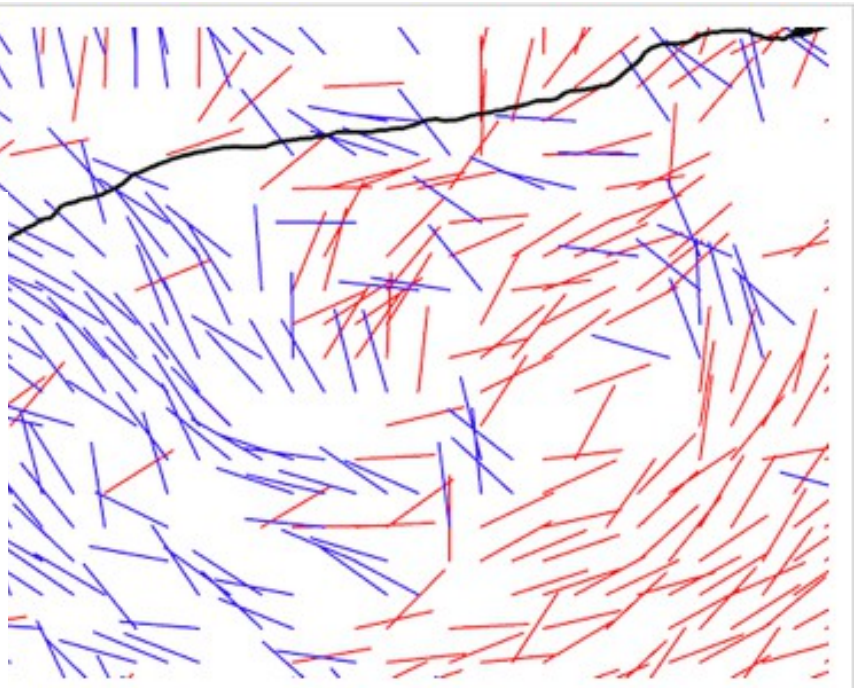

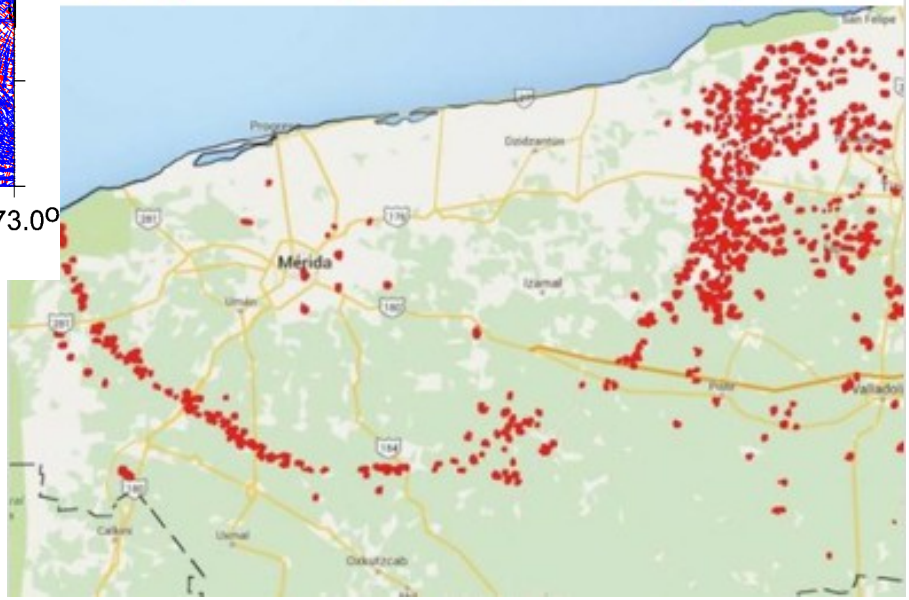
Mérida
Izamal
Valladolid

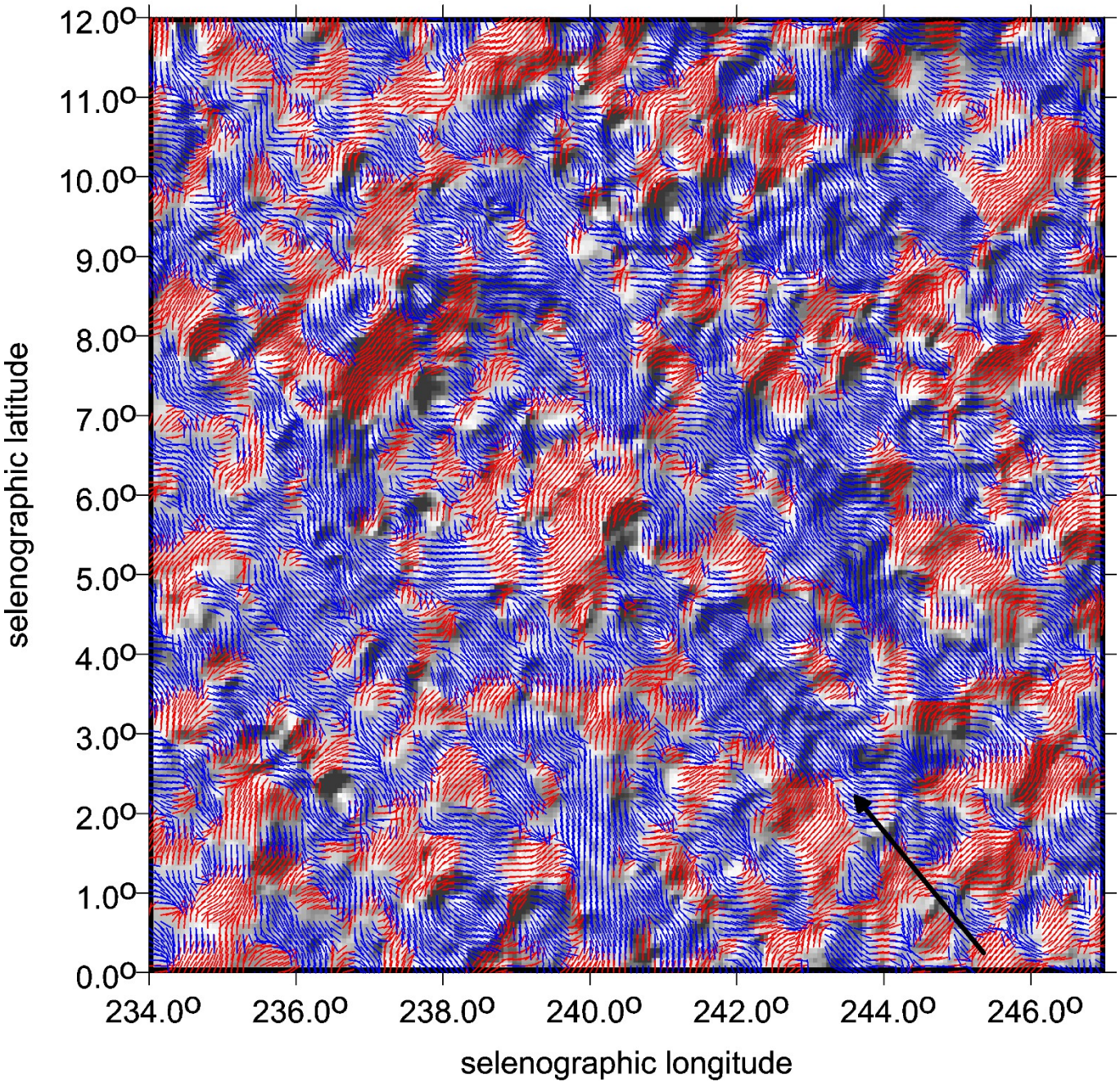

Michelson

crater and catena

Fig. Supp. 65
for Michelson

θ [deg]

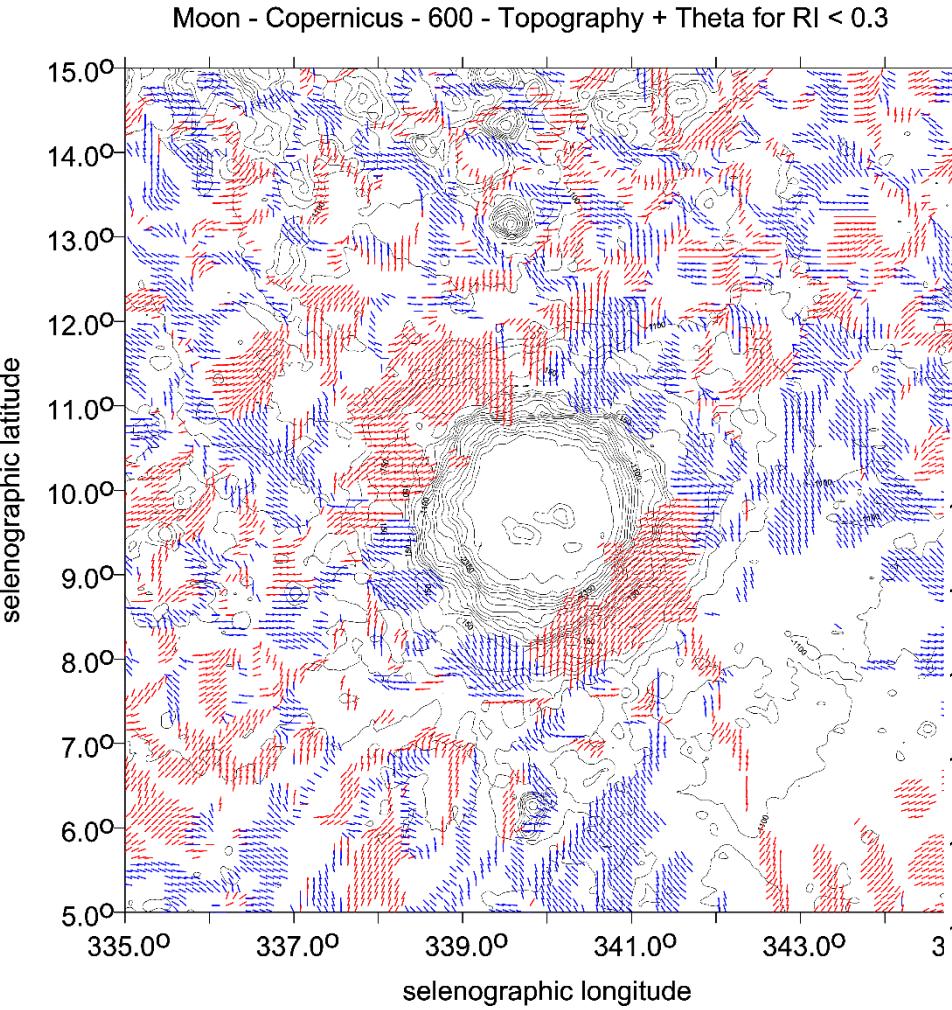

Strike angles for

I<0.3 (left) and
I<0.9 (right down)

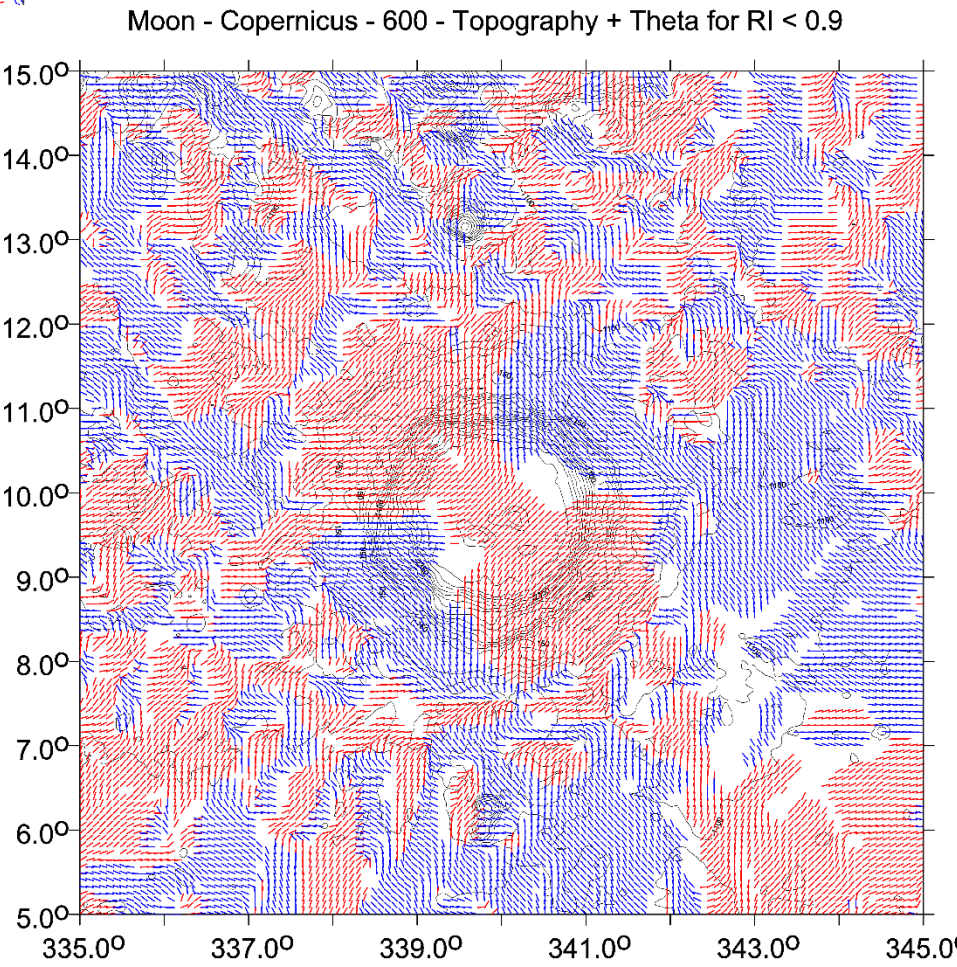

the Moon/ Copernicus

Comments:

Mars
Isidis

Left
combed in plates

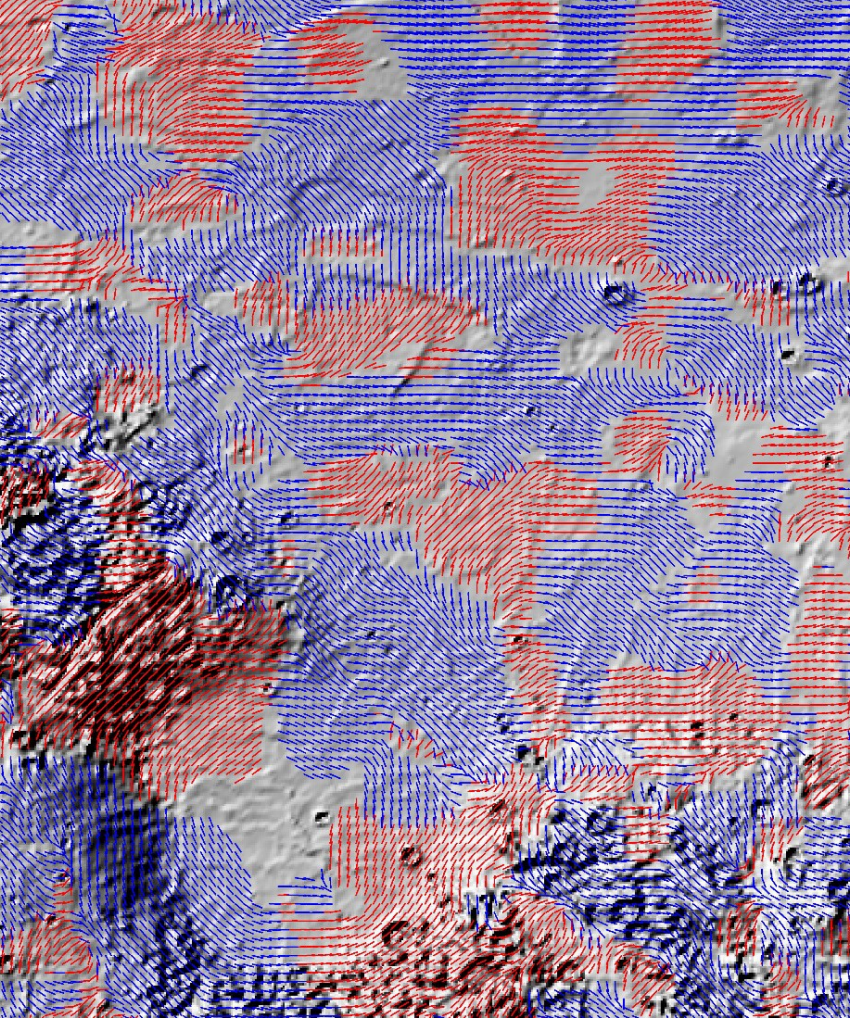

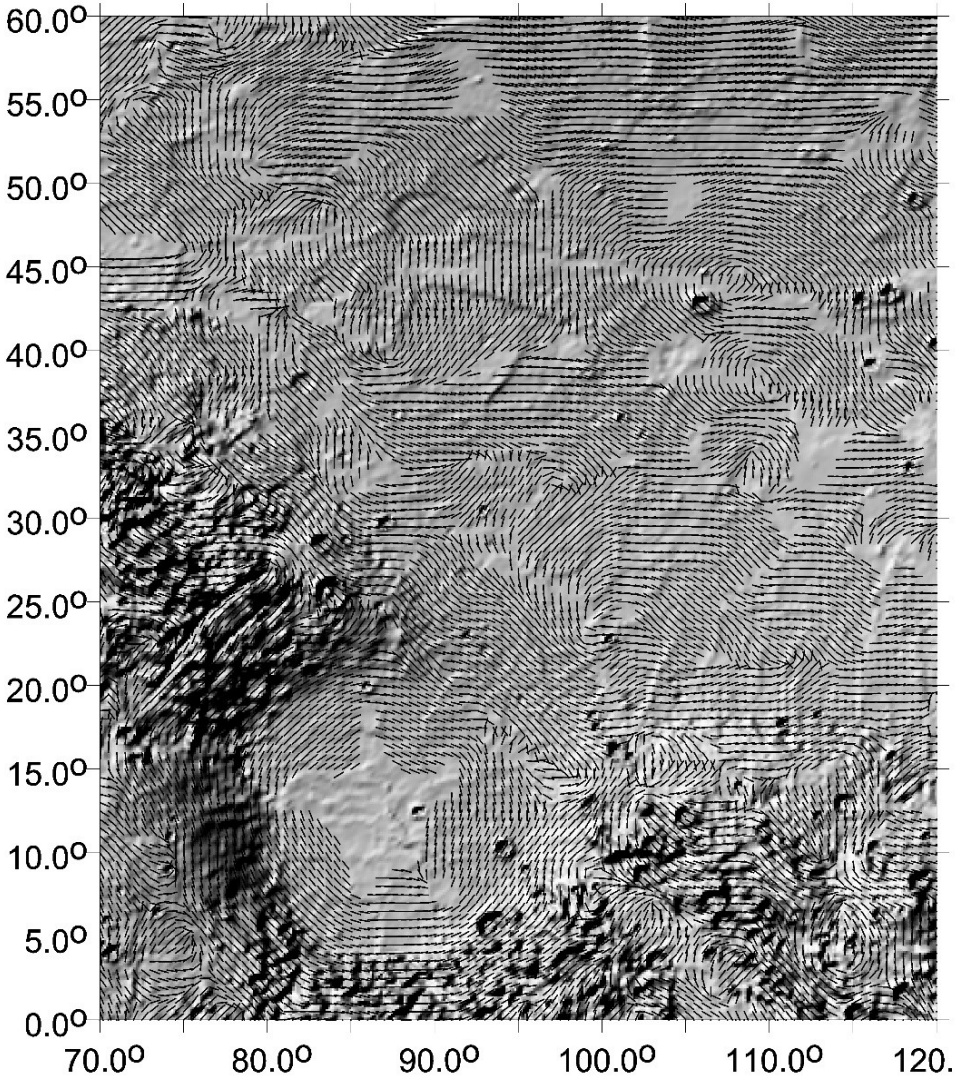

Right
combed in plates
b&w version

Example of the strike angles plotted as a color comb scale (not dashes)

Strike angles with the comb factor to emphasize highly combed areas
Mars, Nothern paleoocean - potential water more probably for red areas

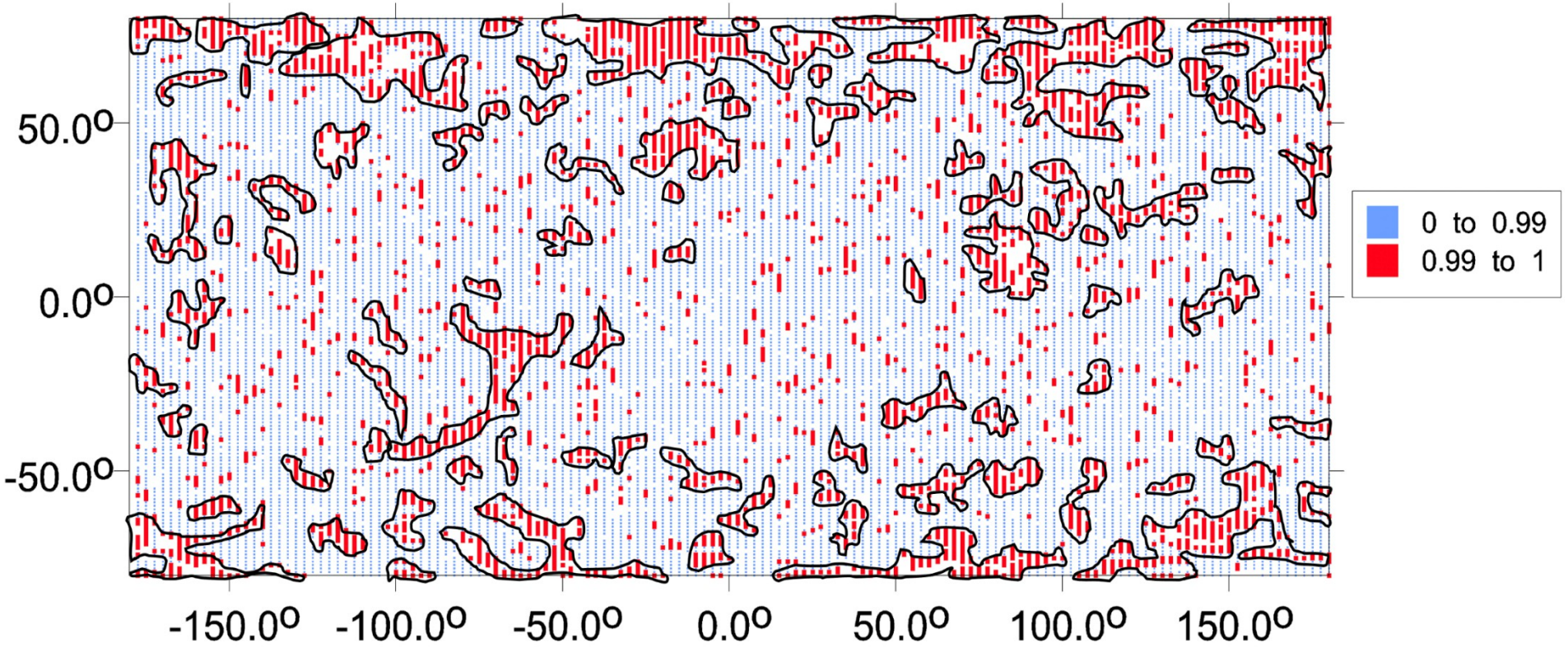

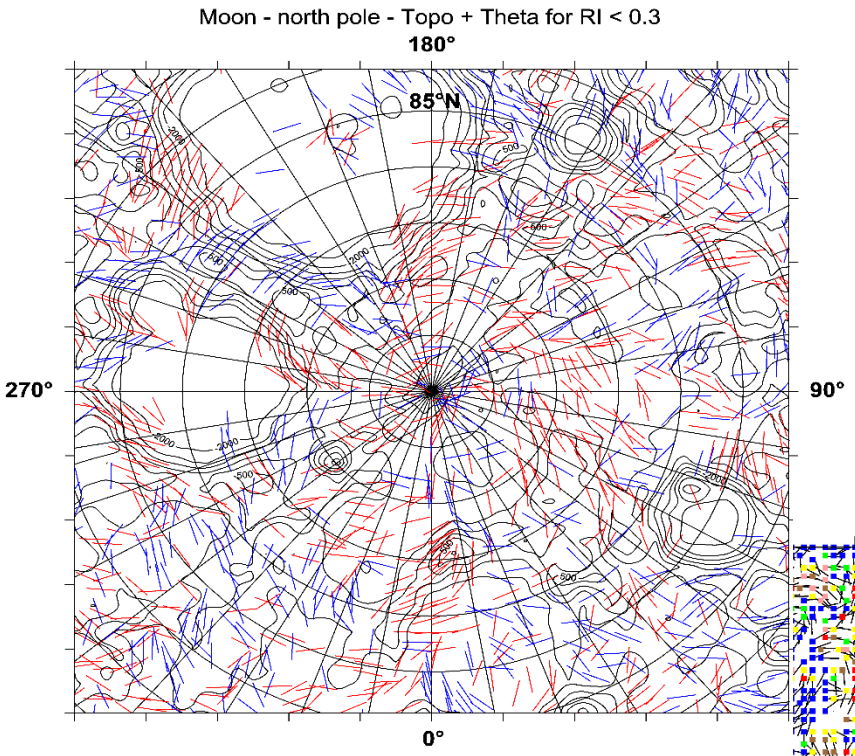

Example of the strike angles

plotted as a color comb scale (not lines)

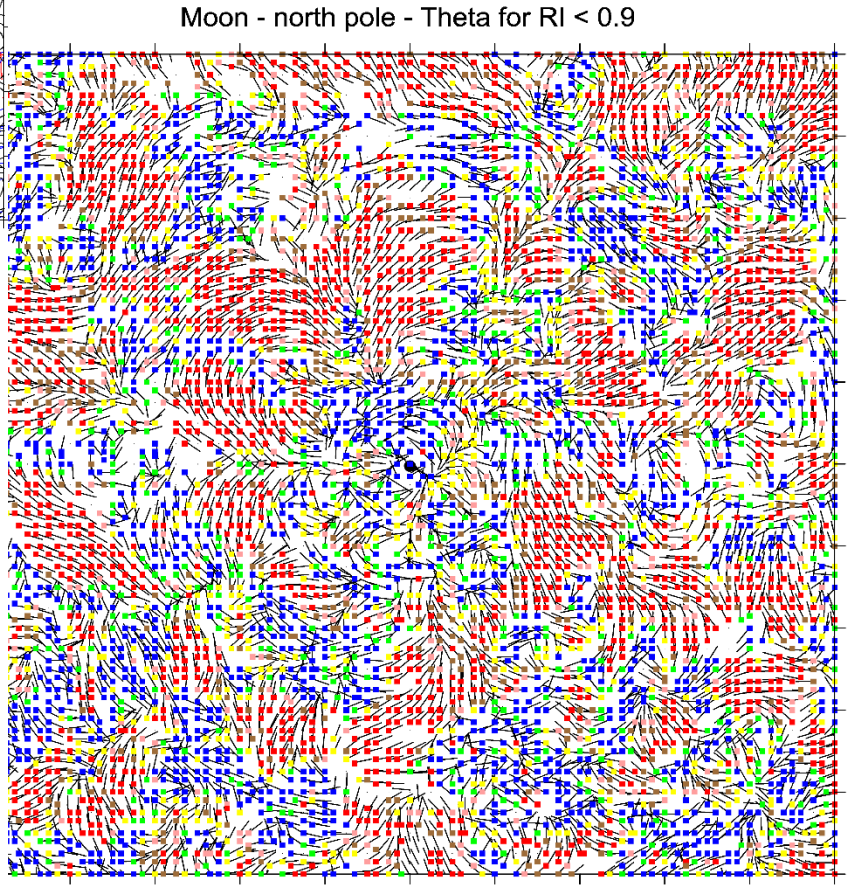

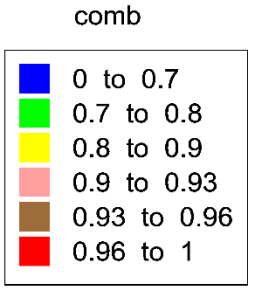

Strike angles with the comb factor scaled

to quantify a degree of strike angle alignment

the polar zone of the Moon

Ground Resolution

A usual simple estimate of the smallest representable feature of the gravity field or the **shortest half-wavelength *Lhalf* (as a distance on a sphere) that can be resolved with all *Clm*, *Slm* to *Lmax,* is**

$$Lhalf = \pi R / Lmax$$

or equivalently, taking the circumference $2\pi R$ = 40 050 km for the Earth:

$$Lhalf = 2 \pi R / (2\, Lmax) = 40\,050 / (2\, Lmax).$$

This *Lhalf* is what we call the "ground resolution". For *Lmax= 300* and *2190,* we have *Lhalf* = 67 and 9 km, respectively. The former limit roughly corresponds to the resolution of the GOCE data alone, and the latter belongs to the combined models, EGM 2008, EIGEN 6C4 or SatGavRET2014 (in the case of the Earth).

Body	**R [km] rounded**	**max *d/o* of model used**	**resolution [km]**
Earth	6380	2190	9
Moon	1740	600	9
Mars	3400	80-120	130-90
Venus	6050	120	160

The gravity field of Mars *used here*

Konopliv et al 2020

Name: JPL-MARS-MRO120F (d/o =120) "Mars - gravitační pole JGMRO"
Ground resolution: ~ 100 km

Geophysical Research Letters
47, e2020GL090568 13 October 2020

Detection of the Chandler Wobble of Mars From Orbiting Spacecraft

Alex S. Konopliv , Ryan S. Park , Attilio Rivoldini , Rose-Marie Baland Sebastien Le Maistre Tim Van Hoolst Marie Yseboodt, Veronique Dehant

https://doi.org/10.1029/2020GL090568

For the first time for any planetary body other than the Earth, the free wobble of the pole called the Chandler wobble has been detected for Mars with a period of 206.9 ± 0.5 days and amplitude of 10 cm from radio tracking observations of Mars Odyssey, Mars Reconnaissance Orbiter (MRO), and Mars Global Surveyor (MGS), in order of decreasing sensitivity. The motion of the rotation pole location on the surface of Mars, or polar motion, is observed using two different approaches: (1) joint global estimates of Mars' orientation and its gravity field and (2) time series solutions of $C21$ and $S21$. For Mars interior models, the Chandler wobble period is combined with other measurements including the moments of inertia from our estimated precession rate $\dot{\psi} = -7603.9 \pm 1.3$ mas/year and tidal Love number $k2 = 0.169 \pm 0.006$. The Chandler wobble period constrains the rheology of the Martian mantle and in particular its long-term frequency dependence.

The gravity field model of Mars JPL-MARS-MRO120F (to max. d/o =120) used here (Konopliv et al 2020) superseded the older solutions (e.g. GGM 3 by Genova et al 2016). The model is based on data from Mars orbiters: the Mars Reconnaissance Orbiter (MRO), the Mars Global Surveyor (MGS) and Mars Odyssey. The data spanned 18 years (and still coming) was considered to be precise enough even to measure the Chandler wobble of Mars. The model has the ground resolution about 100 km; its nominal precision is 10 mGals.

As many times before in the gravity field modelling for the Earth, the Moon, Venus and Mars, Kaula rule has been used to stabilize least squares adjustment for the harmonic geopotential coefficients. For JPL-MARS-MRO120F, is was applied above d/o=80. Thus, this d/o limit indicates to which maximum d/o the model should actually been used. This is supported by our truncation error tests for various gravity aspects and the d/o limits 80, 100, and 120, showing an increasing graining as a typical first symptom of incoming artefacts in the gravity signal when the user asks for too much details from the model which are not due to the data imperfections of various types contained in.

References:

Alex S. Konopliv , Ryan S. Park , Attilio Rivoldini , Rose-Marie Baland Sebastien Le Maistre Tim Van Hoolst Marie Yseboodt, Veronique Dehant 2020. Detection of the Chandler Wobble of Mars from Orbiting Spacecraft , Geophys Res Letts 47, e2020GL090568, https://doi.org/10.1029/2020GL090568.

Genova, A., Goossens, S., Lemoine, F. G., Mazarico, E., Neumann, G. A., Smith, D. E., & Zuber, M. T. 2016. Seasonal and static gravity field of Mars from MGS, Mars Odyssey and MRO radio science. *Icarus*, *272*, 228-245. doi:10.1016/2016.02.050

Geoide martien[19]	G Balmino, B Moynot and N Vales	1982	18[19] [¬600 km]	Tracking data of Mariner 9, Viking 1 and 2 spacecraft[19]
GMM-1[20]				
Mars50c[21]				
GMM-2B[14]	FG Lemoine, DE Smith, DD Rowlands, MT Zuber, GA Neumann, DS Chinn, and DE Pavlis	2001	80[14]	Tracking data of Mars Global Surveyor (MGS), and MOLA-derived topography data [14]
GGM1041C [22]				
MGS95J[23]				
MGGM08A [7]	JC Marty, G Balmino, J Duron, P Rosenblatt, S Le Maistre, A Rivoldini, V Dehant, T. Van Hoolst	2009	95[7] [~112 km]	Tracking data of Mars Global Surveyor (MGS) and Mars Odyssey, and MOLA-derived topography data [7]
MRO110B2 [24]				
MGM2011[1]				
GMM-3[13]	A Genova, S Goossens, FG Lemoine, E Mazarico, GA Neumann, DE Smith, MT Zuber	2016	120[13] [115 km]	Mars Global Surveyor (MGS), Mars Odyssey and Mars Reconnaissance Orbiter (MRO)[13] • MGS (SPO-1, SPO-2, GCO, MAP)[13]

SURFACE **TOPOGRAPHY OF MARS** used here

Topography of Mars in resolution 0,25°:
http://www.asu.cas.cz/~bezdek/JK&JK/Mars/topografie_MOLA/
topography of Mars from the MOLA experiment:
https://pgda.gsfc.nasa.gov/products/62

Smith, D. E., M. T. Zuber, H. V. Frey, J. B. Garvin, J. W. Head, D. O. Muhleman, et al. (2001), Mars Orbiter Laser Altimeter: Experiment summary after the first year of global mapping of Mars, *J. Geophys. Res*., 106, 23689–23722, DOI: 10.1029/2000JE001364.
http://www.asu.cas.cz/~bezdek/JK&JK/Mars/topografie_MOLA/ref/

The Mars Orbiter Laser Altimeter (MOLA), an instrument on
the Mars Global Surveyor spacecraft
as measured the topography, surface roughness and 1.064-/•m
reflectivity of Mars and the heights of volatile and dust clouds.

Radial precision 1 meter with respect o the planet‘s center of mass.

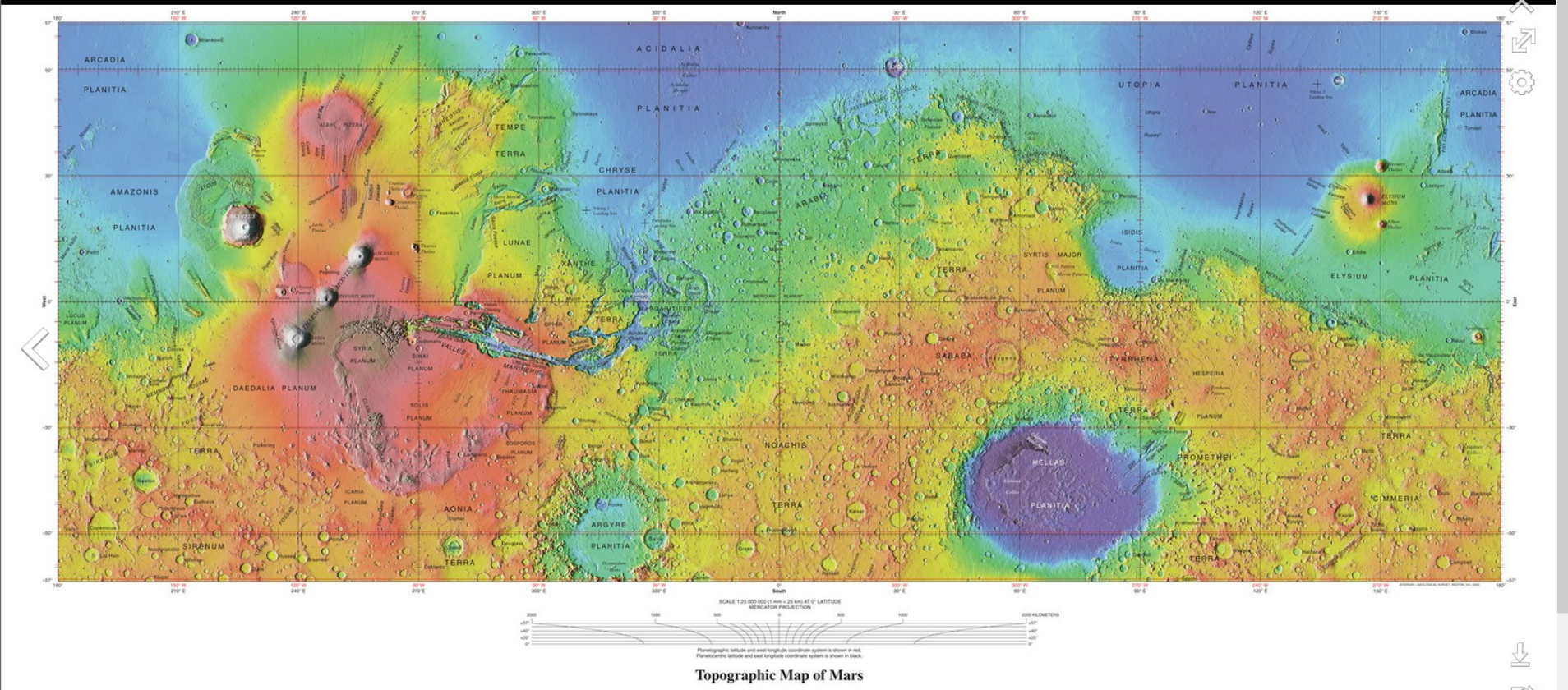

Planet Mars - Topographical Map (USGS; 2005)

More details

U.S. Geological Survey - https://pubs.usgs.gov/imap/i2782/; https://pubs.usgs.gov/imap/i2782/i2782_sh1.pdf

Public Domain

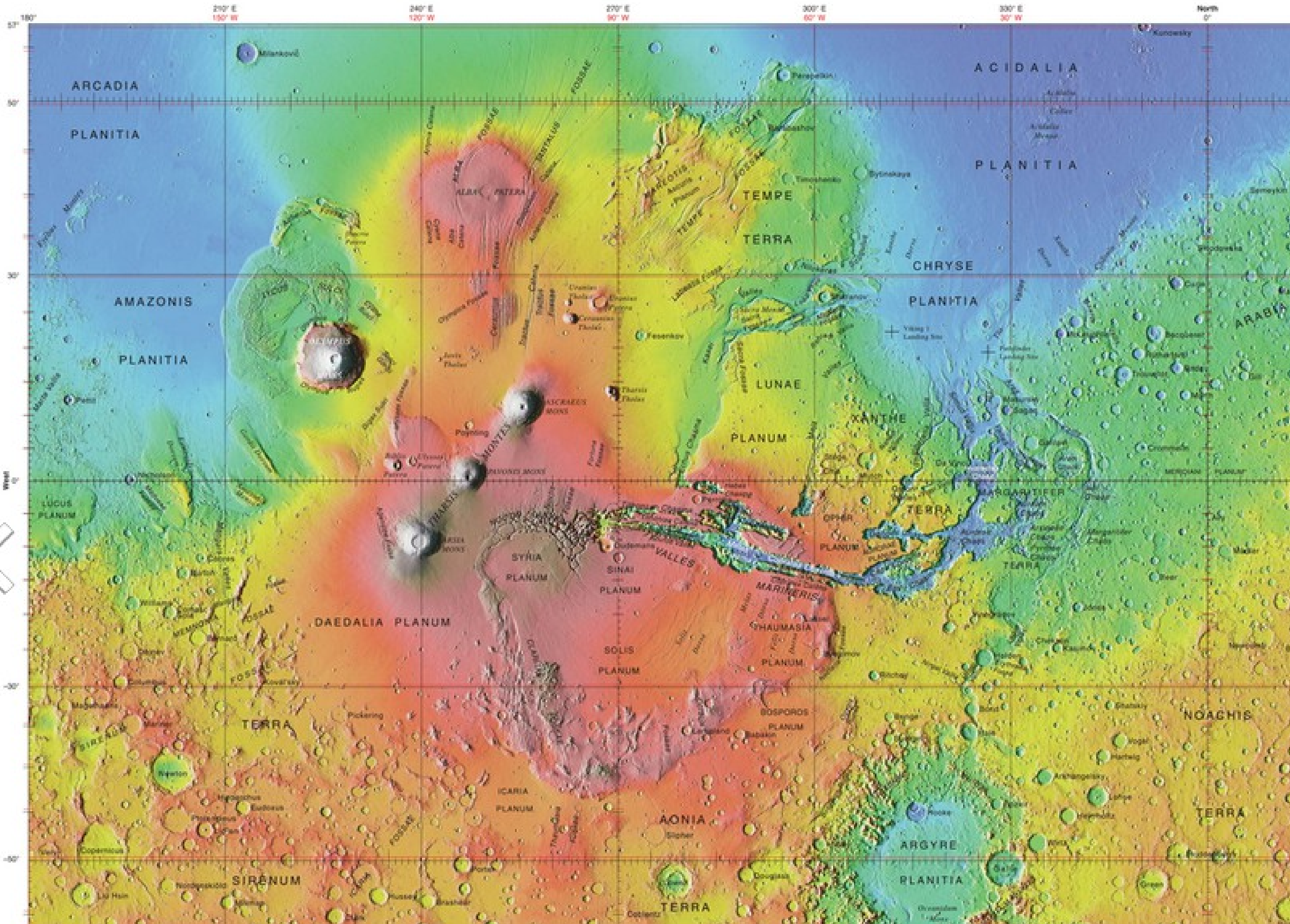

180°
210° E
150° W
240° E
120° W
270° E
90° W
300° E
60° W
330° E
30° W
North
0°
57°
50°
30°
0°
-30°
-50°
West
ARCADIA
PLANITIA
AMAZONIS
PLANITIA
ACIDALIA
PLANITIA
TEMPE
TERRA
CHRYSE
PLANITIA
ARABIA
LUNAE
XANTHE
PLANUM
LUCUS
PLANUM
MARGARITIFER
TERRA
OPHIR
PLANUM
SYRIA
PLANUM
SINAI
PLANUM
VALLES
MARINERIS
DAEDALIA PLANUM
THAUMASIA
SOLIS
PLANUM
PLANUM
TERRA
BOSPOROS
PLANUM
NOACHIS
TERRA
ICARIA
PLANUM
AONIA
ARGYRE
PLANITIA
SIRENUM
TERRA

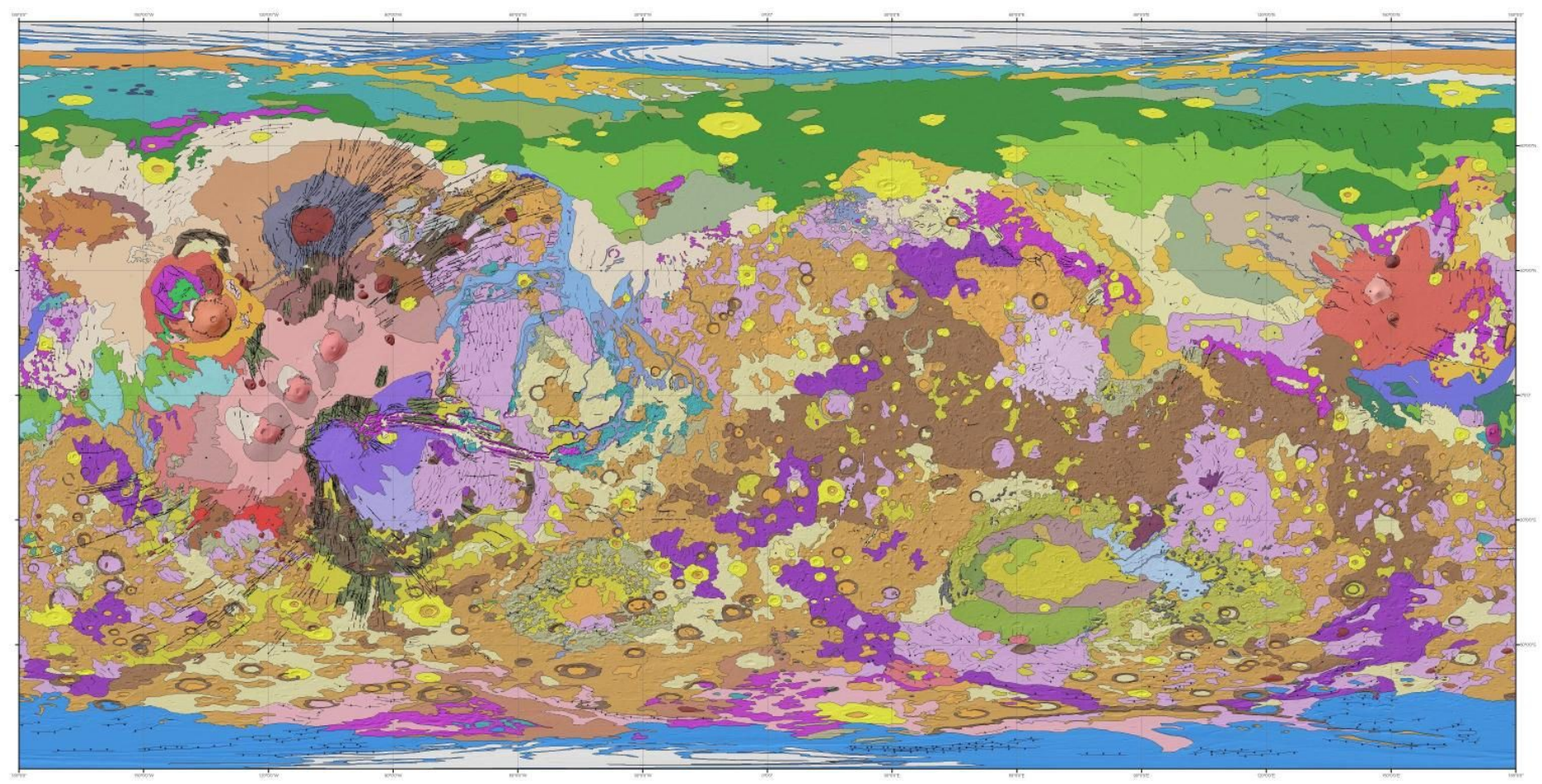

1,100 550 0 1,100 2,200 3,300 4,400 Km

1:28,267,459

N W E S

Mars Global Geologic Map 1802ABC

Legend

APPROX
CERTAIN

geo_structure_EquidistCyl

<all other values>

SrucType

Large scarp, symbol points downslope
Crater rim
Caldera.
Crest of basal scarp on Olympus Mons, exposed.
Crest of basal scarp on Olympus Mons, buried.
Depression.
Fault with differentiated offset.
Fault with undifferentiated and (or) unmapped offset.
Mare-type structural ridge; symbol on crest.
Channel

AHa Adl Aop Hdu Hvm
AHat Ae Aos Hf Hvr
AHcf Aol1 Api Hh2 Nb
AHh Aol2 Apk Hh3 Nf
AHpe Aol3 Apl Hhet Nh1
AHt Aol4 Aps Hpl3 Nm
AHt3 Ah4 As Hplm Npl1
Aa1 Ah5 At4 Hr Npl2
Aa2 Ah6 At5 Hs Npld
Aa3 Ah7 At6 Hsl Nple
Aa4 Ah8 Avf Hsu Nplh
Aa5 Am HNu Ht1 Nplr
Aam Aml Had Ht2 b
Aau Amm Hal Htl cb
Ach Amu Hap Htm cs
Achu Aoa1 Hch Htu d
Achp Aoa2 Hchp Hvg m
Ad Aoa3 Hcht Hvk s
Adc Aoa4 Hdl Hvl v

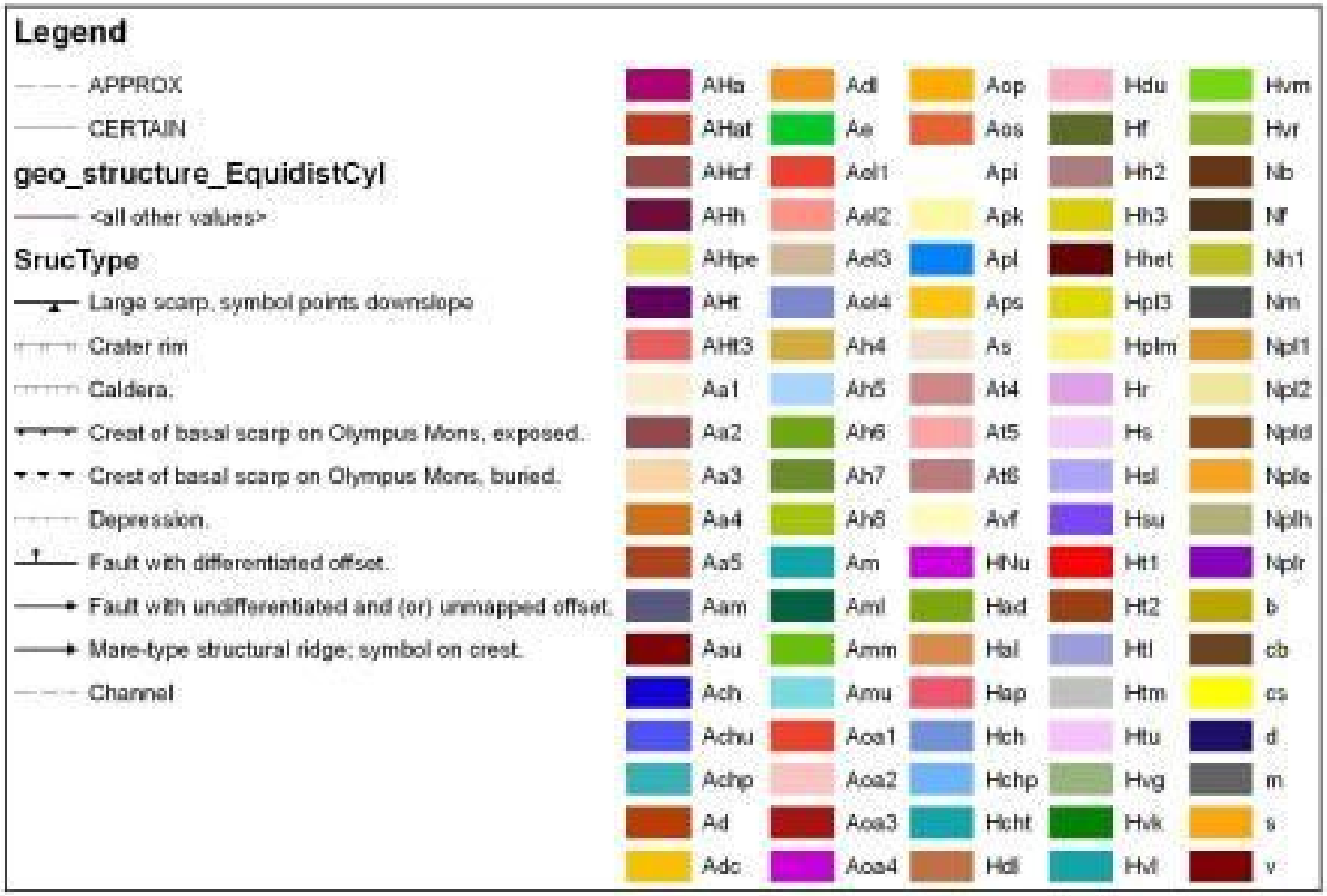
Legend
APPROX
CERTAIN
geo_structure_EquidistCyl
<all other values>
SrucType
Large scarp, symbol points downslope
Crater rim
Caldera.
Crest of basal scarp on Olympus Mons, exposed.
Crest of basal scarp on Olympus Mons, buried.
Depression.
Fault with differentiated offset.
Fault with undifferentiated and (or) unmapped offset.
Mare-type structural ridge; symbol on crest.
Channel
AHa
AHat
AHcf
AHh
AHpe
AHt
AHt3
Aa1
Aa2
Aa3
Aa4
Aa5
Aam
Aau
Ach
Achu
Achp
Ad
Adc
Adl
Ae
Ael1
Ael2
Ael3
Ael4
Ah4
Ah5
Ah6
Ah7
Ah8
Am
Aml
Amm
Amu
Aoa1
Aoa2
Aoa3
Aoa4
Aop
Aos
Api
Apk
Apl
Aps
As
At4
At5
At8
Avf
HNu
Had
Hal
Hap
Hch
Hchp
Hcht
Hdl
Hdu
Hf
Hh2
Hh3
Hhet
Hpl3
Hplm
Hr
Hs
Hsl
Hsu
Ht1
Ht2
Htl
Htm
Htu
Hvg
Hvk
Hvl
Hvm
Hvr
Nb
Nf
Nh1
Nm
Npl1
Npl2
Npld
Nple
Nplh
Nplr
b
cb
cs
d
m
s
v

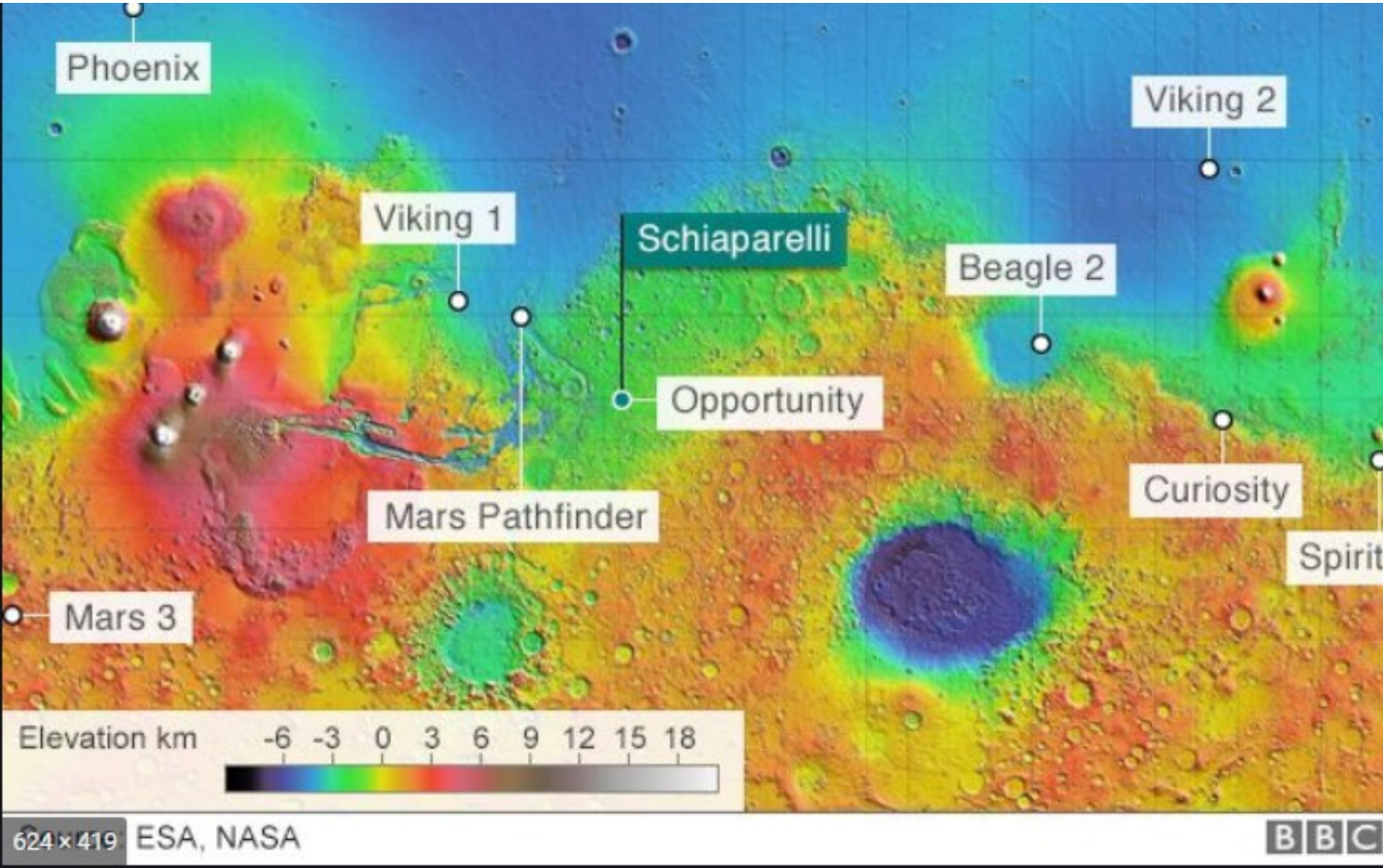
Phoenix
Viking 2
Viking 1
Schiaparelli
Beagle 2
Opportunity
Curiosity
Mars Pathfinder
Spirit
Mars 3
Elevation km
-6 -3 0 3 6 9 12 15 18
624 × 419
ESA, NASA
BBC

Perseverance
is a near clone of Curiosity with better equipment designed to answer difficult question:
Could there have been Martians living on Mars long ago?
Crater named Jezero Crater, an ancient Martian lake roughly the size of Lake Tahoe has been chosen as the target landing area.
Not suprisinly it is in our hypothetical NMPO. We did not know about it.

TARGET LANDING AREA 1/2 mile
By Jonathan Corum | Image by NASA, Jet Propulsion Laboratory, European Space Agency, German Aerospace Center, Freie Universität Berlin and Justin Cowart. Inset image by NASA and J.P.L.

Sdílet pristani

https://youtu.be/4czjS9h4Fpg

Jezero Crater's ancient lake-delta system offers many promising sampling targets. Parts of Jezero may be especially rich in carbonates, minerals that, on Earth, can preserve fossilized signs of ancient life and can be associated with biological processes. And new landing technologies will allow Perseverance to touch down even closer to the most promising locations than any Mars mission before it.

Martian polar ice caps

From Wikipedia, the free encyclopedia

The planet Mars has two permanent polar ice caps. During a pole's winter, it lies in continuous darkness, chilling the surface and causing the deposition of 25–30% of the atmosphere into slabs of CO_2 ice (dry ice).[1] When the poles are again exposed to sunlight, the frozen CO_2 sublimes.[2] These seasonal actions transport large amounts of dust and water vapor, giving rise to Earth-like frost and large cirrus clouds.

The caps at both poles consist **primarily of water ice**. Frozen carbon dioxide accumulates as a comparatively thin layer about one metre thick on the north cap in the northern winter, while the south cap has a permanent dry ice cover about 8 m thick.[3]

The northern polar cap has a diameter of about 1000 km during the northern Mars summer,[4] and contains about 1.6 million cubic km of ice, which if spread evenly on the cap would be 2 km thick.[5] (This compares to a volume of 2.85 million cubic km (km3) for the Greenland ice sheet.)

The southern polar cap has a diameter of 350 km and a thickness of 3 km.[6] The total volume of ice in the south polar cap plus the adjacent layered deposits has also been estimated at 1.6 million cubic km.

Unlike the northern polar cap, the southern ice cap stands on heavily cratered ground in the southern highlands. It is elevated about 6 km (4 mi) higher than Martian "sea level," which is the average radius of Mars The southern also covers part of the ancient Prometheus impact basin.

The polar cap has a thickness similar to the northern one — about 3,000 m (10,000 ft) — but it spreads only about 400 km (250 mi) wide. The cap's highest point lies at –87° latitude and 0° longitude, not the actual pole (–90°) but about 180 km (112 mi) away from it. Polar materials also extend hundreds of kilometers toward the equator in a direction centered on 150° east longitude.

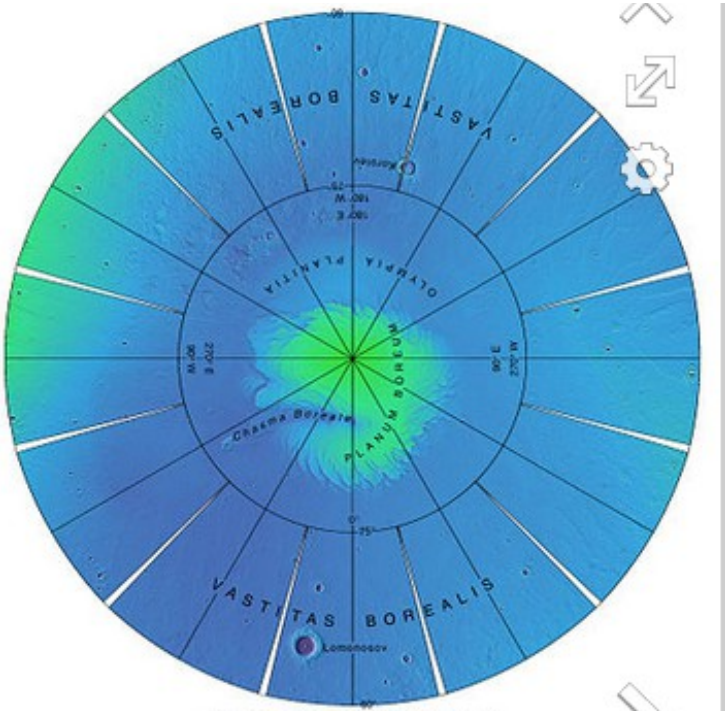

0° E or W, 60° N or S

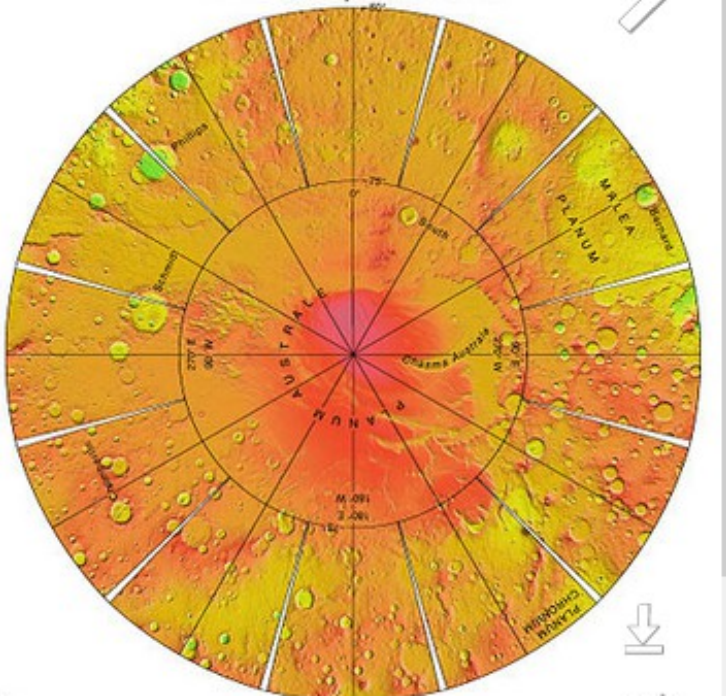

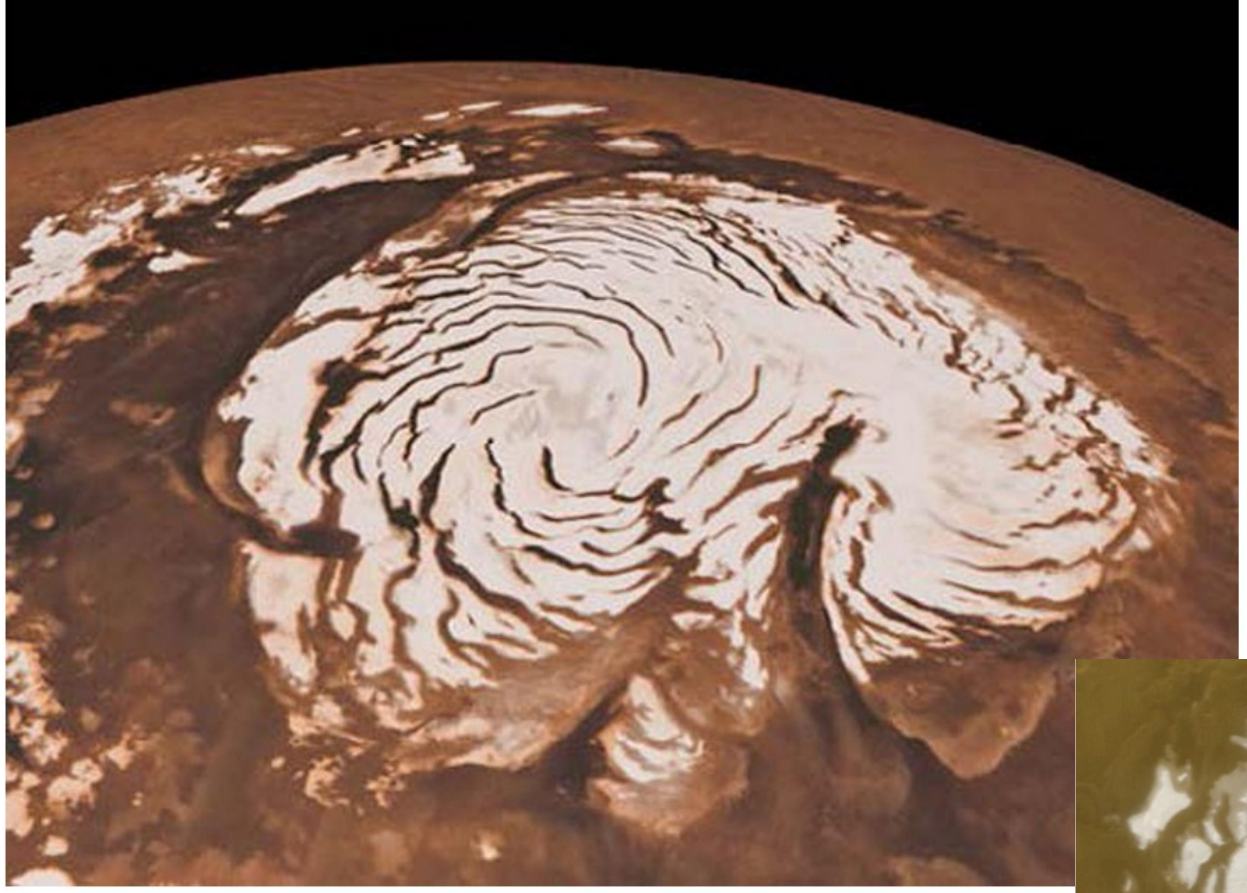

northern

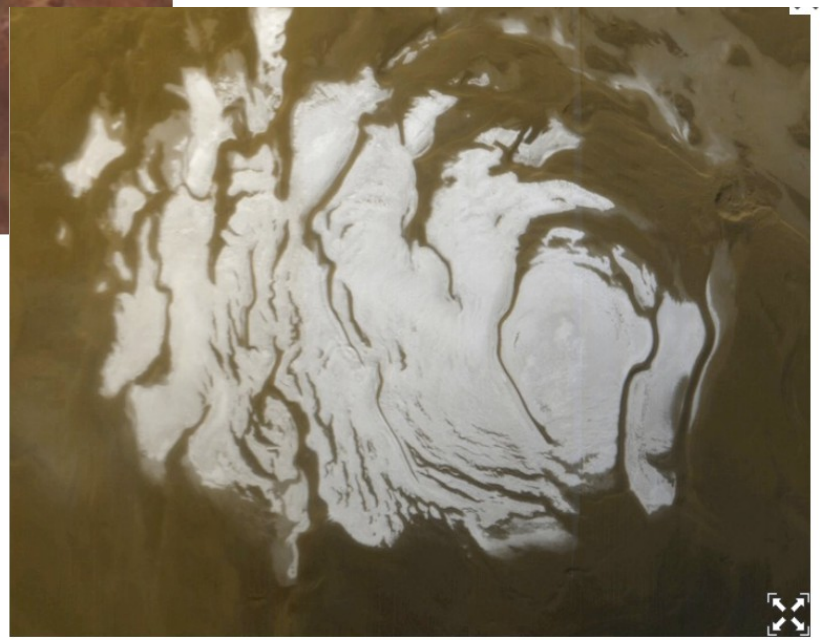

southern

The south polar cap spreads about 420 kilometers (260 miles) wide. This image was made in summer and shows the ice at its smallest extent. In winter and early spring this entire scene would be covered by frost. Like the northern ice cap, the southern one is cut into by troughs. (NASA/JPL-Caltech/Malin Space Science Systems)

Download Image

Northern cap

Southern cap

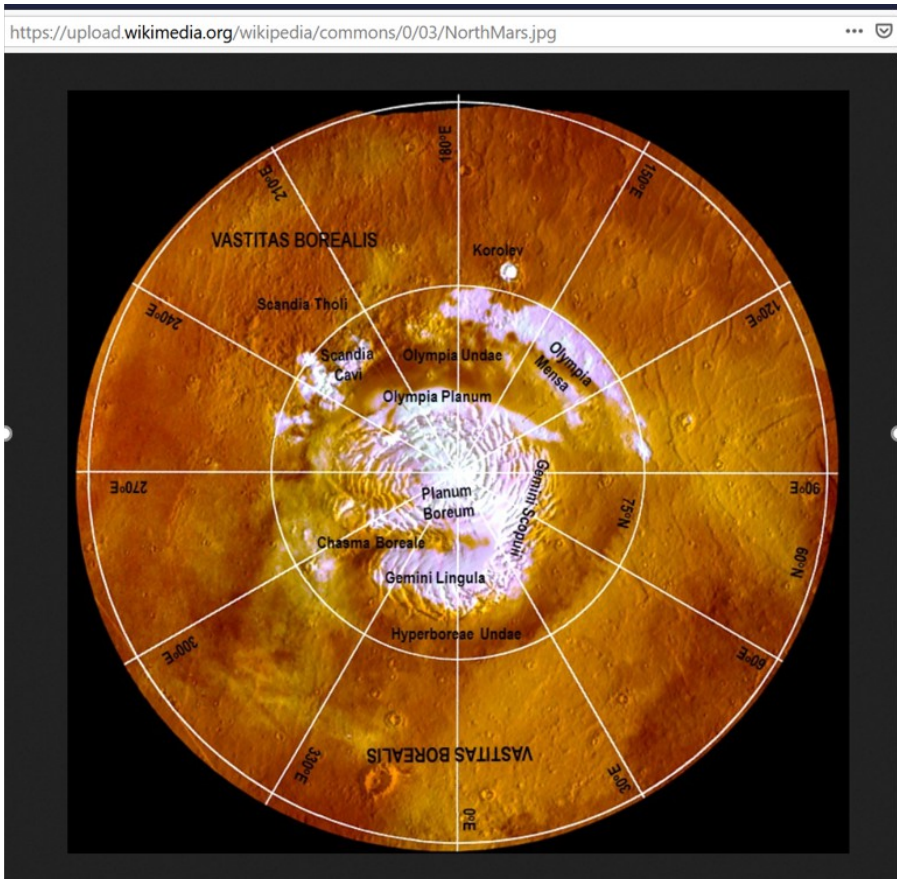

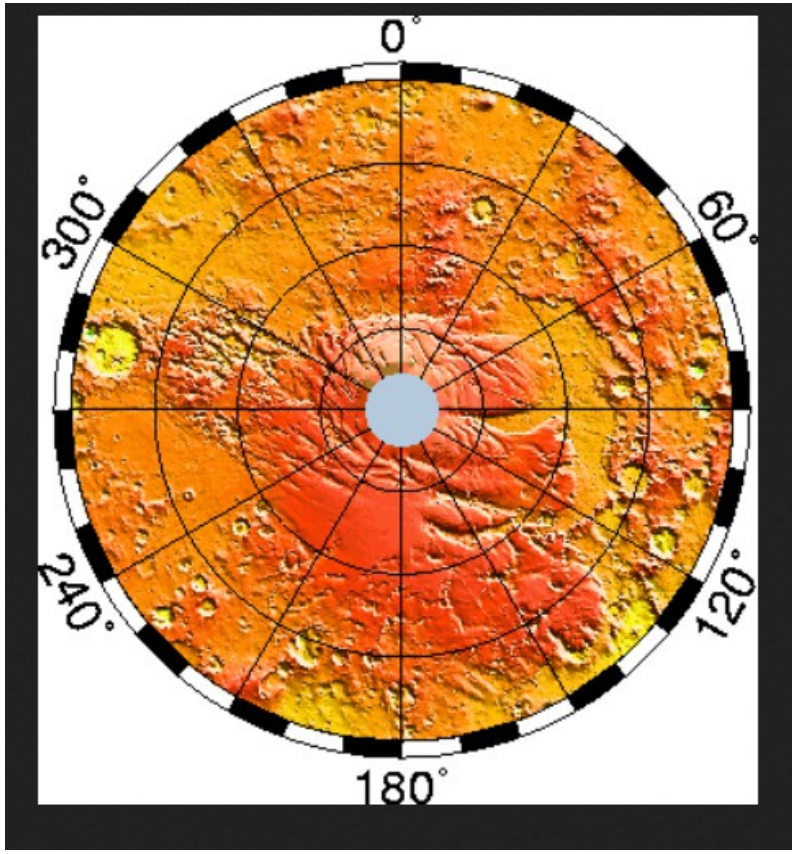

Assymetry around poles, different size and thickness (southern smaller), effect of Corriolis force, see also strike angles for more study

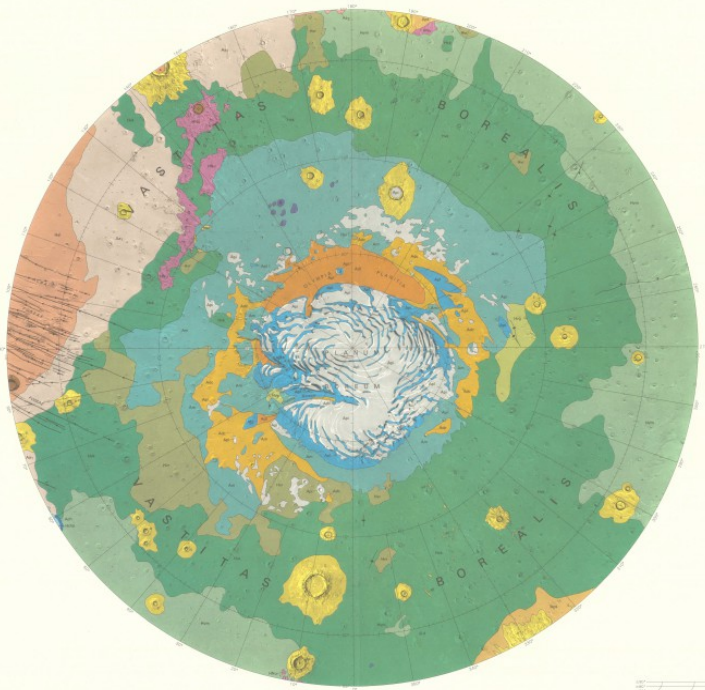

NORTH POLAR REGION

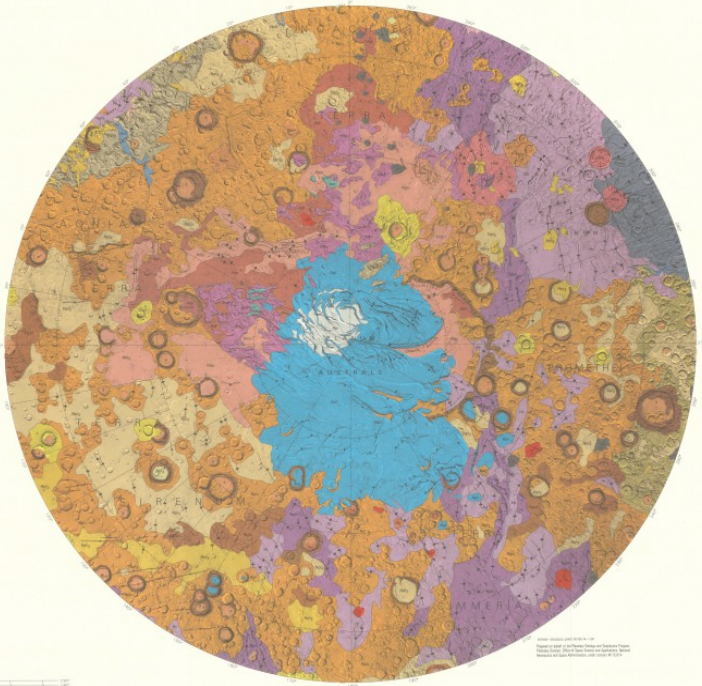

SOUTH POLAR REGION

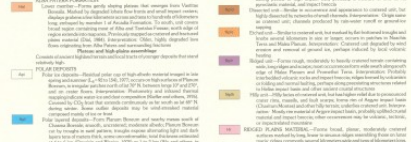

Our main results

global

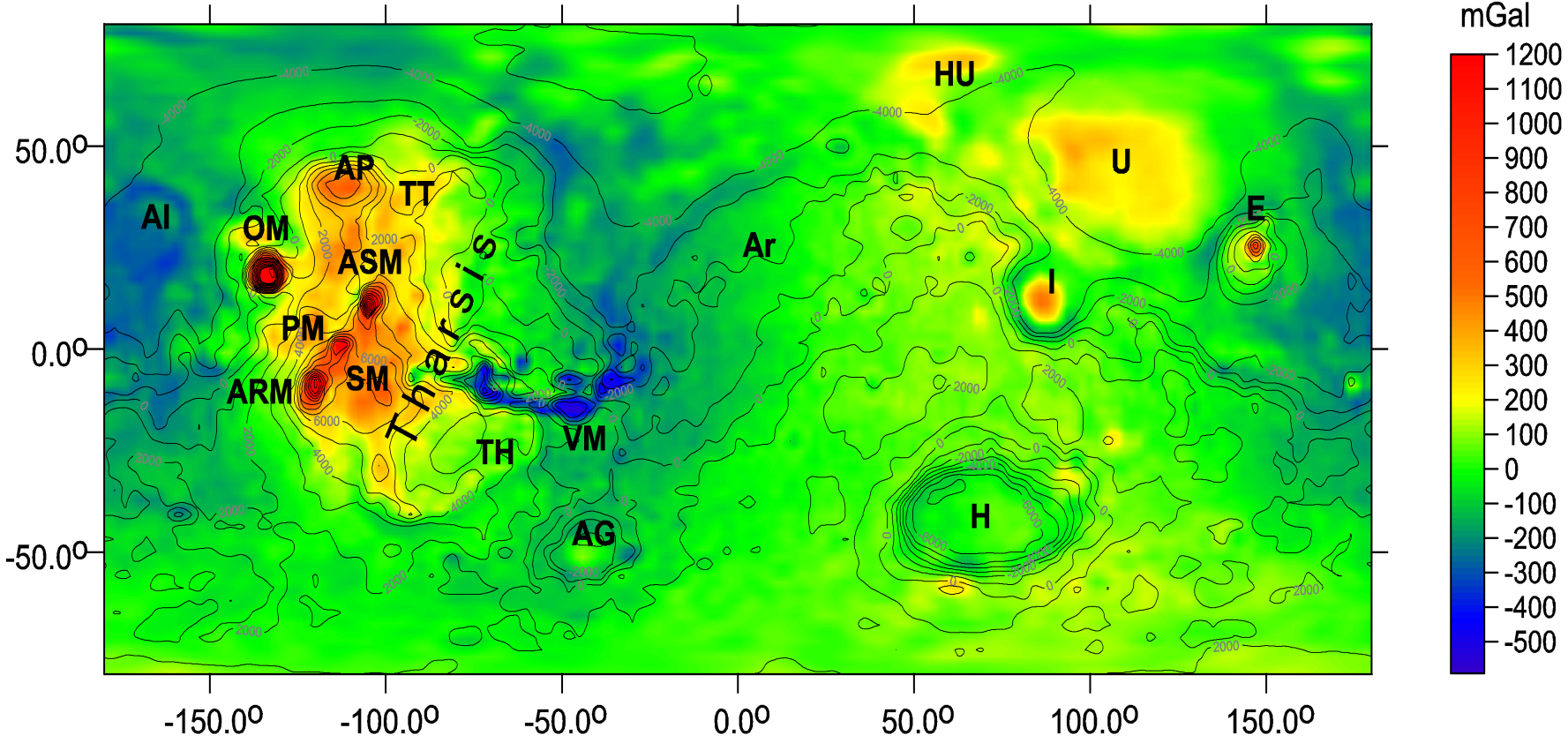

Gravity disturbances Δ*g* [mGal] on Mars

according to the gravity field model JGMRO_120 F (Konopliv et al. 2020), used here everywhere to plot the gravity aspects, cut always at maximum degree and order d/o = 80, as recommended by the authors of the model, together with contour lines derived from the MOLA topography [m] (metres above the reference ellipsoid).

Valles Marineris (VM). Hellas (H), area at the Crater Lake (Syrtis Major/Isidis) I, Utopia (U), Hustak (HU), Elysium (E), Tharsis area (T), Olympus Mt (OM) and other volcanoes in T, Ascraeus Mons (ASM), Pavonis and Arsia Mons (PM and ARM), Alba Patera and Syria Mons (AP and SM), Tempe Terra (TT), Thaumasia Highlands (TH), one of ancient structures (AI).

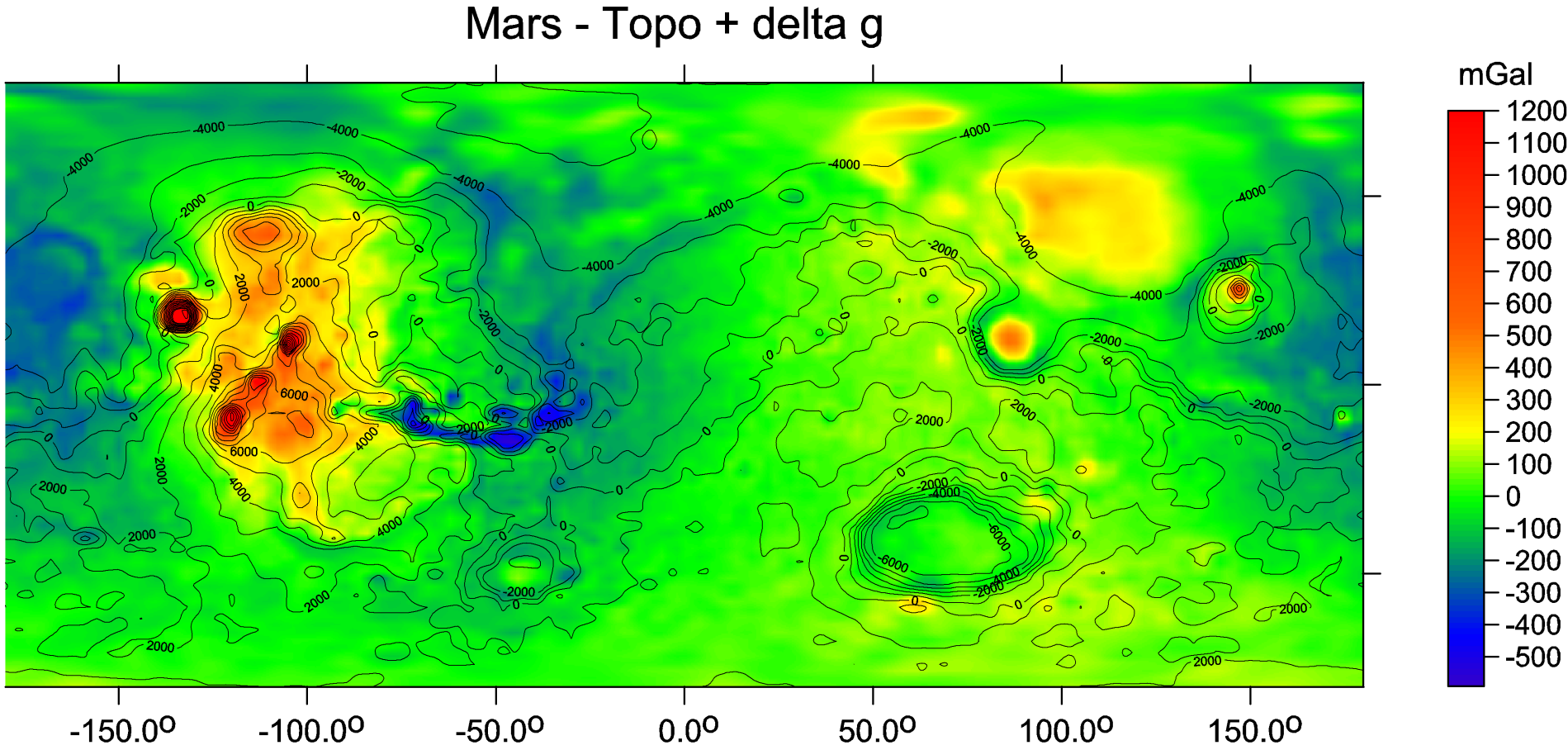
Mars - Topo + delta g
mGal
1200
1100
1000
900
800
700
600
500
400
300
200
100
0
-100
-200
-300
-400
-500
-150.0°
-100.0°
-50.0°
0.0°
50.0°
100.0°
150.0°

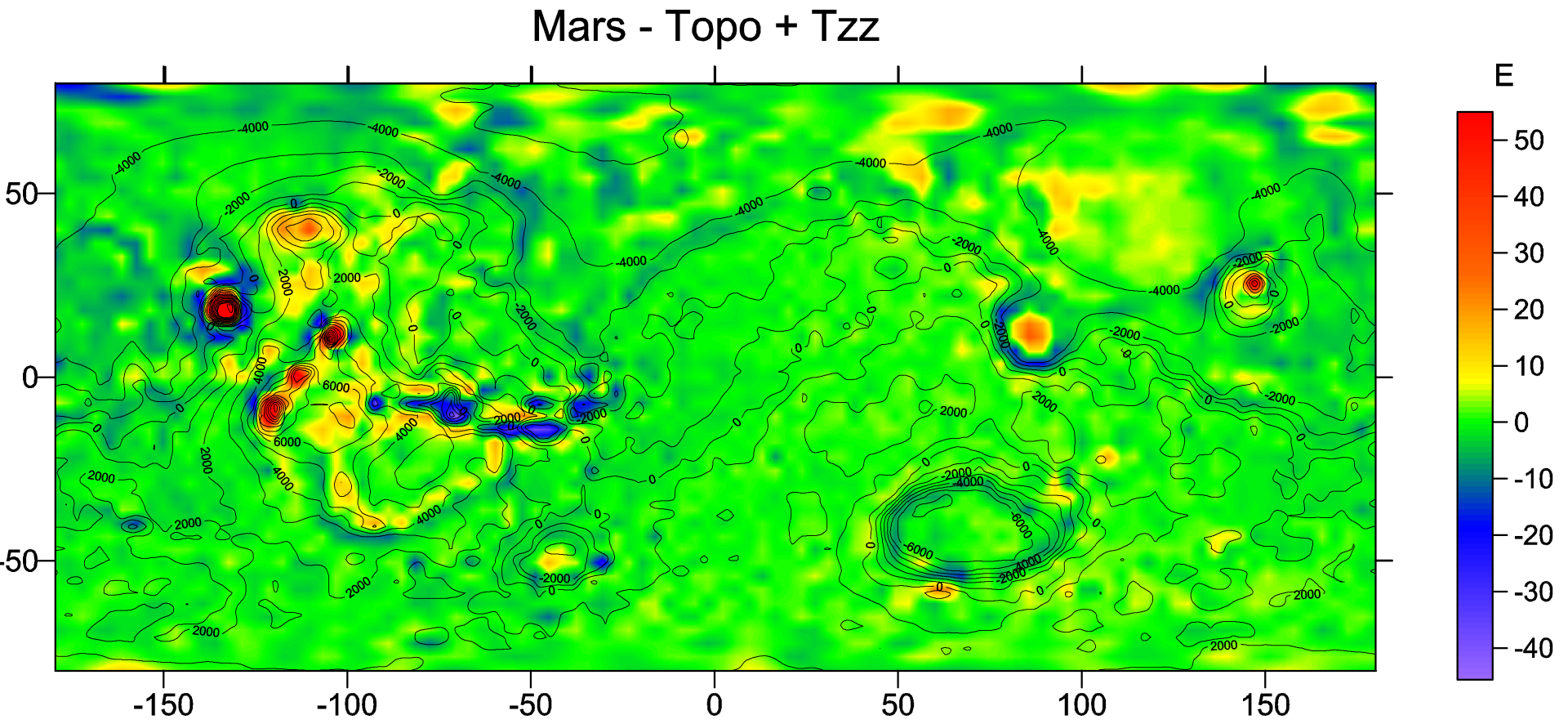
Mars - Topo + Tzz
E
50
40
30
20
10
0
-10
-20
-30
-40
50
0
-50
-150
-100
-50
0
50
100
150

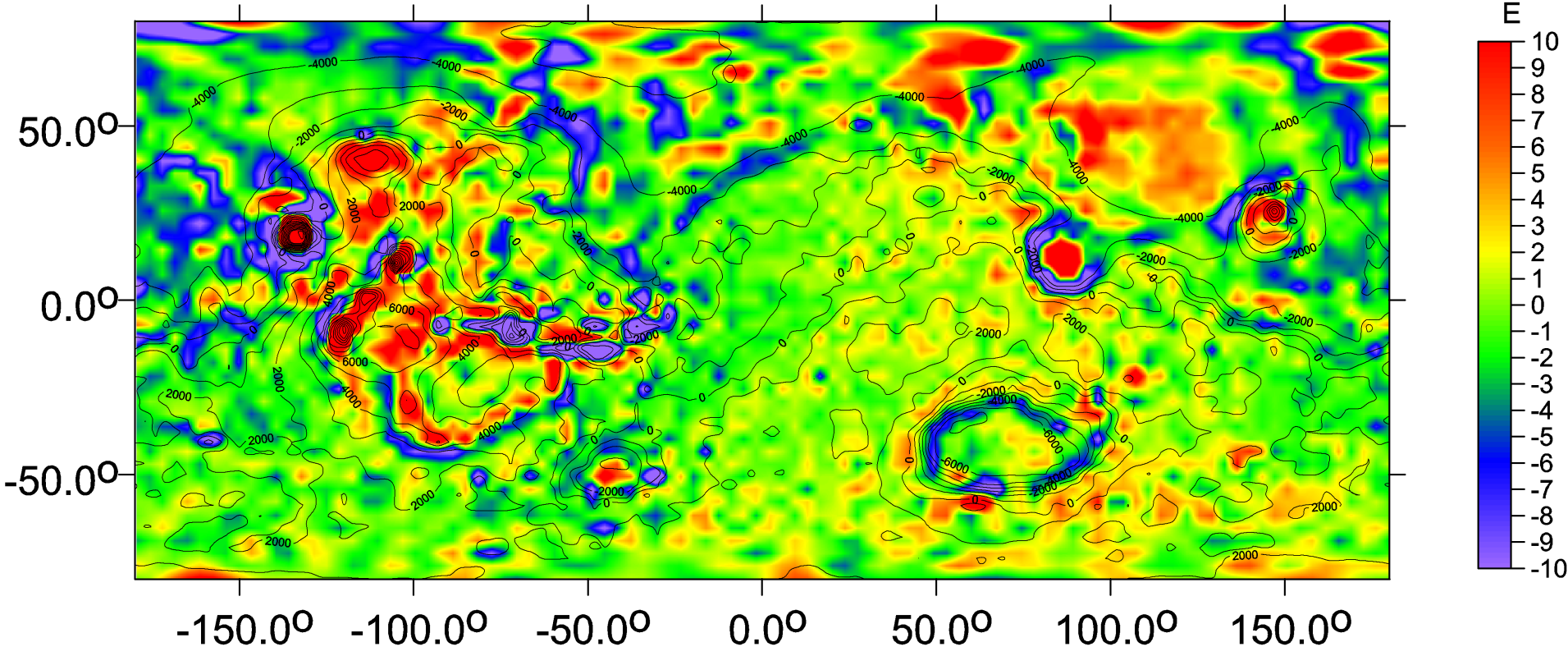
Mars - Topo + Tzz
E
10
9
8
7
6
5
4
3
2
1
0
-1
-2
-3
-4
-5
-6
-7
-8
-9
-10
50.0°
0.0°
-50.0°
-150.0°
-100.0°
-50.0°
0.0°
50.0°
100.0°
150.0°

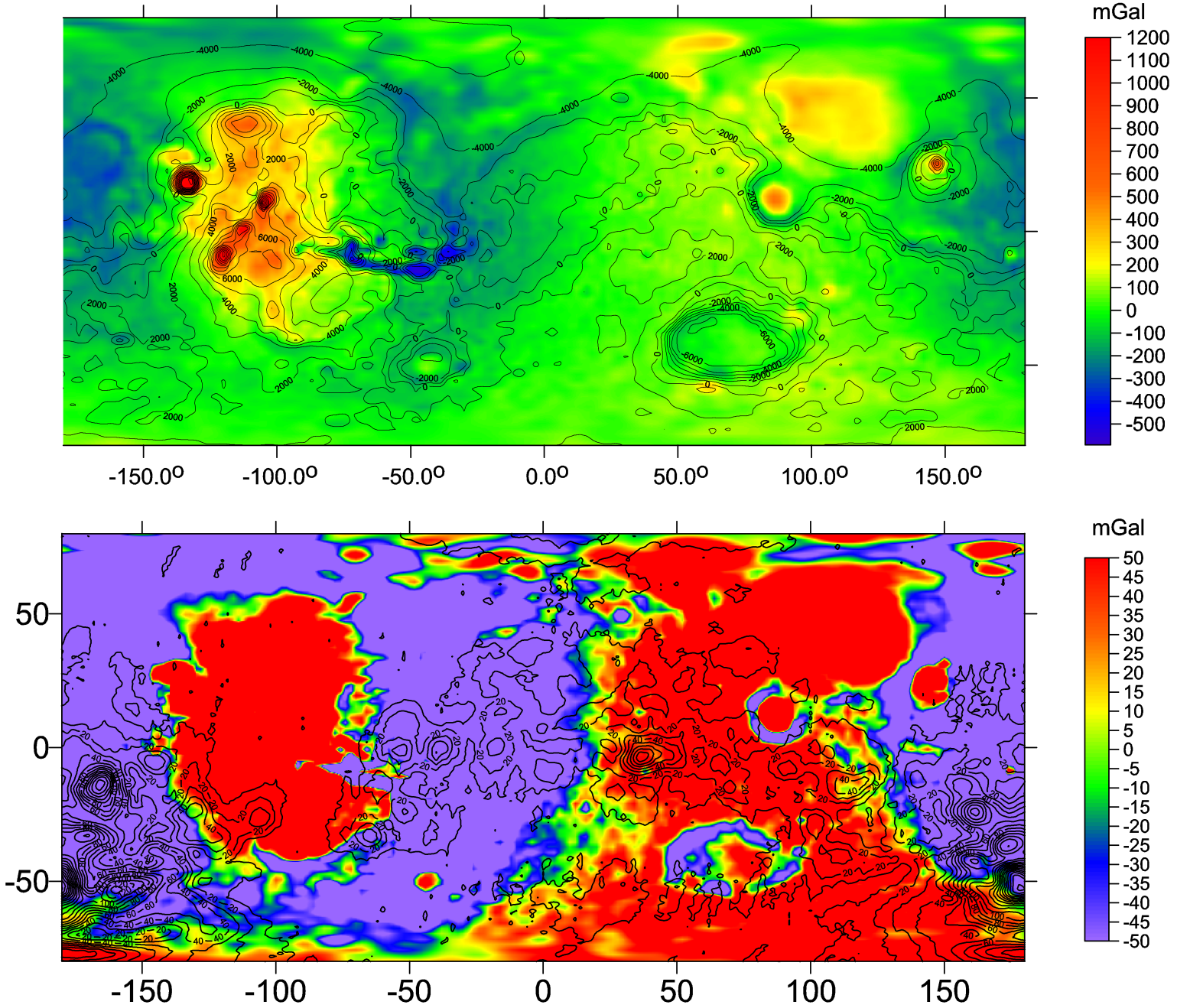
Mars - Topo + delta g
mGal
1200
1100
1000
900
800
700
600
500
400
300
200
100
0
-100
-200
-300
-400
-500
-150.0°
-100.0°
-50.0°
0.0°
50.0°
100.0°
150.0°
mGal
50
45
40
35
30
25
20
15
10
5
0
-5
-10
-15
-20
-25
-30
-35
-40
-45
-50
50
0
-50
-150
-100
-50
0
50
100
150

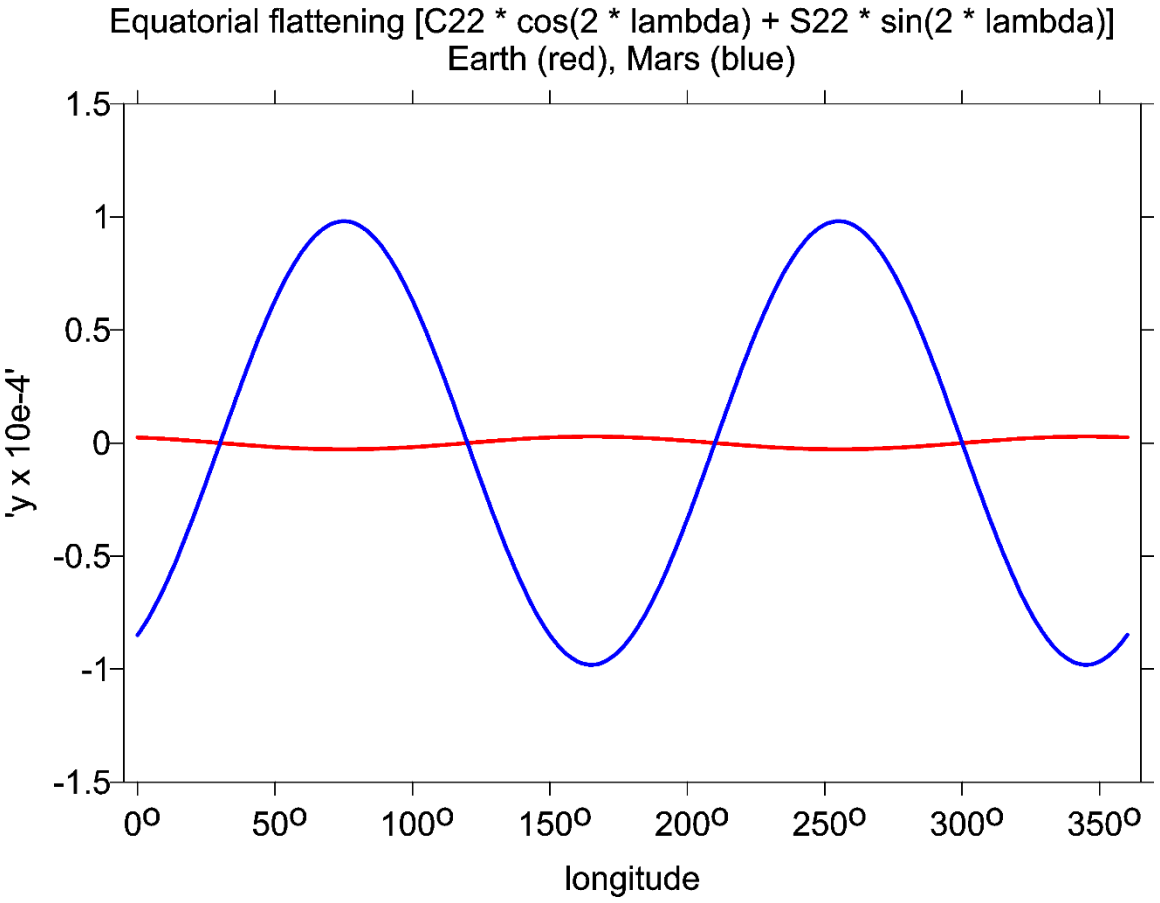

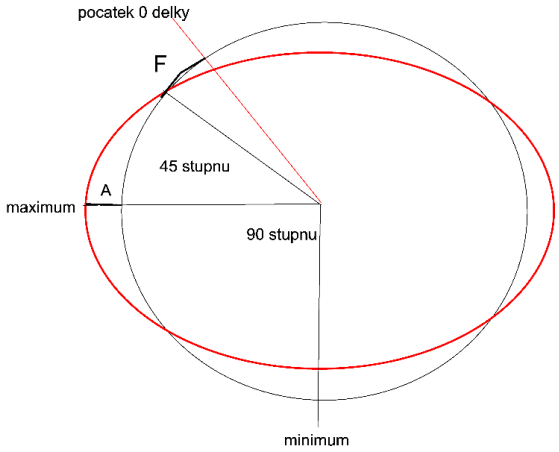

Mars (gravity model JGMRO_120 F):

GM (C00) = 0.4282837×1014 [m3 s−2]

C20 = -0.88 10-3
C30 = -0.12 10-4
C50 = -0.17 10-5

C22 = -0.85 10-4, S22= 0.49 10-4

J22 = 0.98 10-4, λ22stable = 165. 3o E,

λ22unstab = 75. 2o E

The Earth (gravity model EIGEN 6C4):

GM (C00) = 3.986004419×1014 [m3 s−2]

C20 = -0.48 10-3
C30 = +0.01 10-4
C50 = +0.69 10-7

C22 = 2.44 10-6, S22 = -1.40 10-6;

J22 = 2.81 10-6 = 0.03 10-4, λ22stable = 75. 2o E, λ22unstab = 165. 3o E

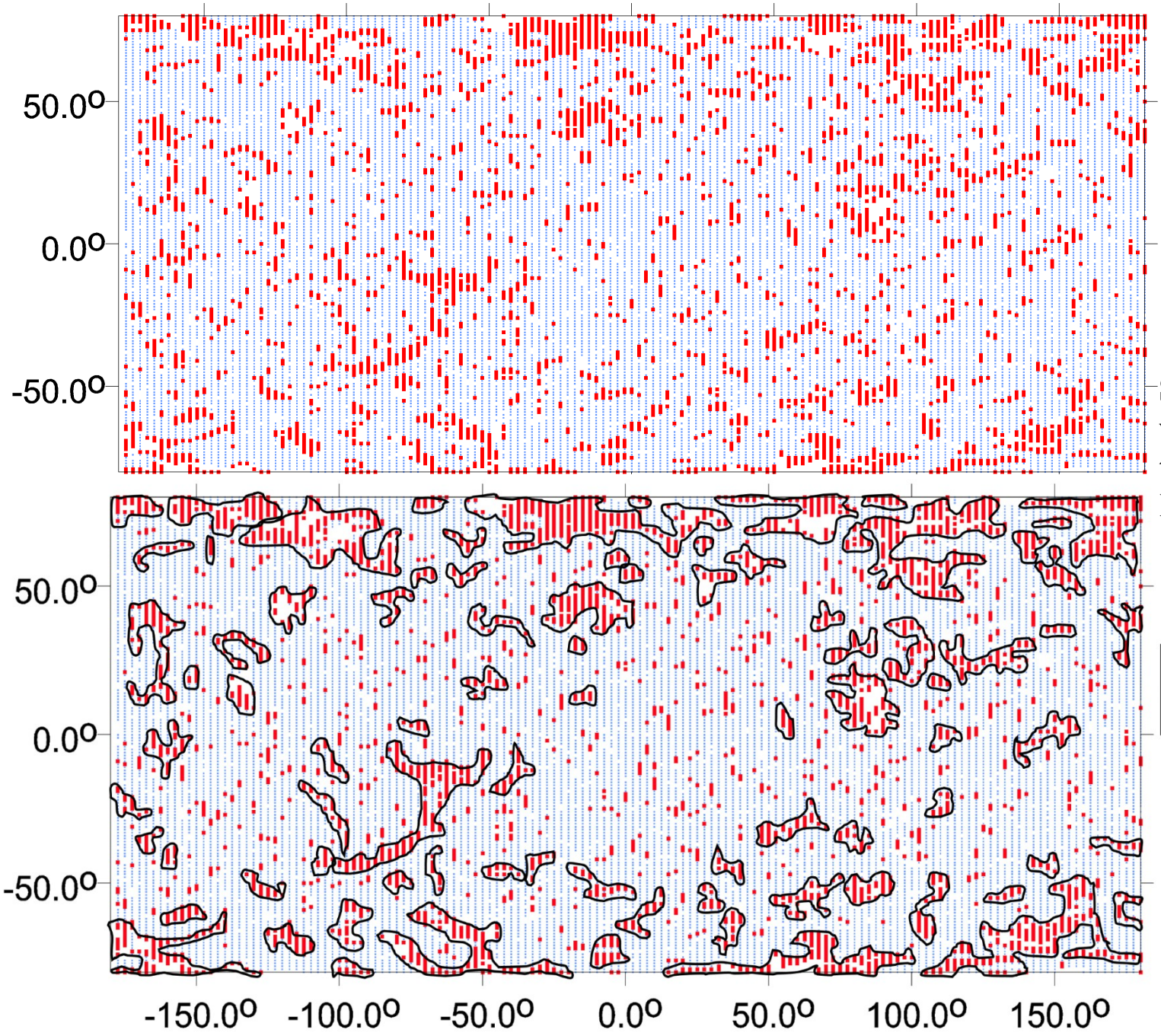

Strike angles with the comb factor to emphasize highly combed areas

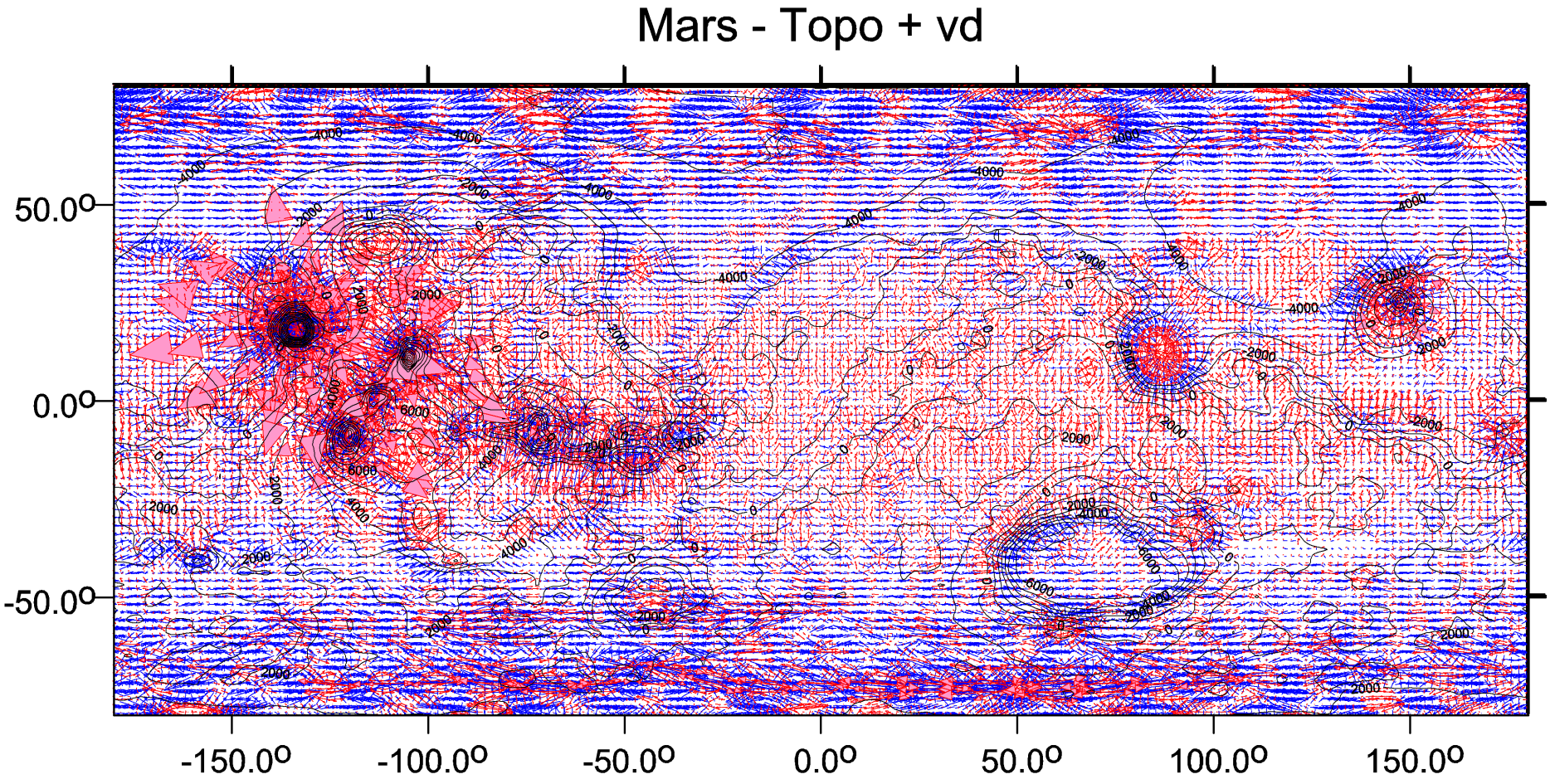
Mars - Topo + vd
50.0°
0.0°
-50.0°
-150.0°
-100.0°
-50.0°
0.0°
50.0°
100.0°
150.0°

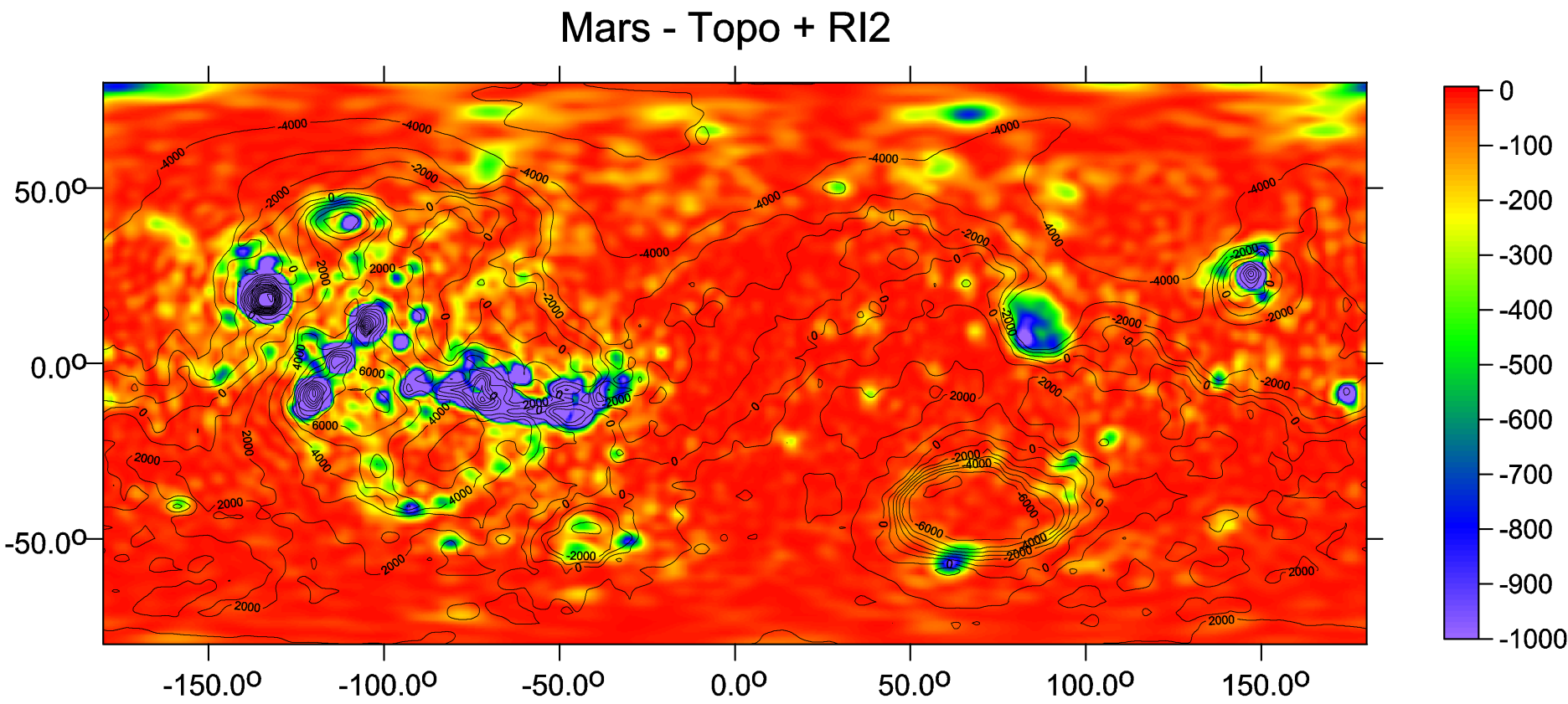
Mars - Topo + RI2
50.0°
0.0°
-50.0°
-150.0°
-100.0°
-50.0°
0.0°
50.0°
100.0°
150.0°
0
-100
-200
-300
-400
-500
-600
-700
-800
-900
-1000

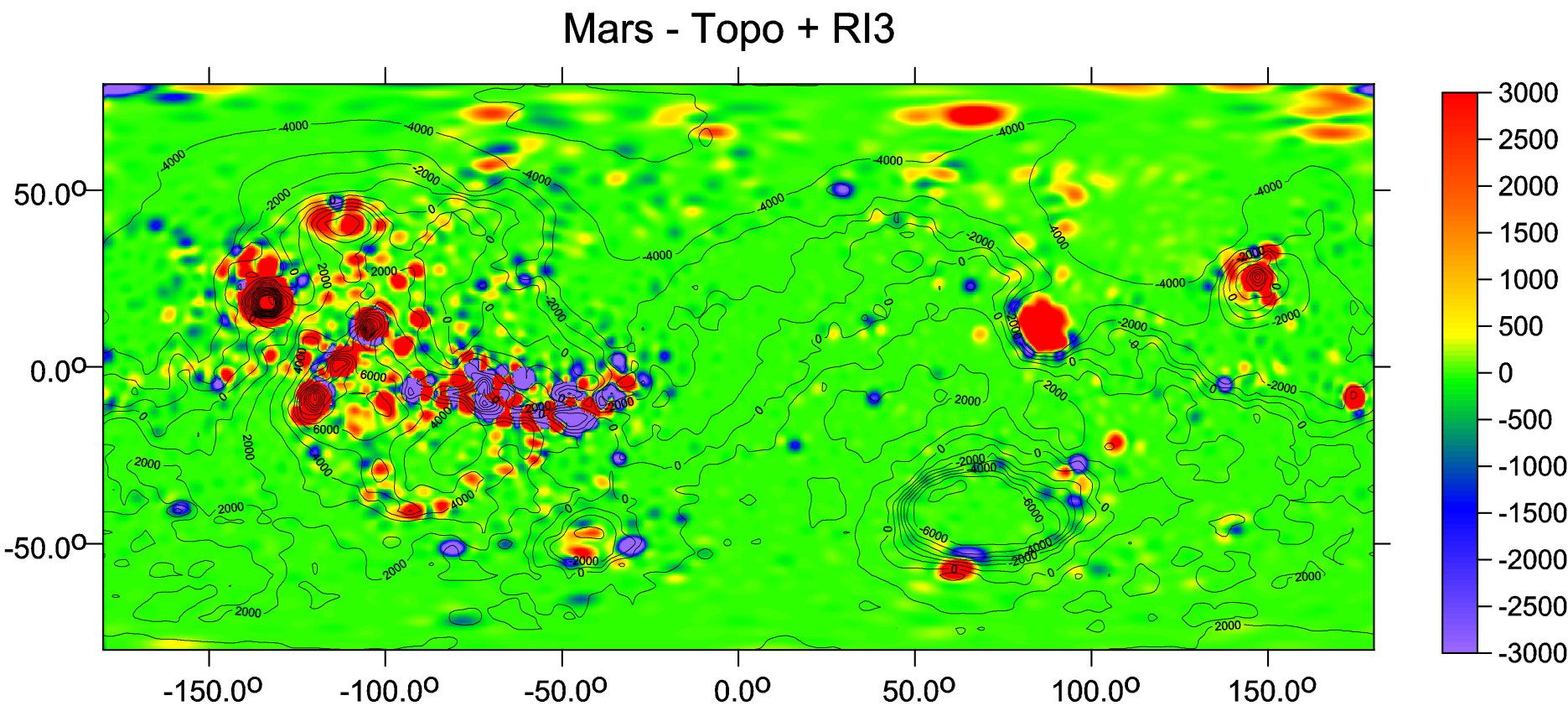
Mars - Topo + RI3
50.0°
0.0°
-50.0°
-150.0°
-100.0°
-50.0°
0.0°
50.0°
100.0°
150.0°
3000
2500
2000
1500
1000
500
0
-500
-1000
-1500
-2000
-2500
-3000

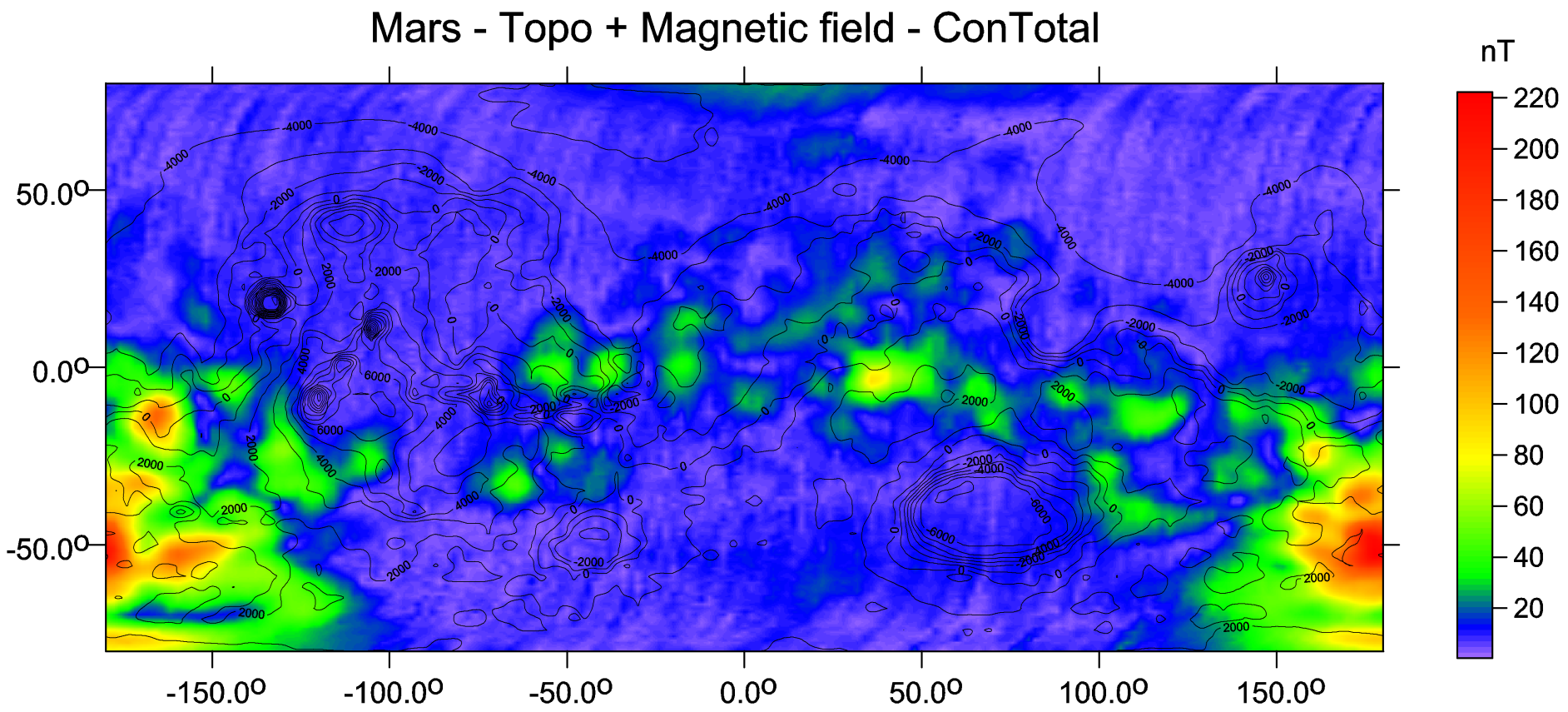
Mars - Topo + Magnetic field - ConTotal
nT
220
200
180
160
140
120
100
80
60
40
20
50.0°
0.0°
-50.0°
-150.0°
-100.0°
-50.0°
0.0°
50.0°
100.0°
150.0°

Our main results

polar

Mars - north pole - Topography + delta g

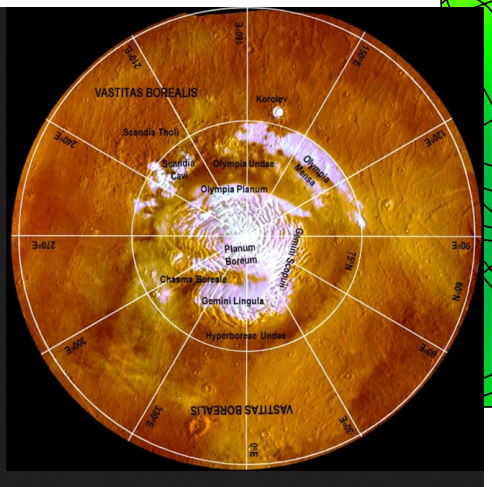

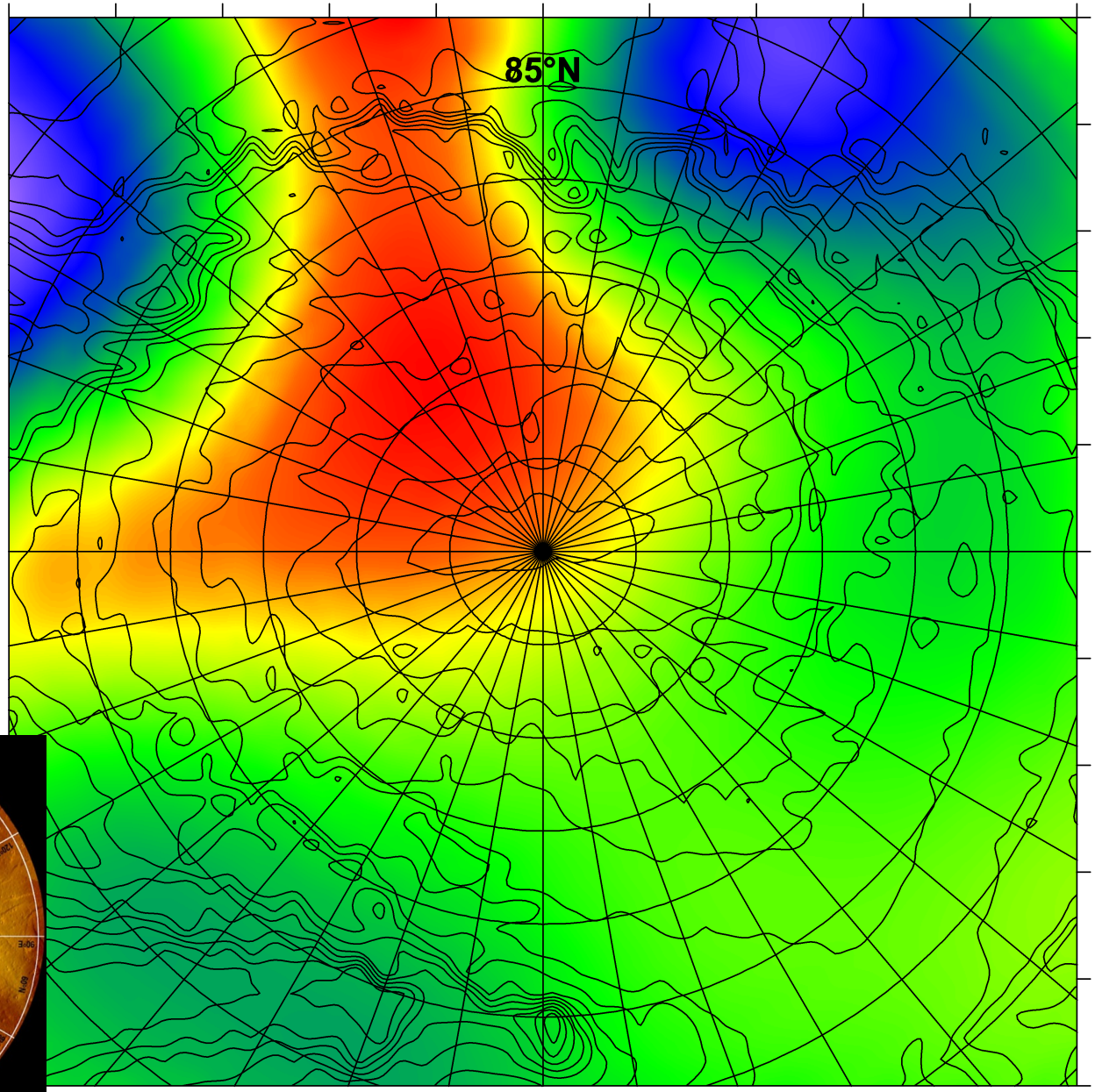

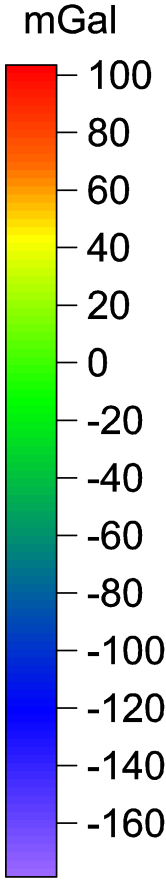

Our resolution ~100 km

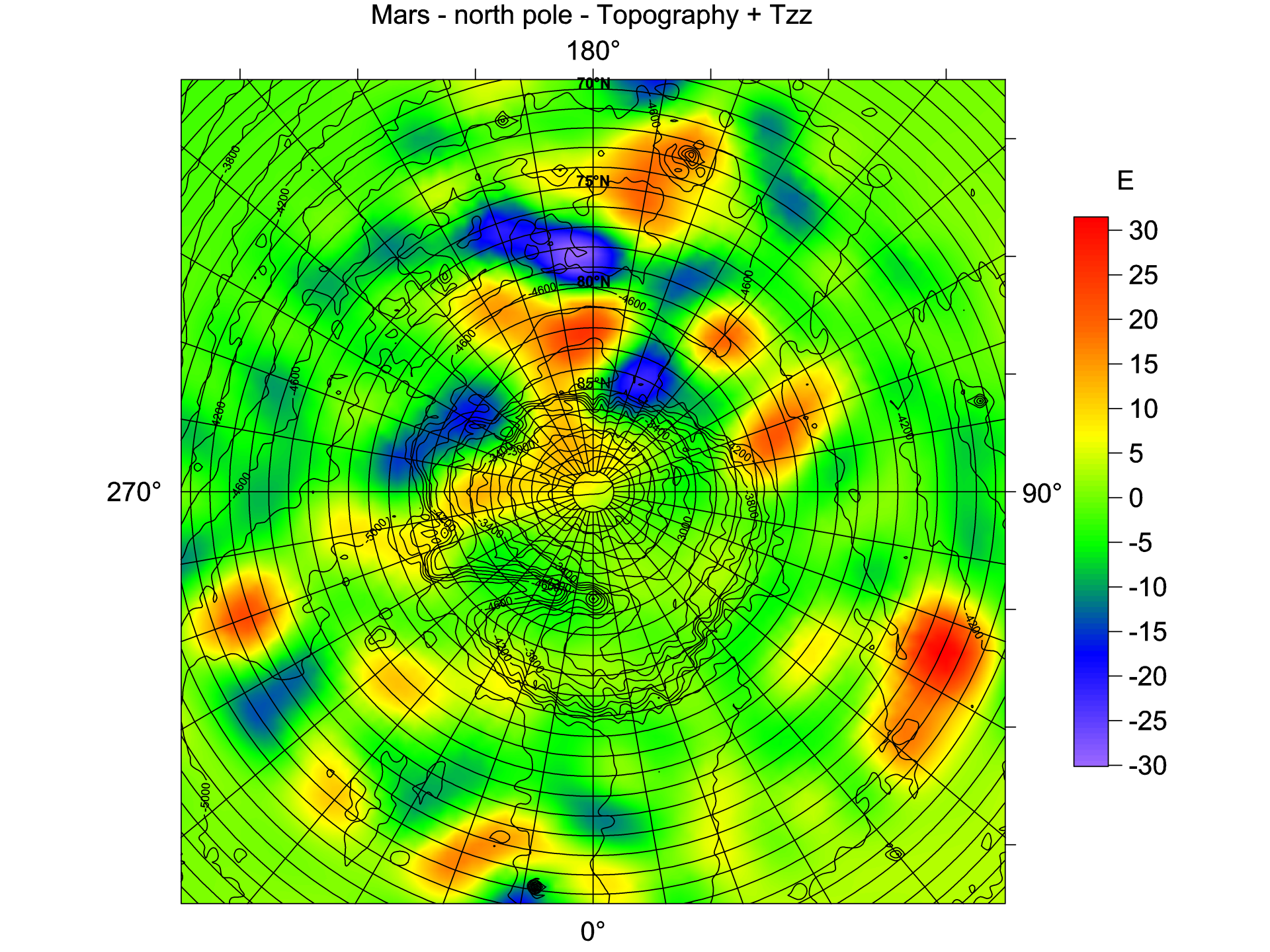
Mars - north pole - Topography + Tzz
180°
270°
90°
0°
70°N
75°N
80°N
85°N
E
30
25
20
15
10
5
0
-5
-10
-15
-20
-25
-30

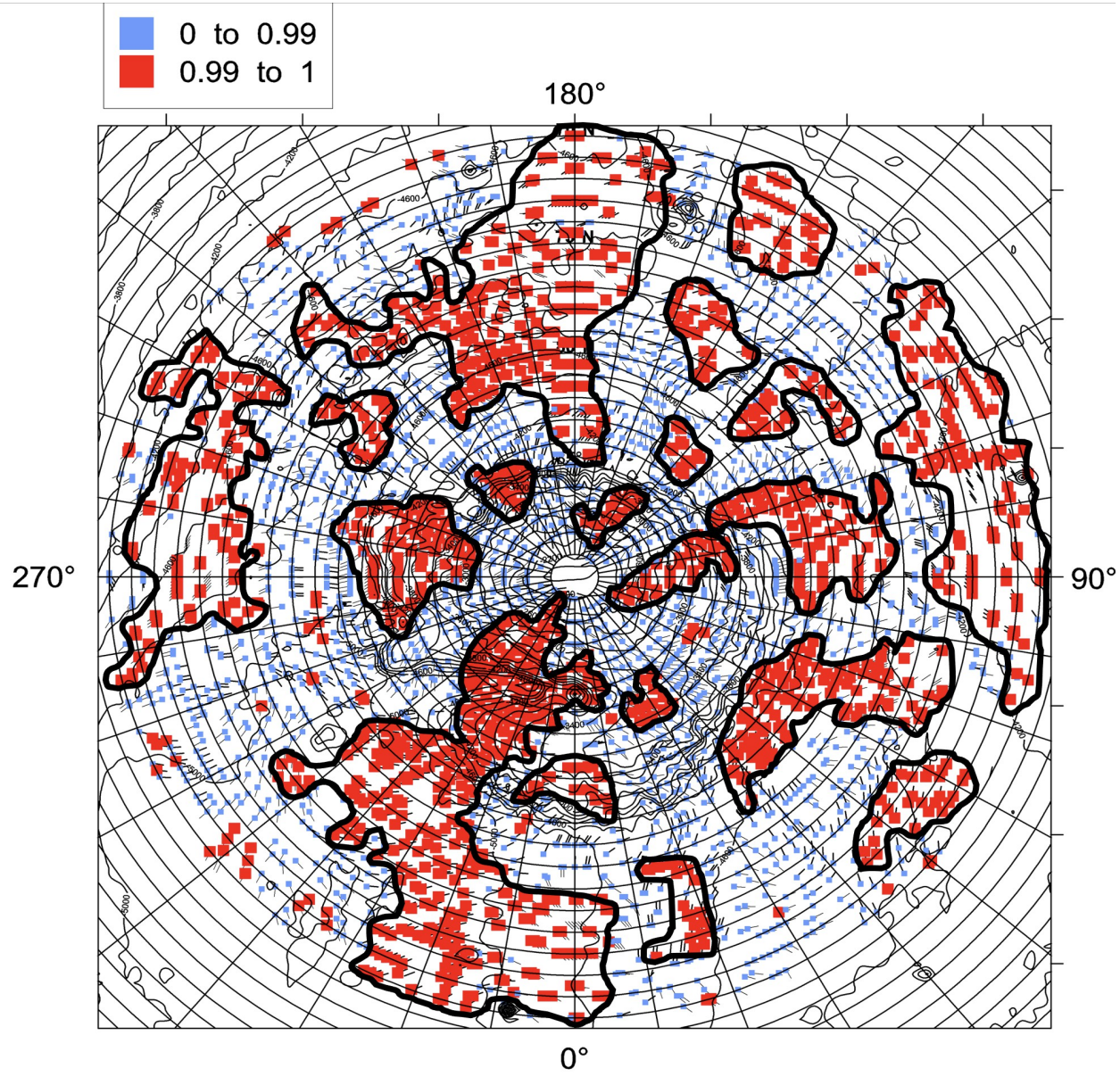

The strike angles θ [deg] (with the *comb* statistics) for the northern polar area.

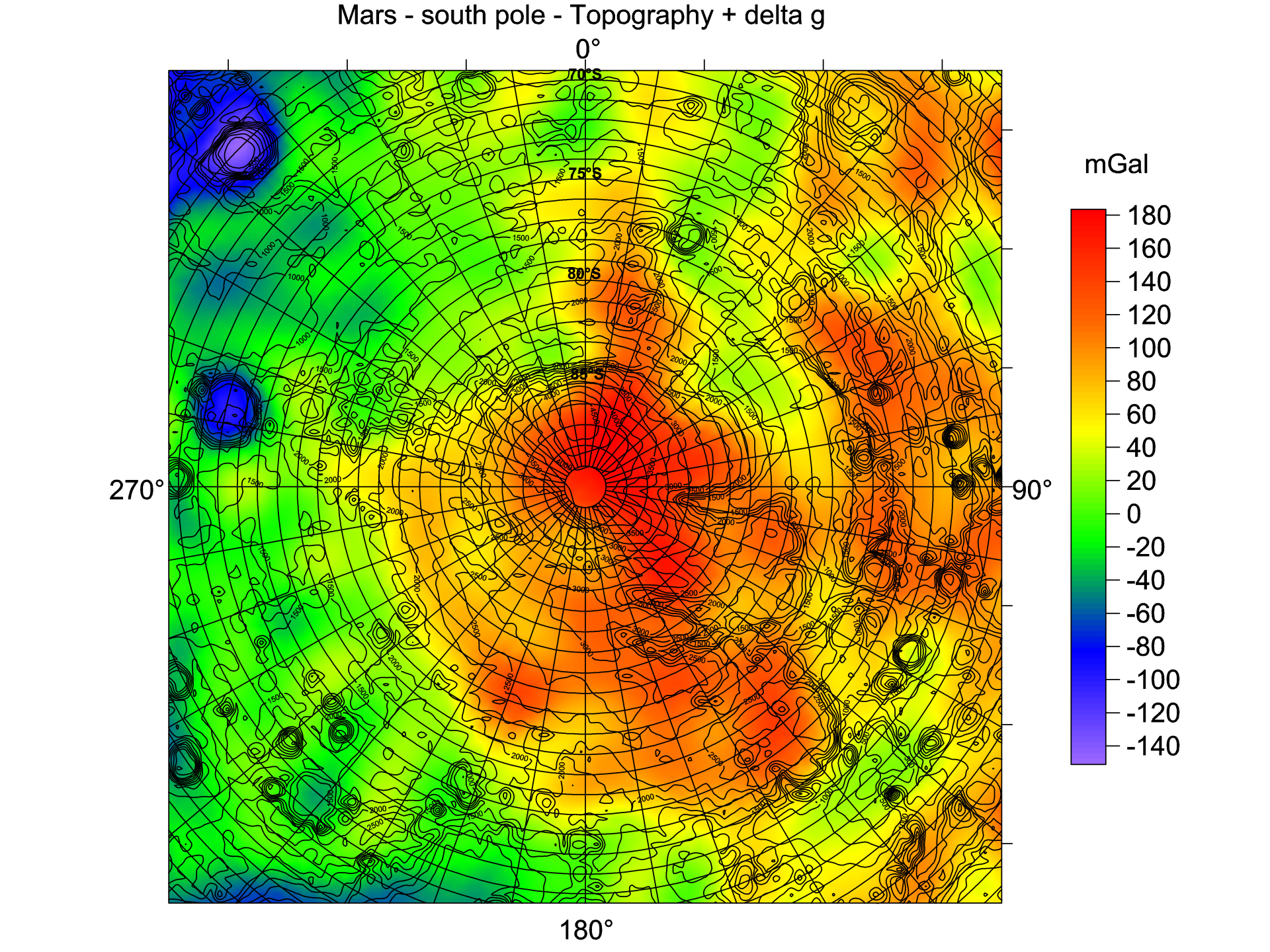
Mars - south pole - Topography + delta g
0°
70°S
75°S
80°S
85°S
270°
90°
180°
mGal
180
160
140
120
100
80
60
40
20
0
-20
-40
-60
-80
-100
-120
-140

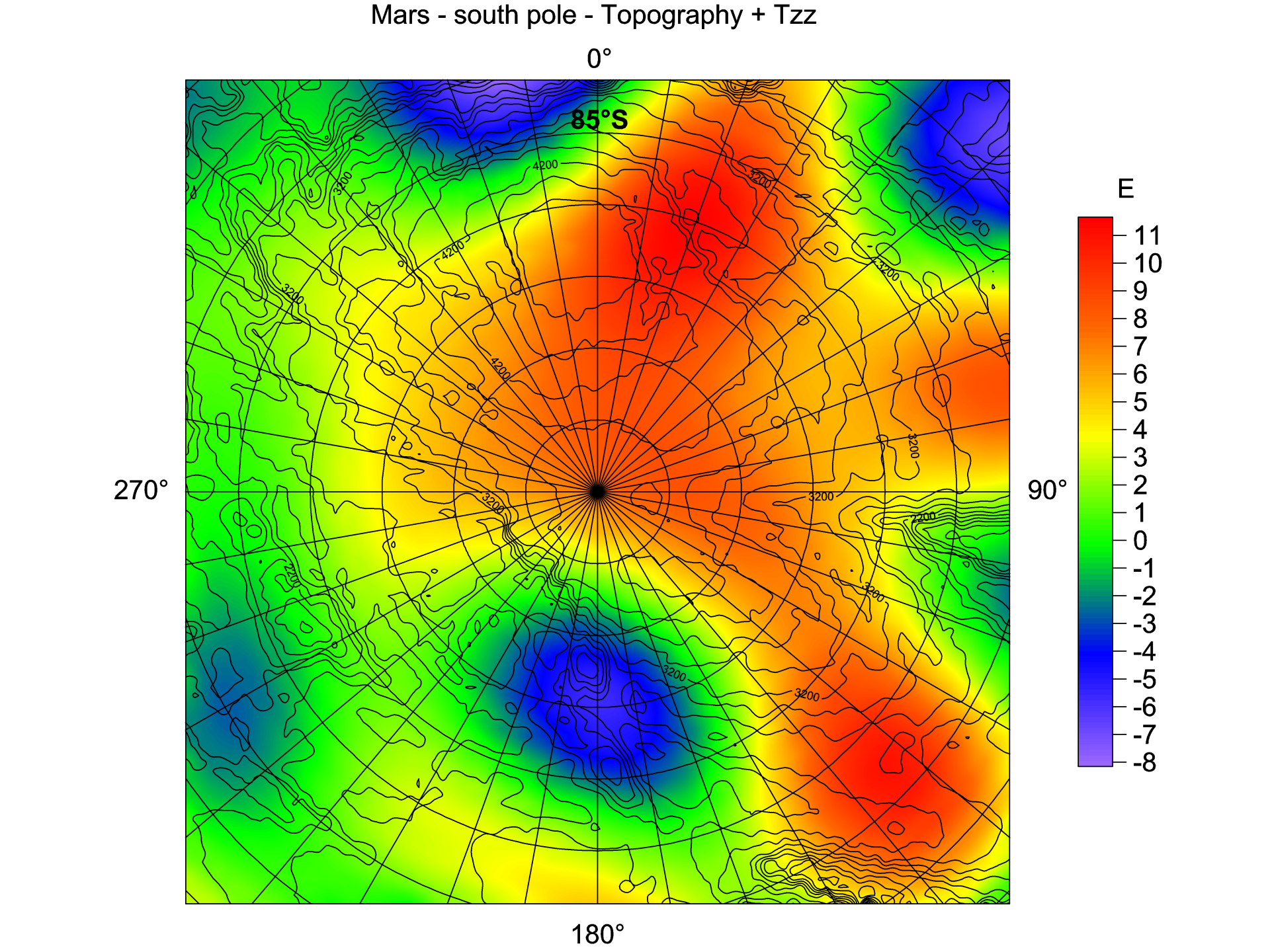
Mars - south pole - Topography + Tzz
0°
85°S
270°
90°
180°
E
11
10
9
8
7
6
5
4
3
2
1
0
-1
-2
-3
-4
-5
-6
-7
-8
4200
3200

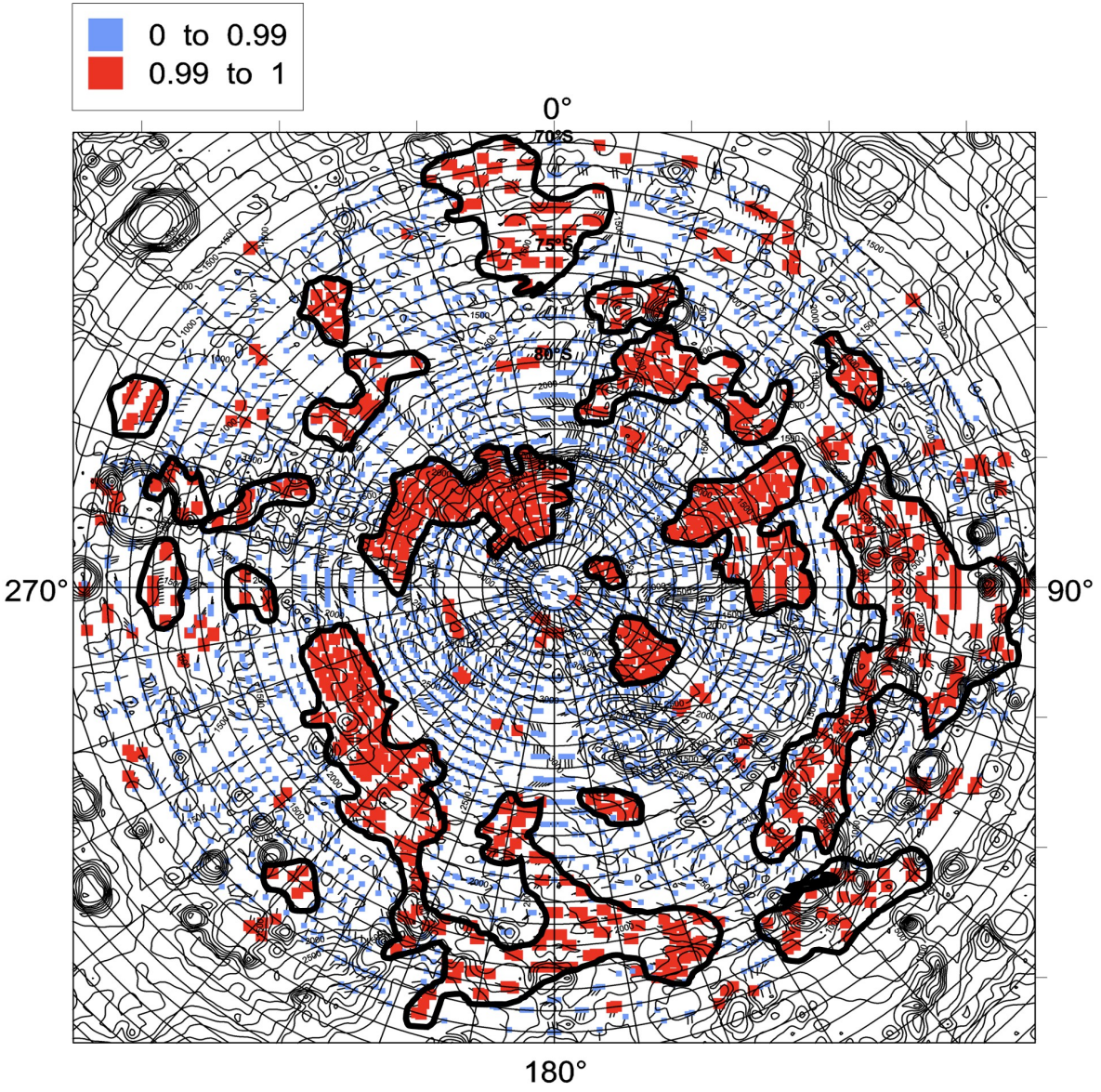

The strike angles θ [deg] (with the *comb* statistics) for the southern polar area.

Our main results

selected regions

Tharsis volcanoes MOLA topo

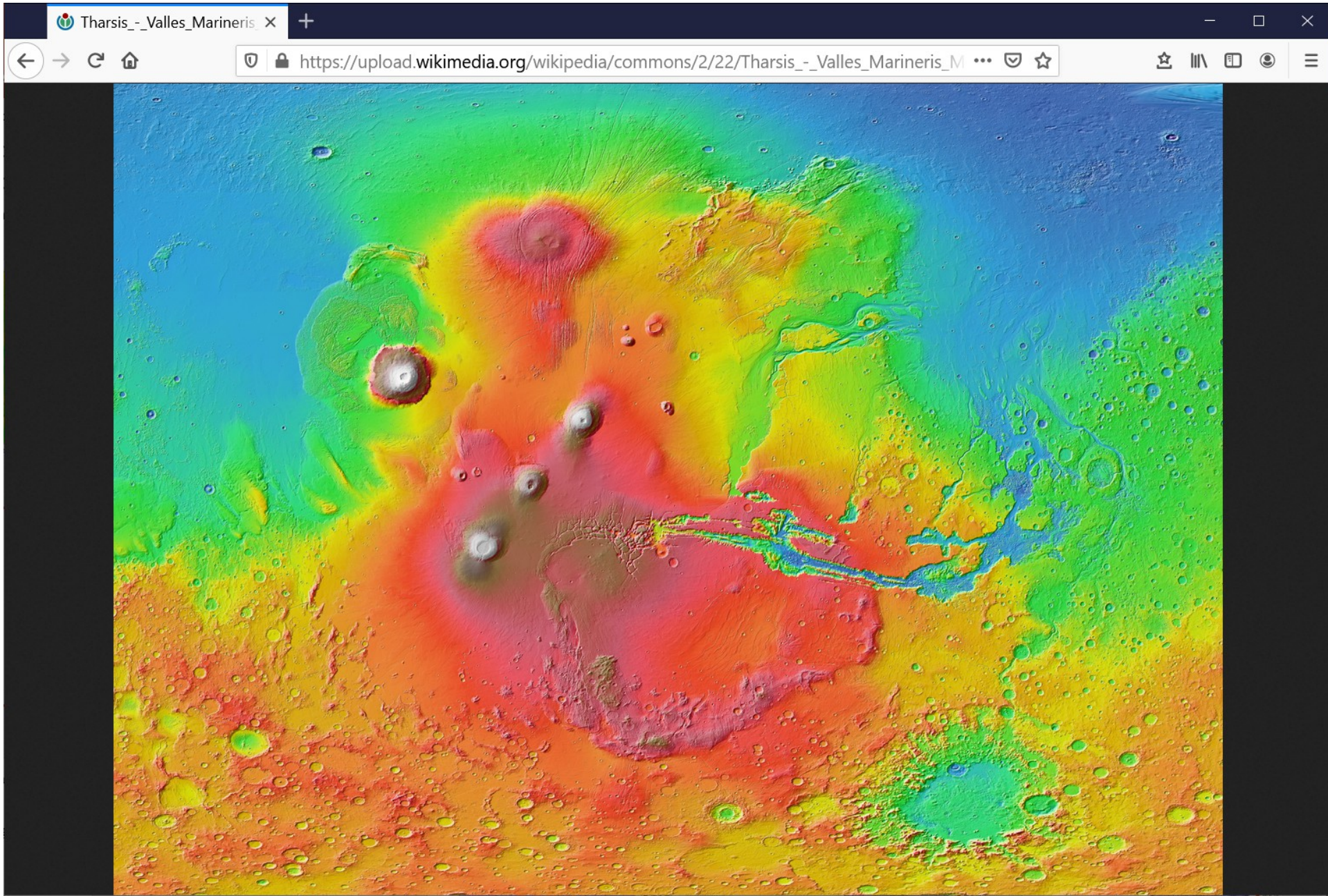

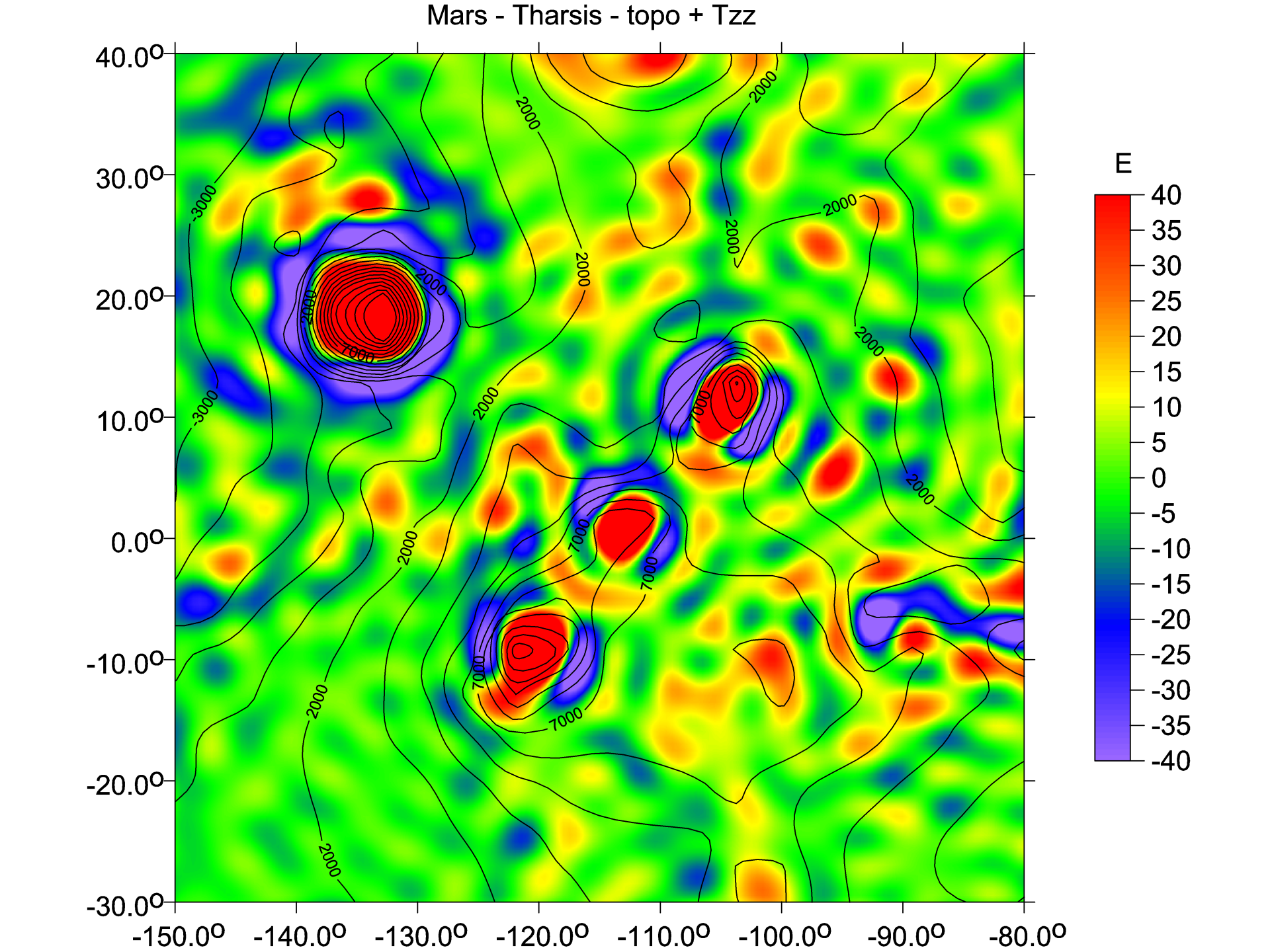
Mars - Tharsis - topo + Tzz
E
40
35
30
25
20
15
10
5
0
-5
-10
-15
-20
-25
-30
-35
-40
40.0°
30.0°
20.0°
10.0°
0.0°
-10.0°
-20.0°
-30.0°
-150.0°
-140.0°
-130.0°
-120.0°
-110.0°
-100.0°
-90.0°
-80.0°
2000
-3000
7000

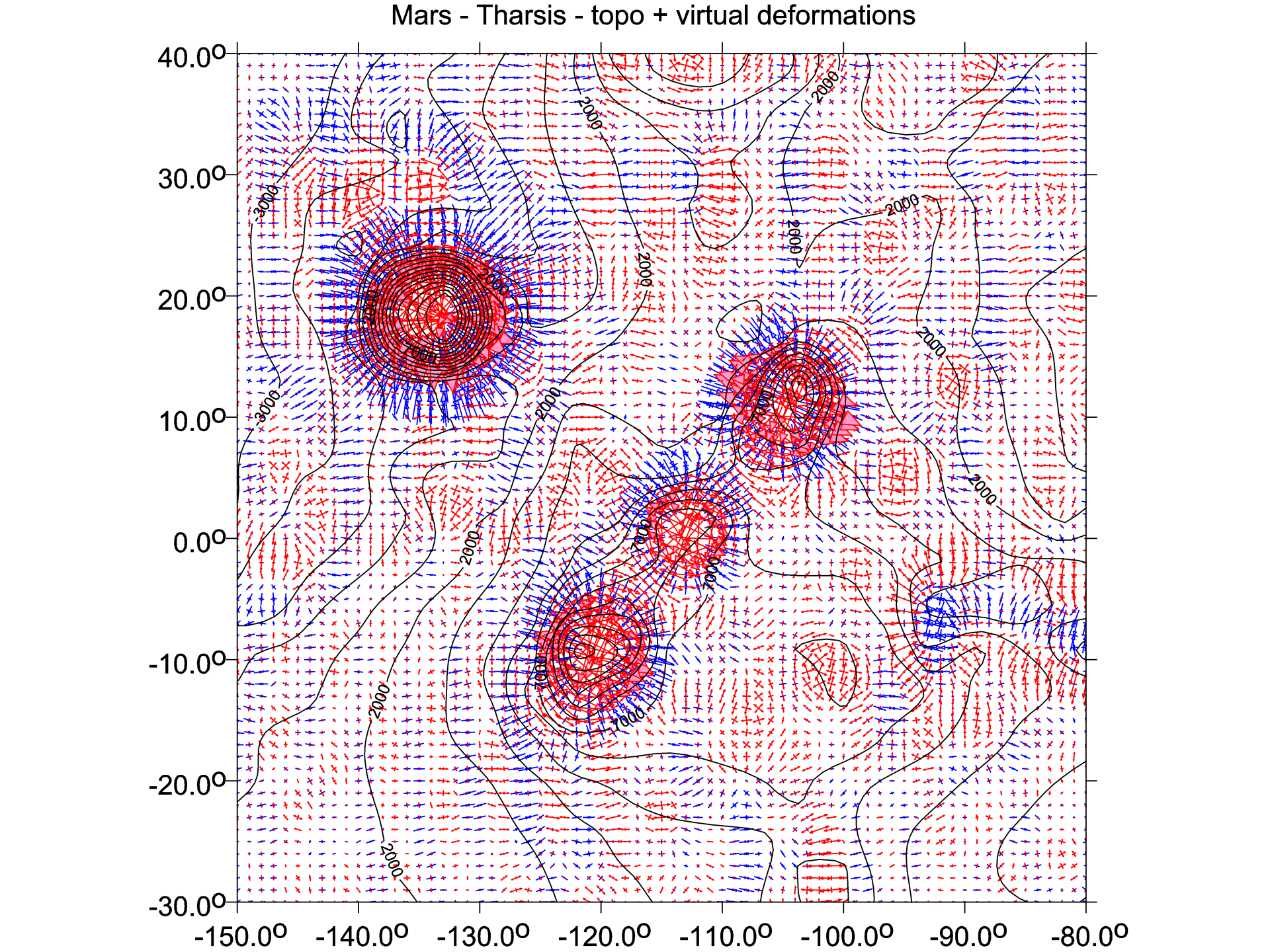
Mars - Tharsis - topo + virtual deformations
40.0°
30.0°
20.0°
10.0°
0.0°
-10.0°
-20.0°
-30.0°
-150.0°
-140.0°
-130.0°
-120.0°
-110.0°
-100.0°
-90.0°
-80.0°
-3000
-2000
-1000

Hellas

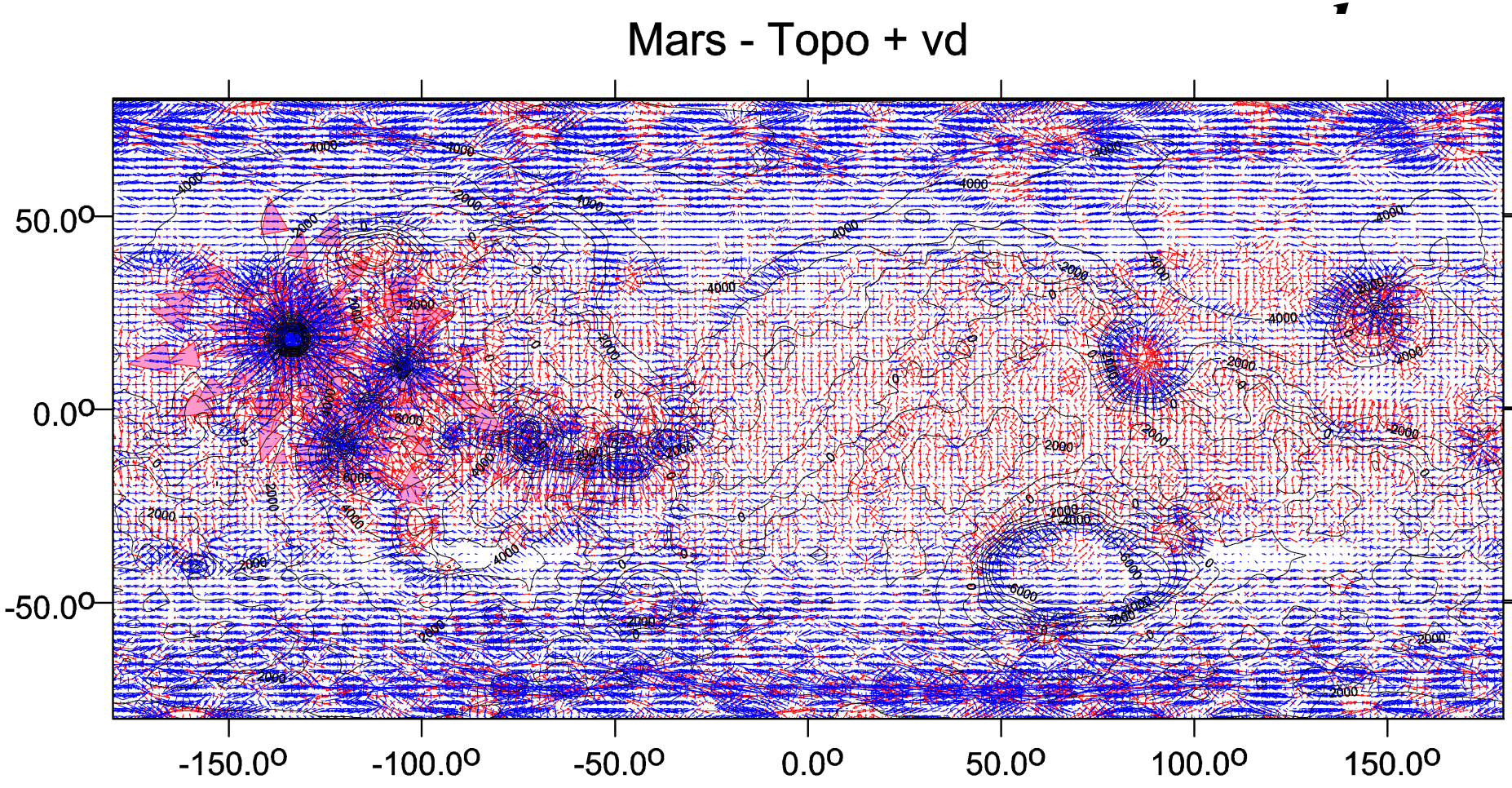

https://cs.wikipedia.org/wiki/Valles_Marineris#/media/Soubor:Valles_marineris_topo.jpg

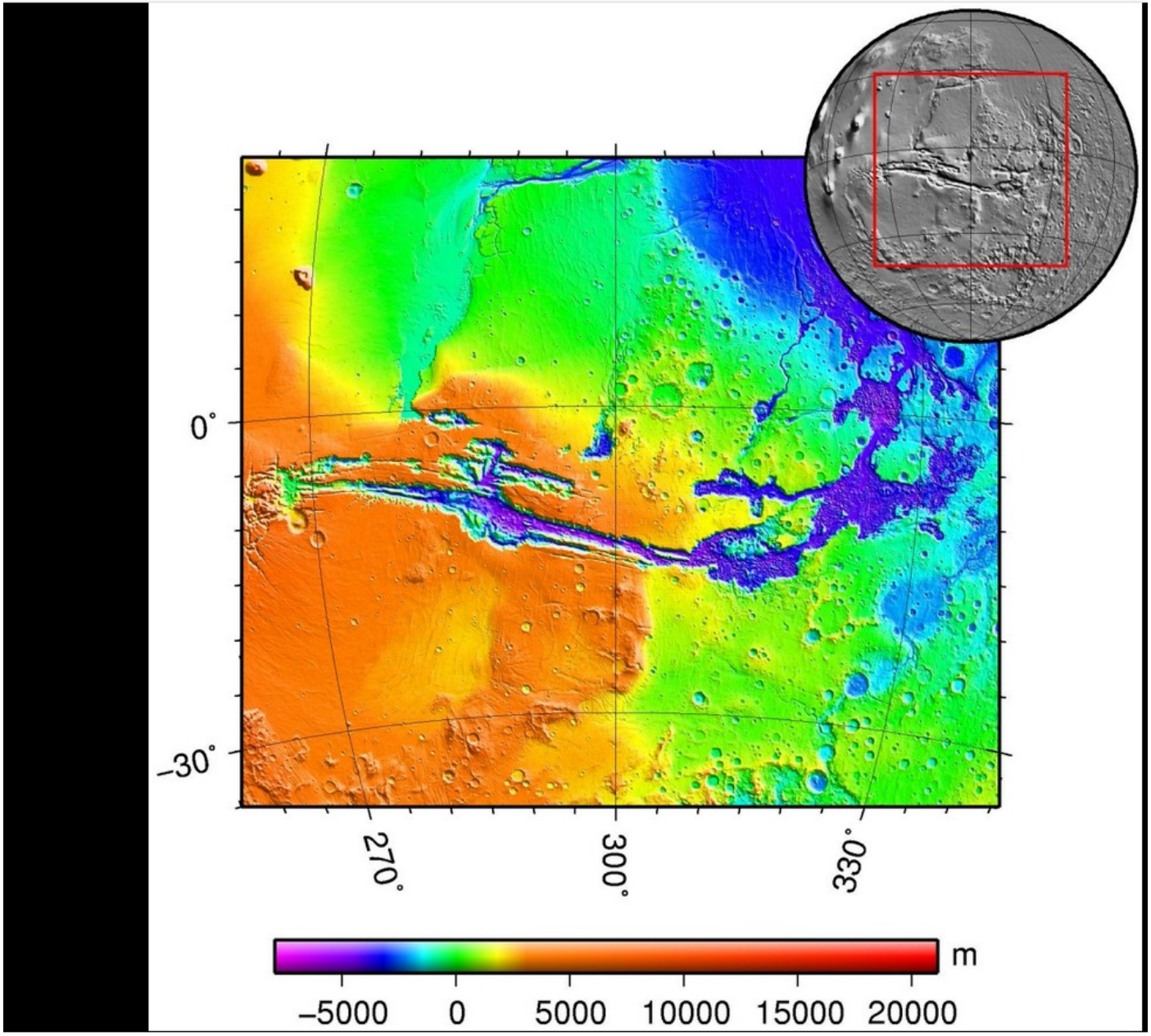

Valles Marineris

Valles Marineris topo

Valles Marineris

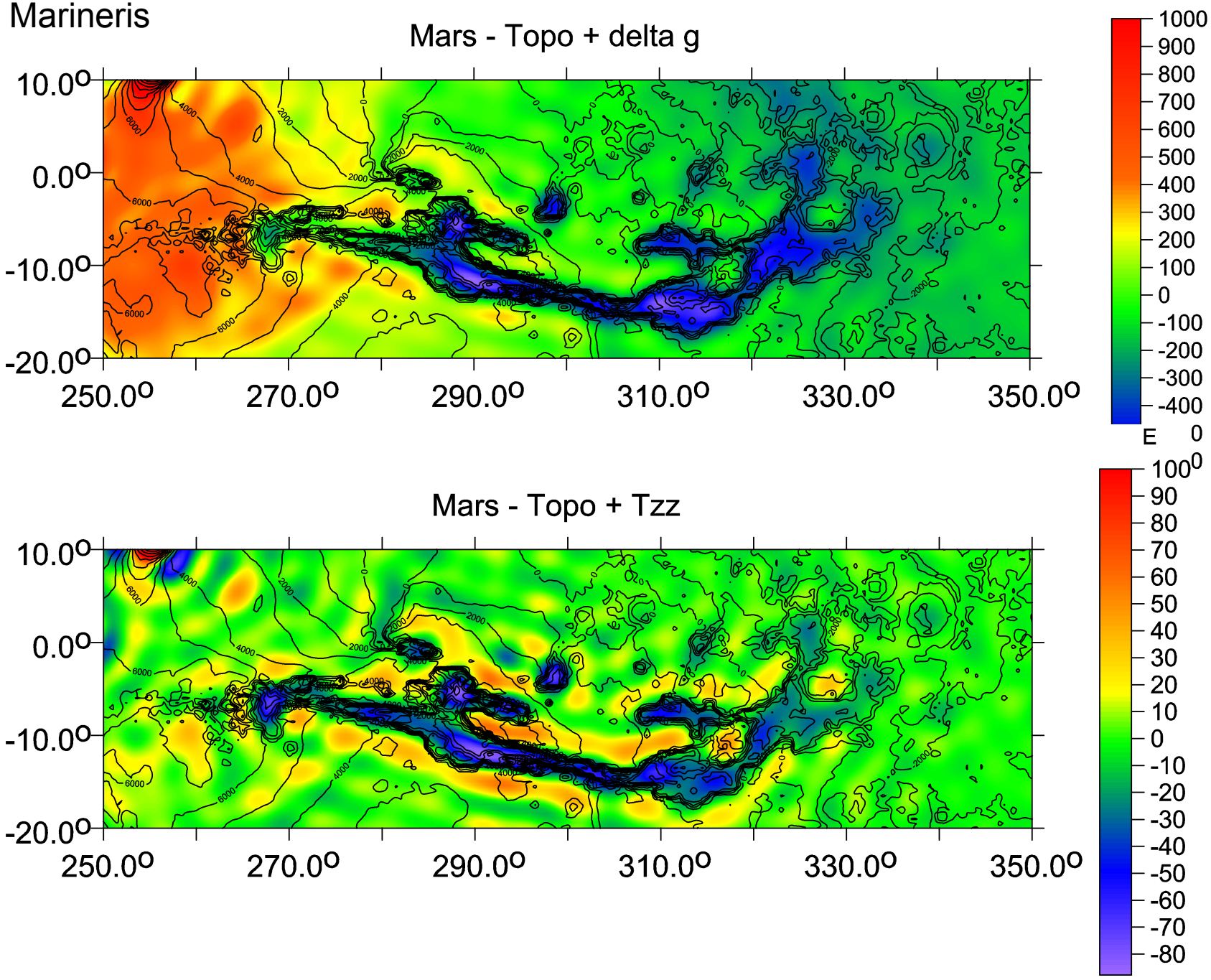

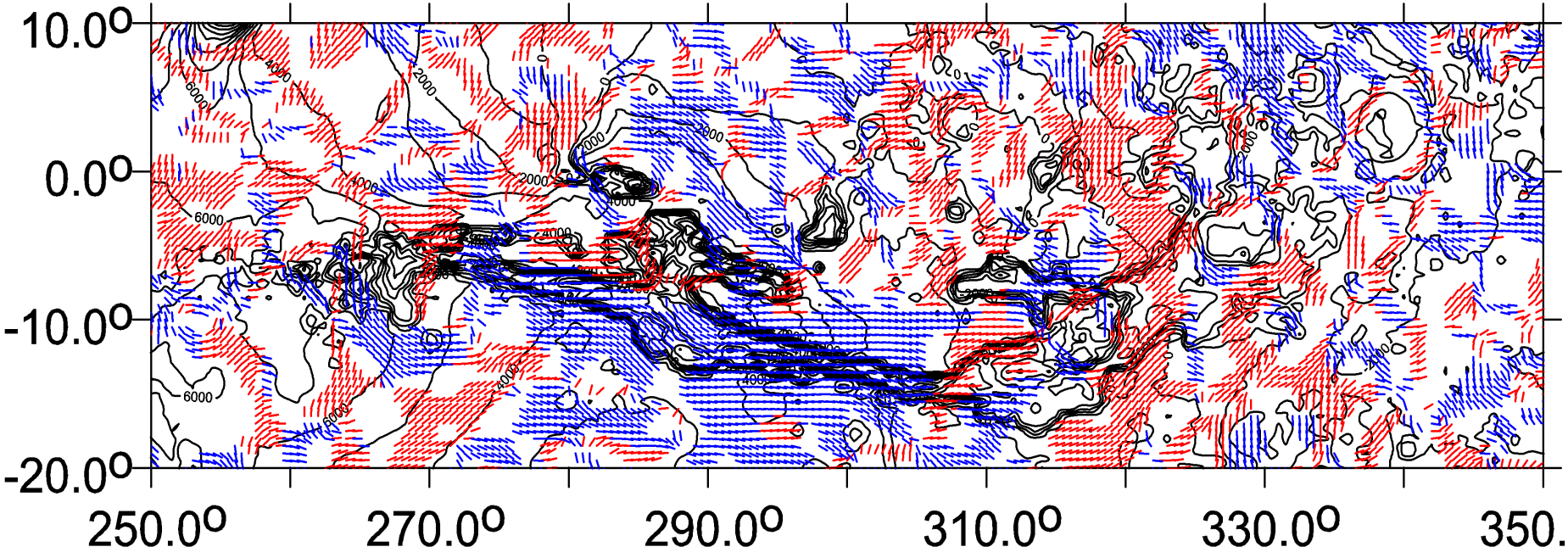
10.0°
0.0°
-10.0°
-20.0°
250.0°
270.0°
290.0°
310.0°
330.0°
350.0°

Isidis Planitia (8.4N, 69.5E) MOLA topo
& Syrtis Major (SM) Planum (black spot) shield volcano

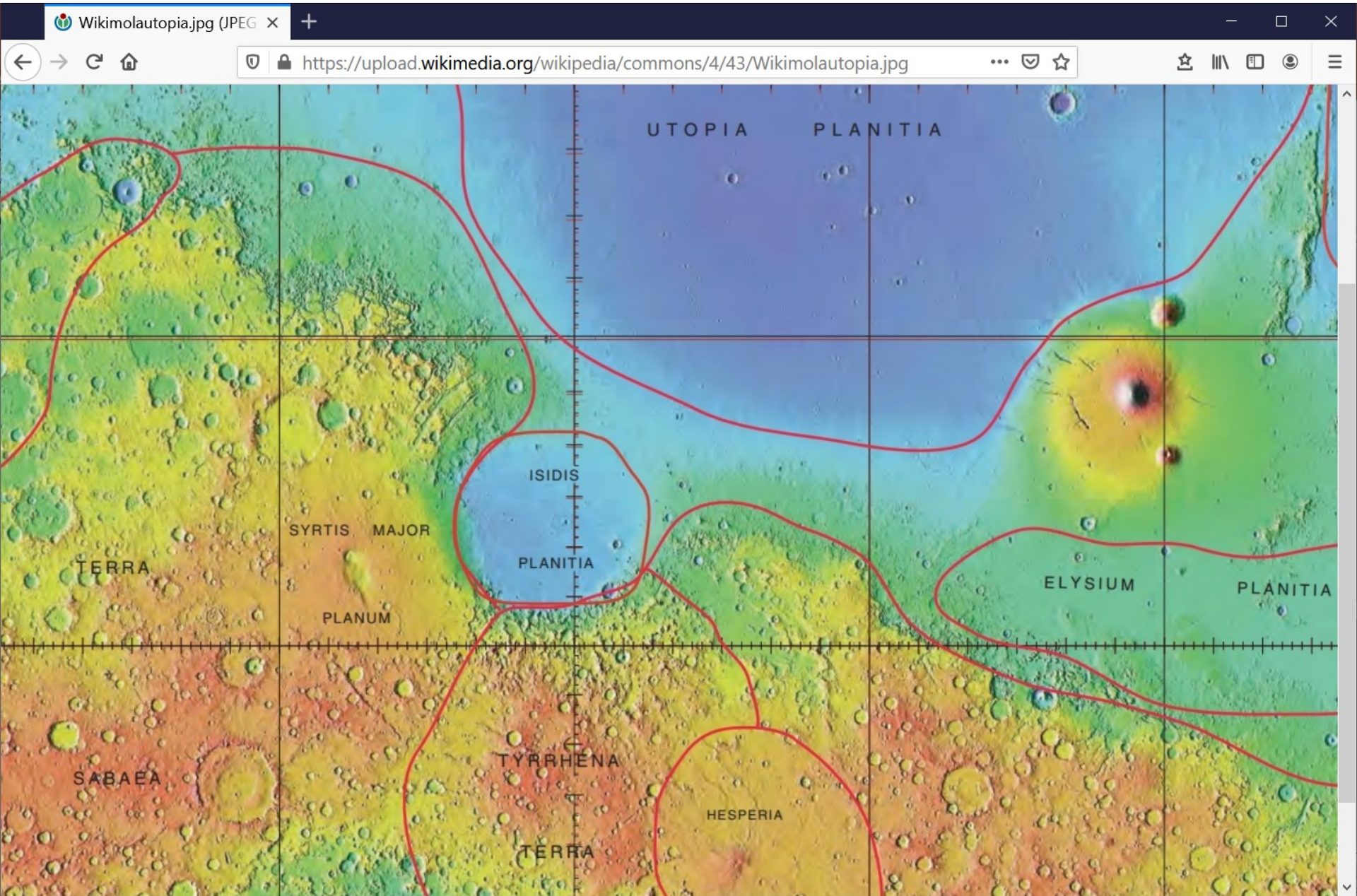

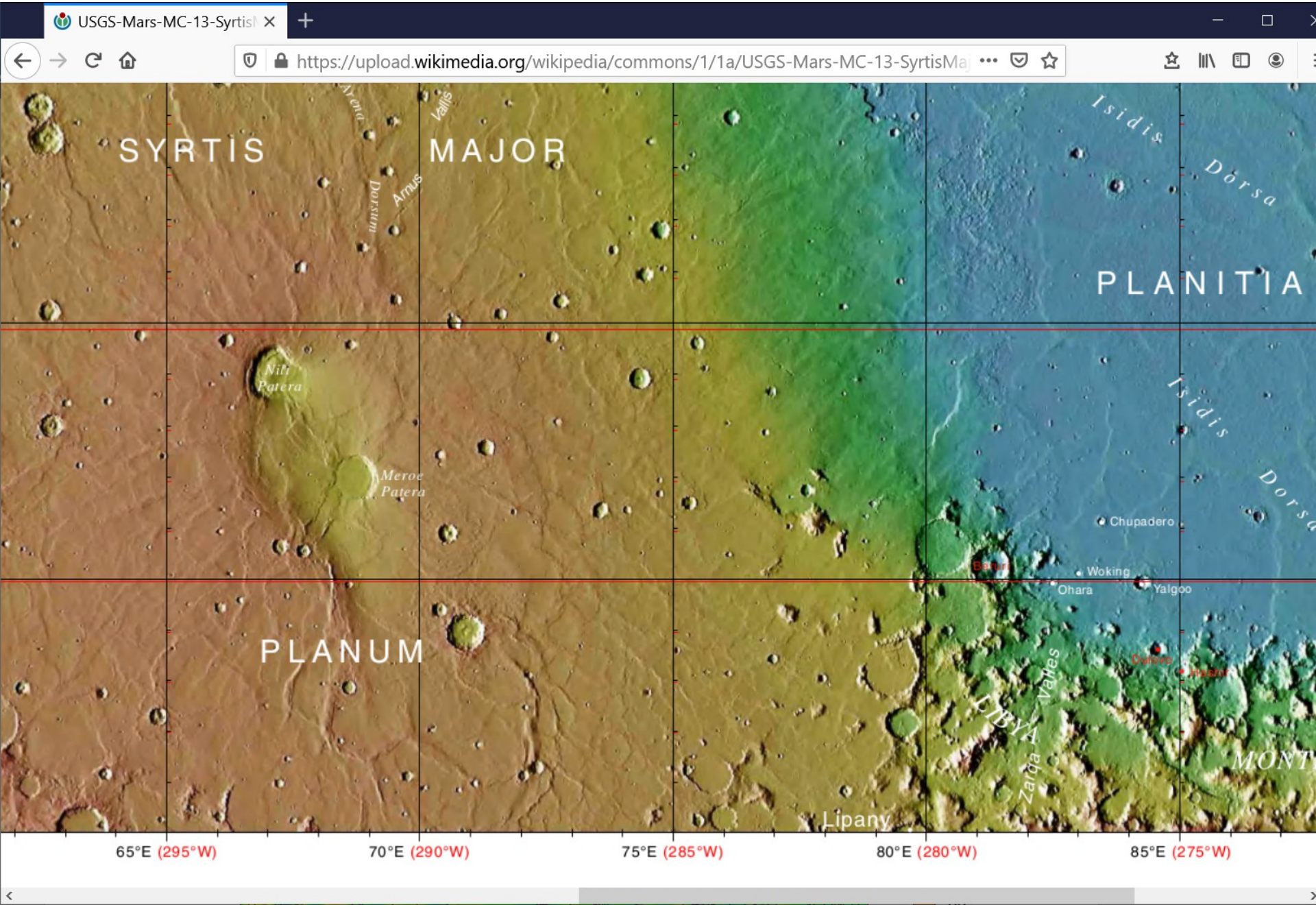
USGS-Mars-MC-13-Syrtis
https://upload.wikimedia.org/wikipedia/commons/1/1a/USGS-Mars-MC-13-SyrtisMa
SYRTIS
MAJOR
Nyctaeus
Vallis
Dorsum
Arnus
Isidis
Dorsa
PLANITIA
Nili
Patera
Meroe
Patera
Isidis
Dorsa
Chupadero
Woking
Ohara
Yalgoo
PLANUM
Zarqa
Valles
LIBYA
MONT
Lipany
65°E (295°W)
70°E (290°W)
75°E (285°W)
80°E (280°W)
85°E (275°W)

ISIDIS = volcano, nothing else

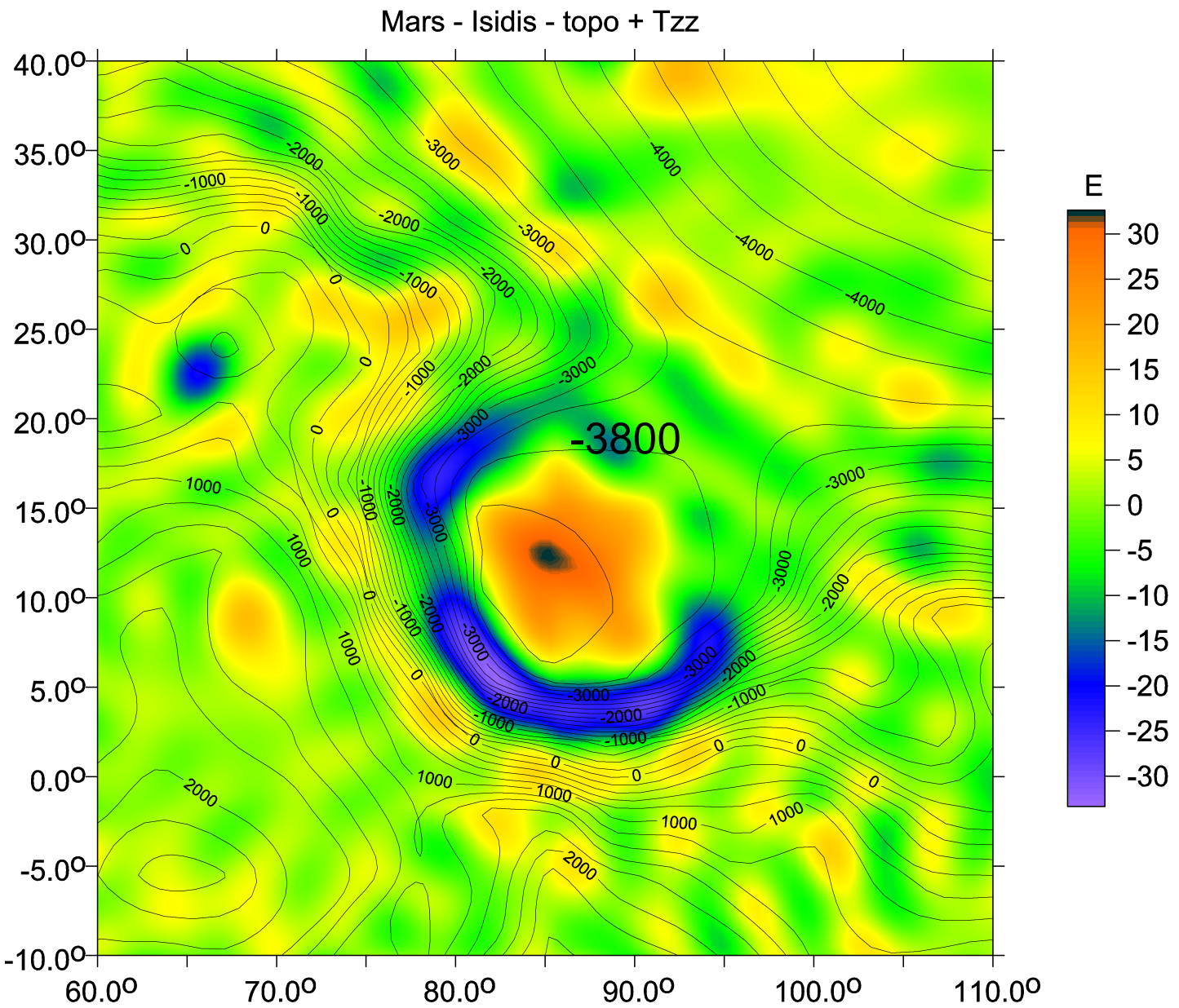

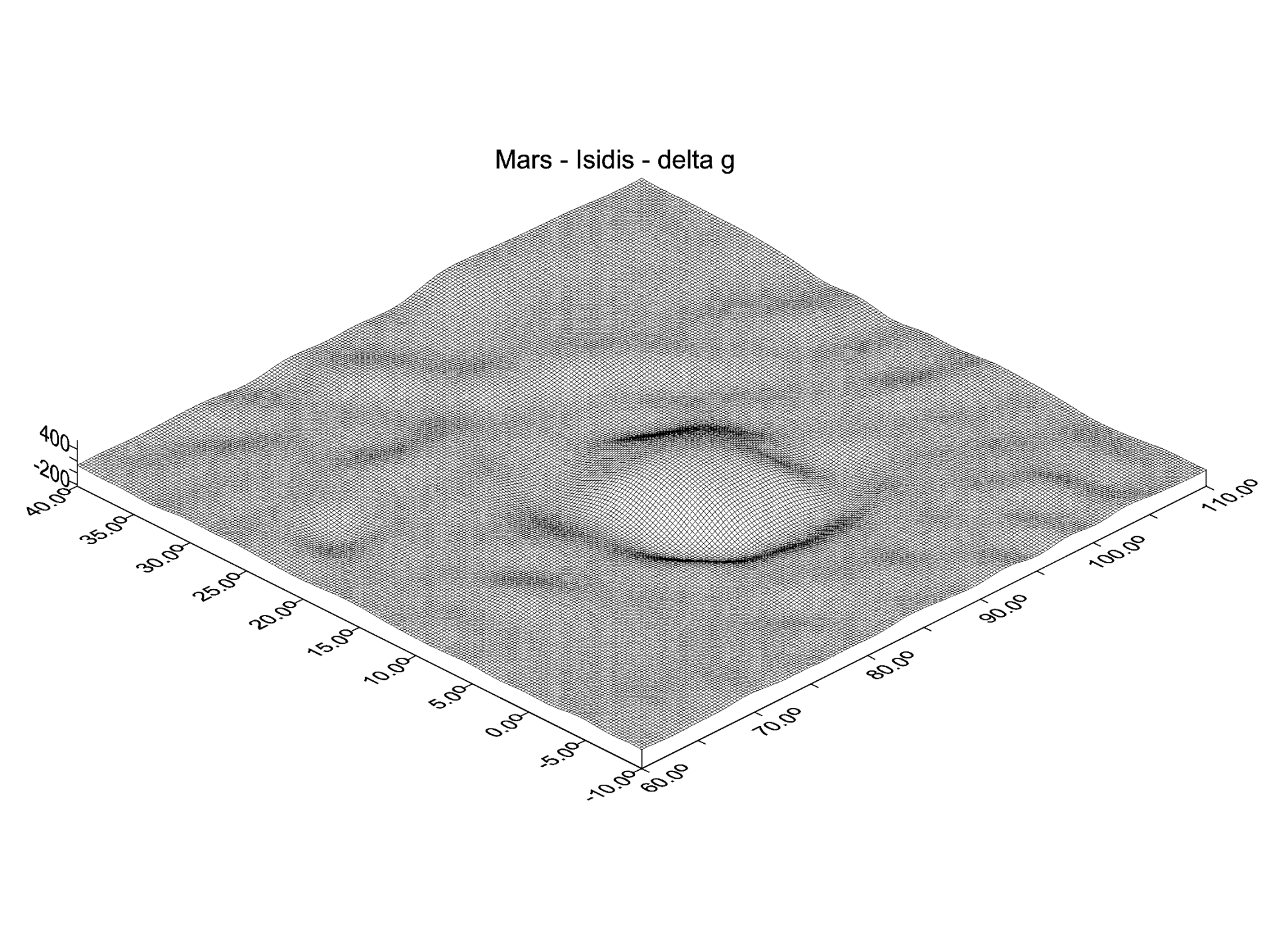
Mars - Isidis - delta g
400
200
40.00
35.00
30.00
25.00
20.00
15.00
10.00
5.00
0.00
-5.00
-10.00
60.00
70.00
80.00
90.00
100.00
110.00

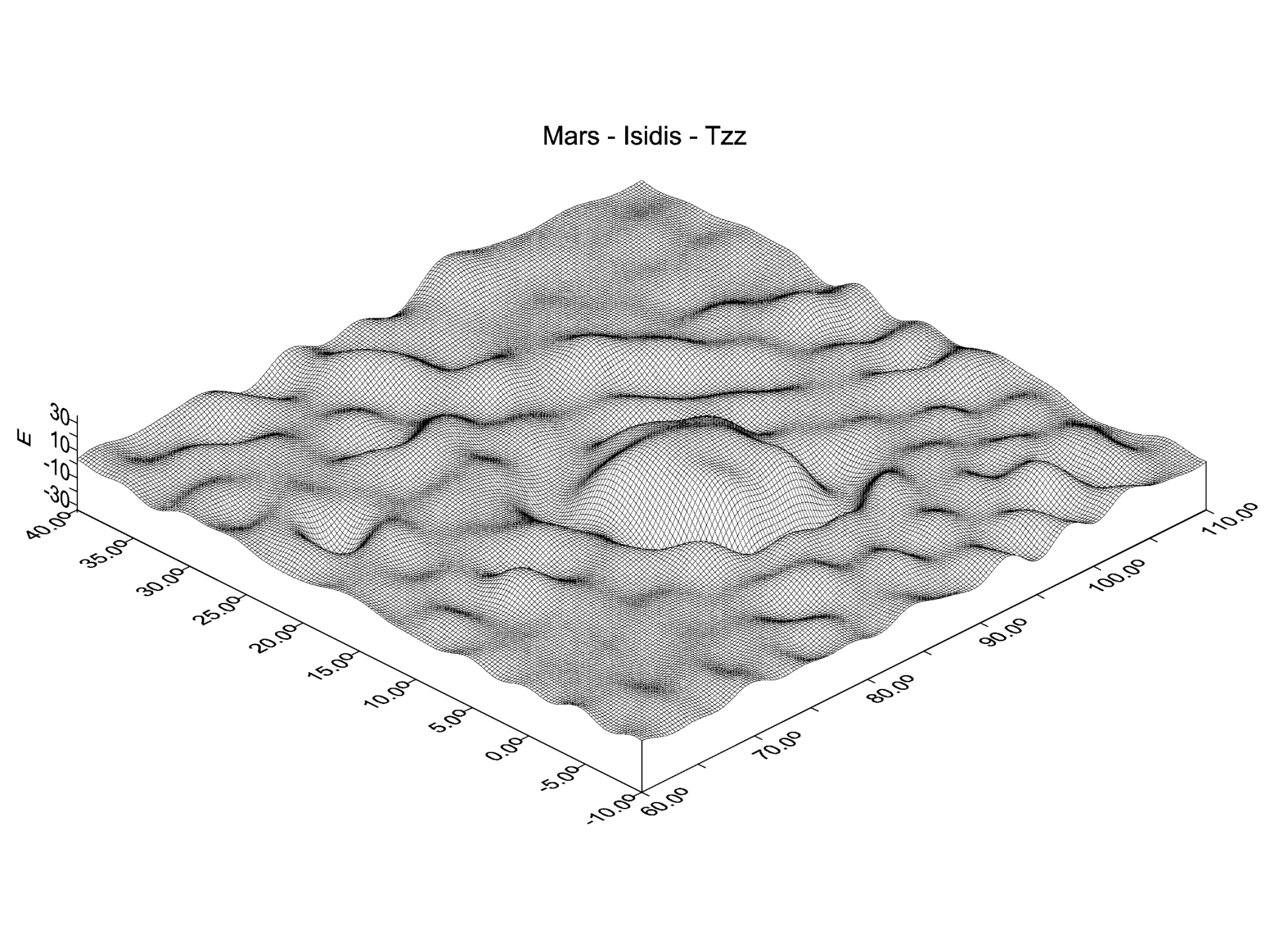
Mars - Isidis - Tzz
E
30
10
-10
-30
40.00
35.00
30.00
25.00
20.00
15.00
10.00
5.00
0.00
-5.00
-10.00
60.00
70.00
80.00
90.00
100.00
110.00

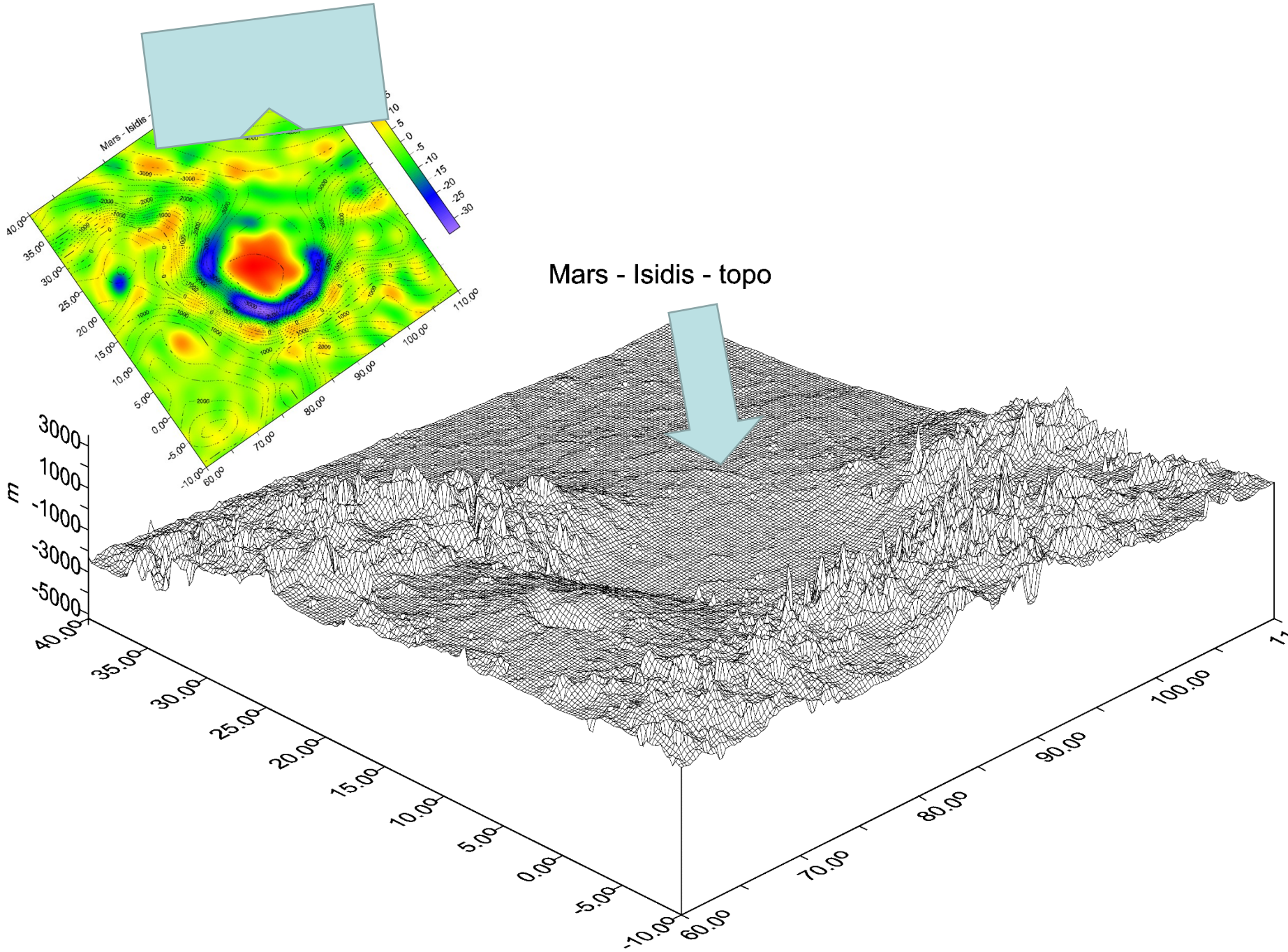
Mars - Isidis - topo
m
3000
1000
-1000
-3000
-5000
40.00
35.00
30.00
25.00
20.00
15.00
10.00
5.00
0.00
-5.00
-10.00
60.00
70.00
80.00
90.00
100.00

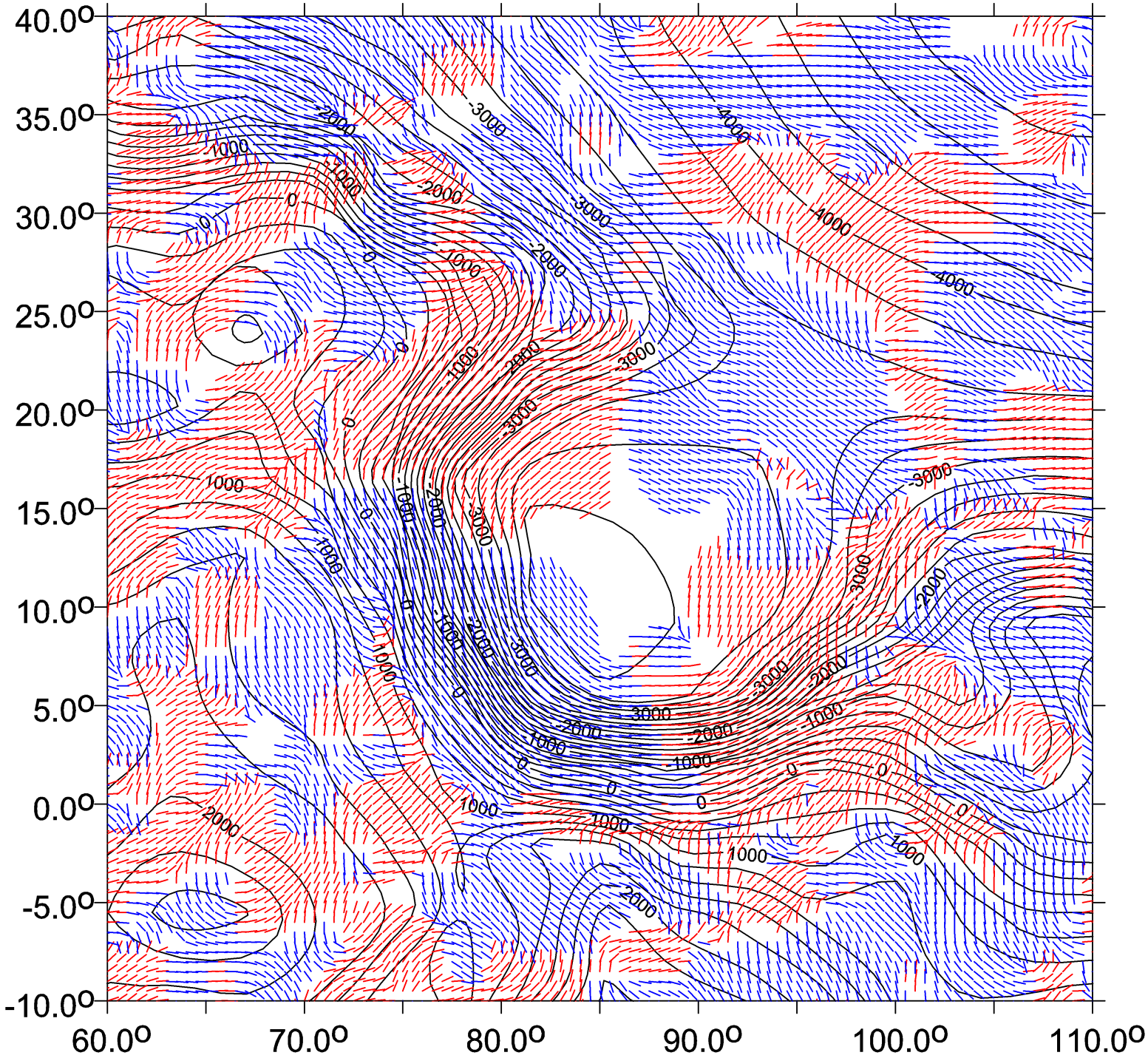
40.0°
35.0°
30.0°
25.0°
20.0°
15.0°
10.0°
5.0°
0.0°
-5.0°
-10.0°
60.0°
70.0°
80.0°
90.0°
100.0°
110.0°

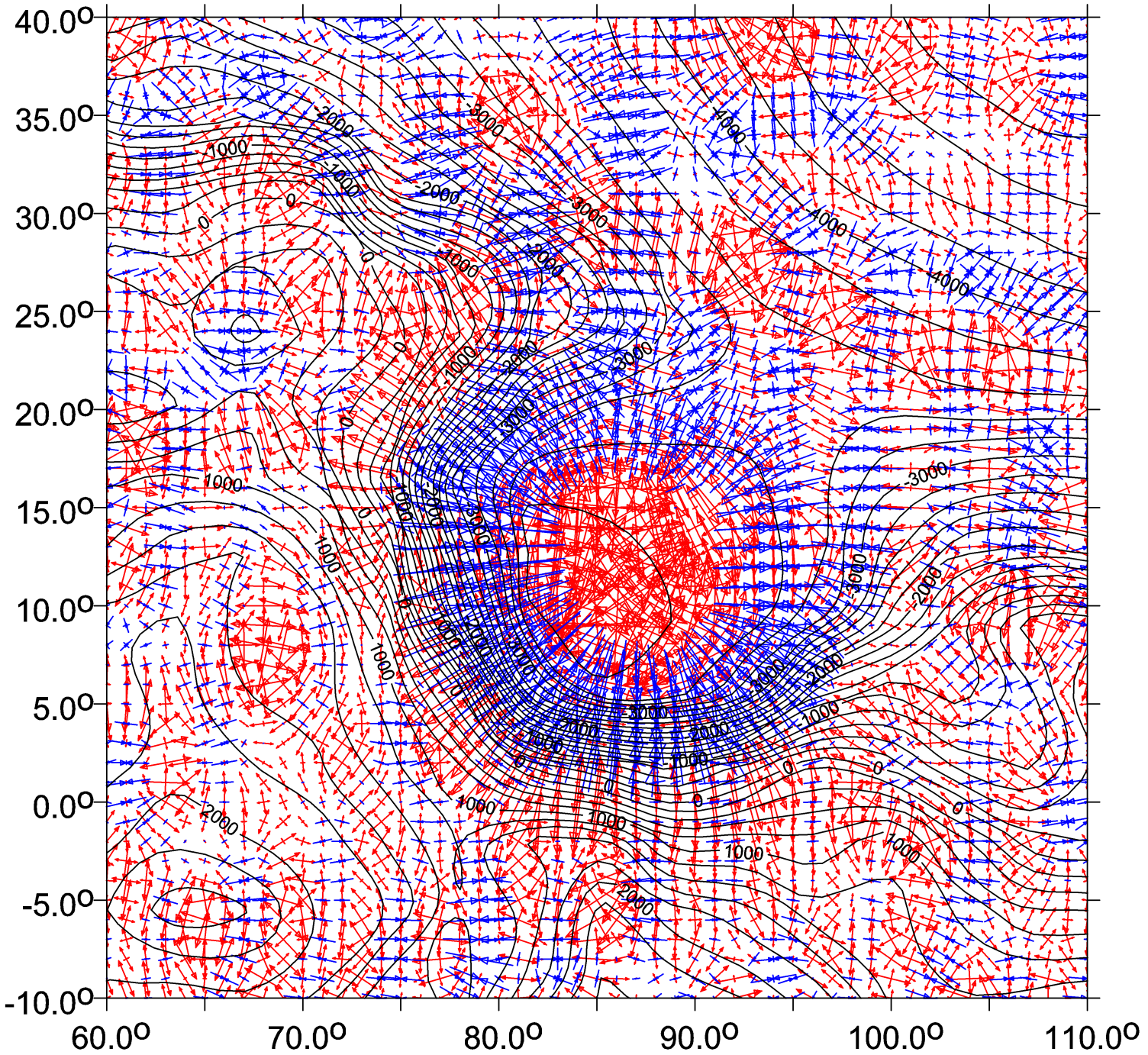
Mars - Isidis - topo + virtual deformations
40.0°
35.0°
30.0°
25.0°
20.0°
15.0°
10.0°
5.0°
0.0°
-5.0°
-10.0°
60.0°
70.0°
80.0°
90.0°
100.0°
110.0°

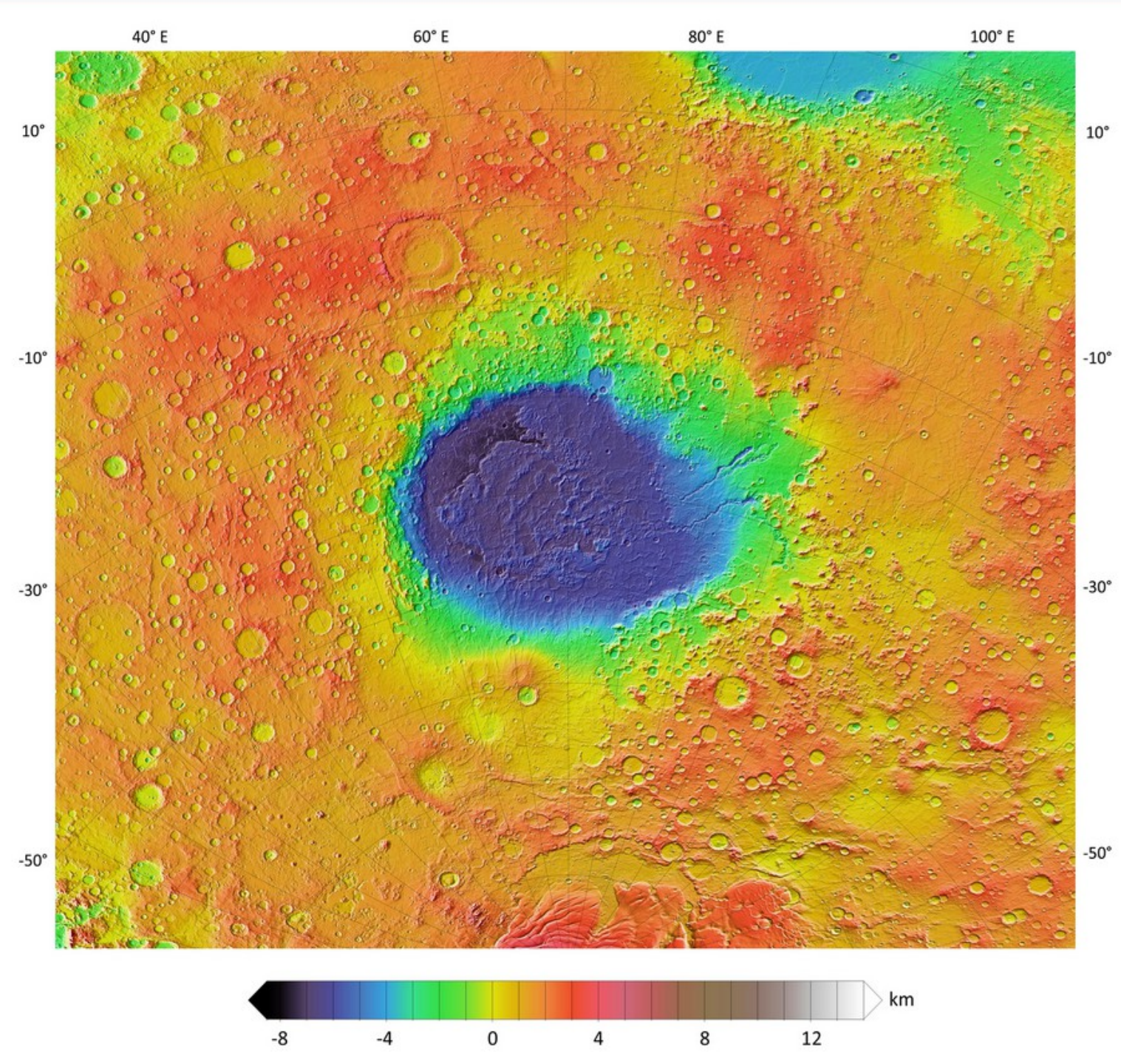

Hellas Planitia *topo*

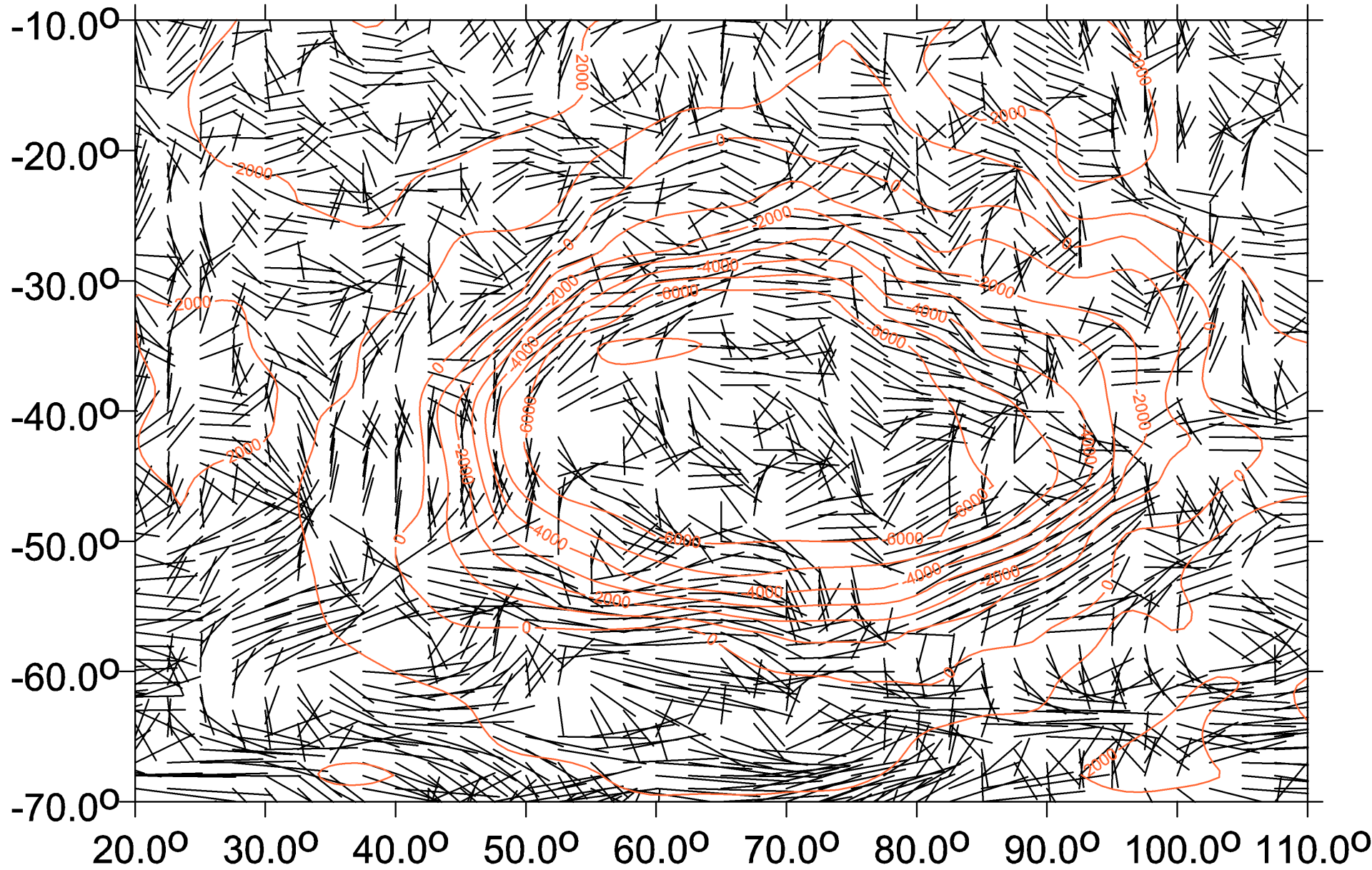
-10.0°
-20.0°
-30.0°
-40.0°
-50.0°
-60.0°
-70.0°
20.0°
30.0°
40.0°
50.0°
60.0°
70.0°
80.0°
90.0°
100.0°
110.0°

dichotomy

Mars dichotomy

The crustal dichotomy of Mars describes the topographic division between the plains in the northern hemisphere and the terrain in the southern hemisphere.
The two hemispheres' geography differ in elevation by 1 to 3 km. The average thickness of the Martian crust is 45 km, with 32 km in the northern lowlands region, and 58 km in the southern highlands.
The boundary between the two regions is quite complex in places. One distinctive type of topography is called **fretted terrain.** It contains mesas, knobs, and flat-floored valleys having walls about a mile high. The Martian dichotomy boundary includes the regions called Deuteronilus Mensae, Protonilus Mensae, and Nilosyrtis Mensae. All three regions have been studied extensively because they contain landforms believed to have been produced by the movement of ice[12][13] or paleoshorelines questioned as formed by volcanic erosion.[14]
The **northern lowlands comprise about one-third of the surface of Mars and are relatively flat,** with as many impact craters as the southern hemisphere.[15] The other two-thirds of the Martian surface are the highlands of the southern hemisphere. The difference in elevation between the hemispheres is dramatic.
Three major hypotheses have been proposed for the origin of the crustal dichotomy: **endogenic (by mantle processes), single impact, or multiple impac**t. Both impact-related hypotheses involve processes that could have occurred before the end of the primordial bombardment, implying that the crustal dichotomy has its origins early in the history of Mars.

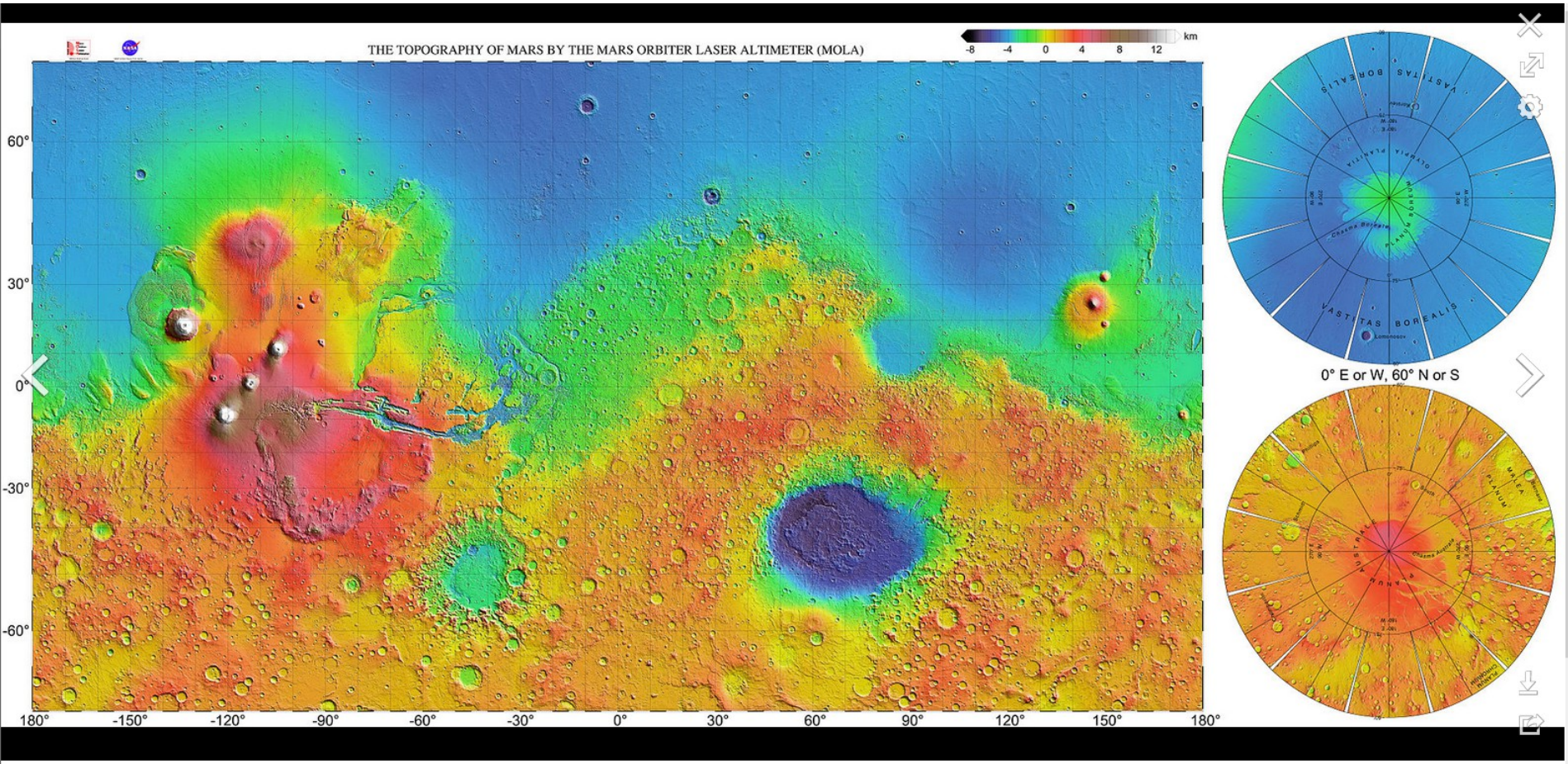

High resolution topographic map of Mars based on the *Mars Global Surveyor* laser altimeter research led by Maria Zuber and David Smith. North is at the top. Notable features include the Tharsis volcanoes in the west (including Olympus Mons), Valles Marineris to the east of Tharsis, and Hellas basin in the southern ...

More details

NASA / JPL / USGS - https://attic.gsfc.nasa.gov/mola/images.html and http://photojournal.jpl.nasa.gov/catalog/PIA02993

Public Domain

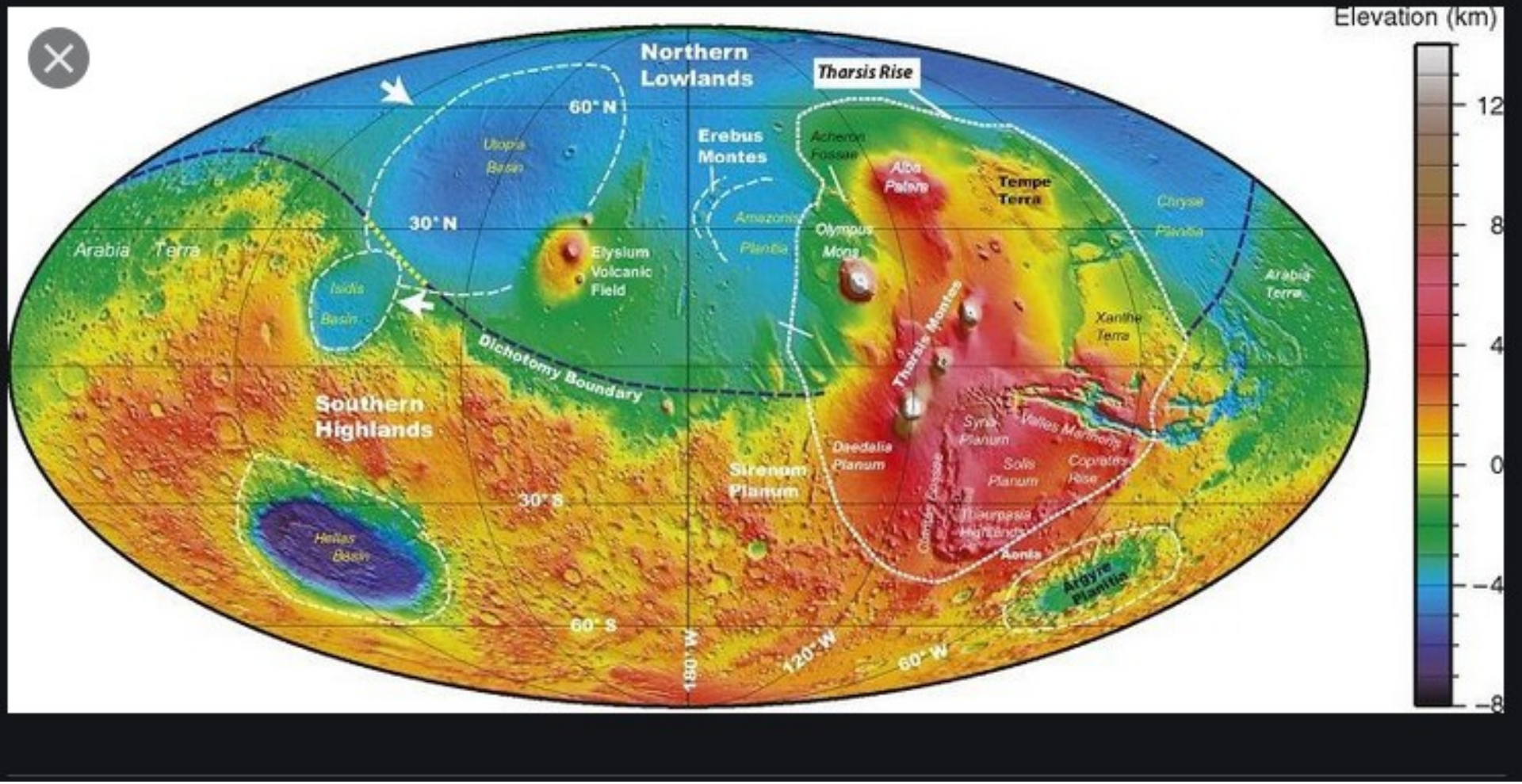
Elevation (km)
12
8
4
0
−4
−8
Northern Lowlands
Tharsis Rise
60° N
30° N
Utopia Basin
Erebus Montes
Acheron Fossae
Alba Patera
Tempe Terra
Chryse Planitia
Amazonis Planitia
Olympus Mons
Arabia Terra
Elysium Volcanic Field
Isidis Basin
Dichotomy Boundary
Xanthe Terra
Tharsis Montes
Southern Highlands
Syria Planum
Valles Marineris
Daedalia Planum
Solis Planum
Coprates Rise
Sirenum Planum
Claritas Fossae
Thaumasia Highlands
Aonia
Argyre Planitia
30° S
Hellas Basin
60° S
180° W
120° W
60° W

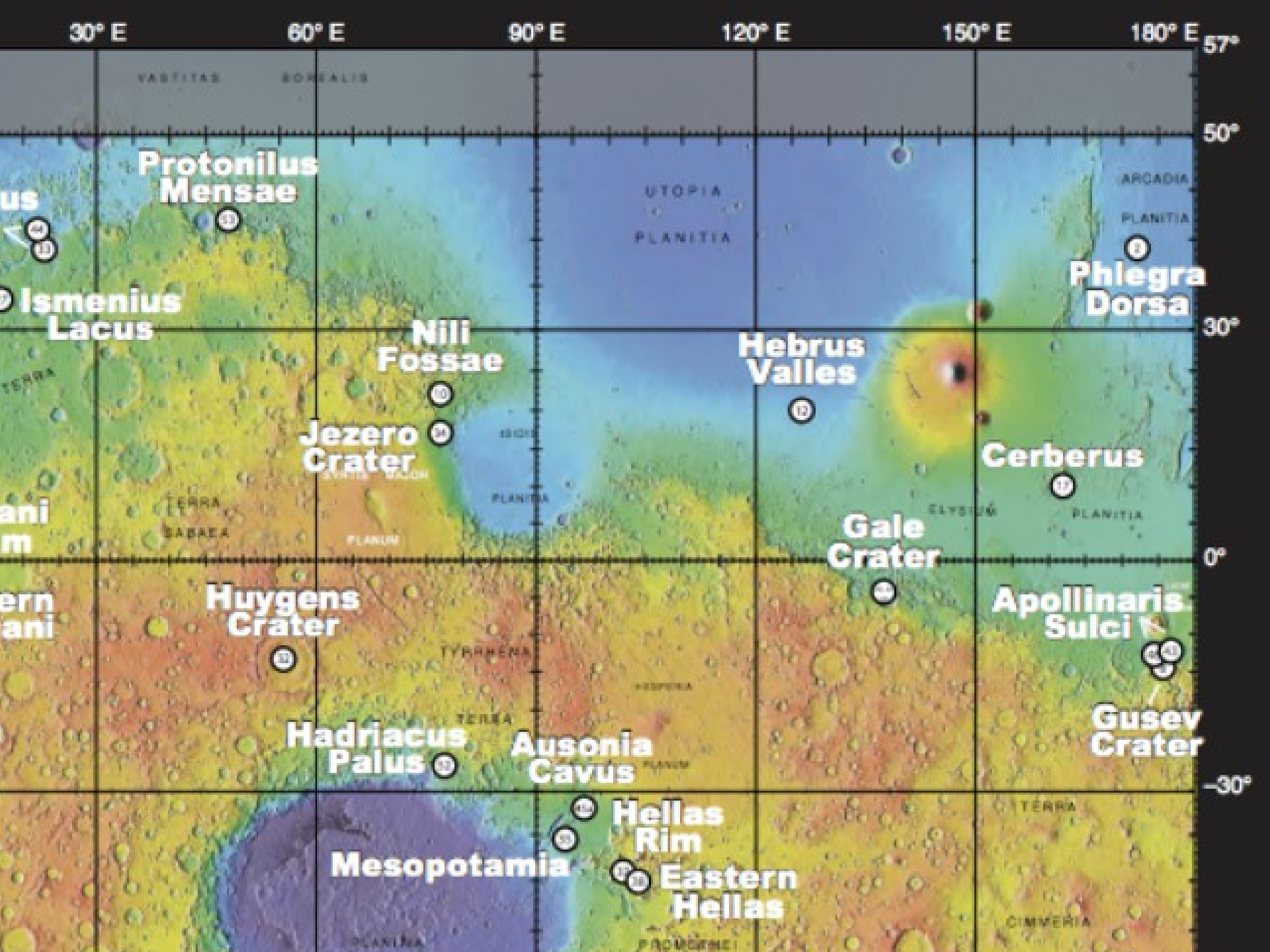
30° E
60° E
90° E
120° E
150° E
180° E
57°
50°
30°
0°
−30°
VASTITAS BOREALIS
UTOPIA PLANITIA
ARCADIA PLANITIA
Protonilus Mensae
Ismenius Lacus
Nili Fossae
Jezero Crater
Hebrus Valles
Phlegra Dorsa
Cerberus
Gale Crater
Huygens Crater
Apollinaris Sulci
Gusev Crater
Hadriacus Palus
Ausonia Cavus
Hellas Rim
Mesopotamia
Eastern Hellas
TERRA SABAEA
TYRRHENA
HESPERIA
CIMMERIA

Fretted terrain Mars

prechodova zona mezi severnimi lowlands a jiznimi highlands

This terrain contains a complicated mix of cliffs, mesas, buttes, and straight-walled and sinuous canyons. It contains smooth, flat lowlands along with steep cliffs. The scarps or cliffs are usually 1 to 2 km high. Channels in the area have wide, flat floors and steep walls. Fretted terrain shows up in northern Arabia, between latitudes 30°N and 50°N and longitudes 270°W and 360°W, and in Aeolis Mensae, between 10 N and 10 S latitude and 240 W and 210 W longitude.Two good examples of fretted terrain are Deuteronilus Mensae and Protonilus Mensae.

Name	centered at latitude	longitude E	range latitudes	longitudes
Arabia Terra Ar	21N	6	large area	
Aeolis Mensae Ae	3S	140	10N-10S	210-240W
Deuteronilus Mensae D	44N	22	40N-48N	325-344W
Protonilus Mensae P	44N	50	40N-47N	37-60E
Nilosyrtis Mensae N	37N	68	30N-37N	51-75E
Nanedi Vallis (Lunae Palus) NV	5N	311		
Meridiani Planus MP	0N	358		
Gusev crater G	15S	175		

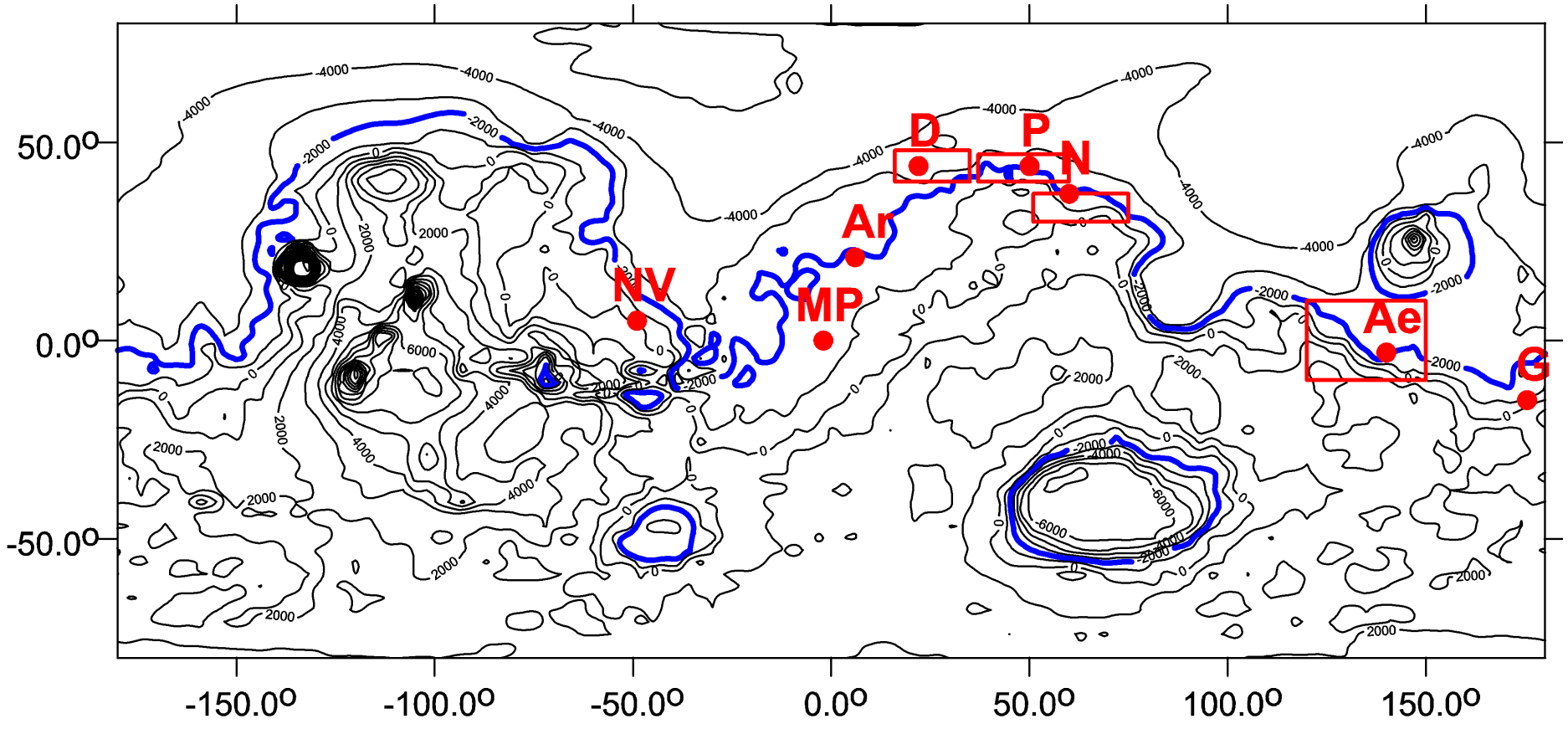
Mars - Topo + oblasti
50.0°
0.0°
-50.0°
-150.0°
-100.0°
-50.0°
0.0°
50.0°
100.0°
150.0°
D
P
N
Ar
NV
MP
Ae
G

Aeolis Mensae

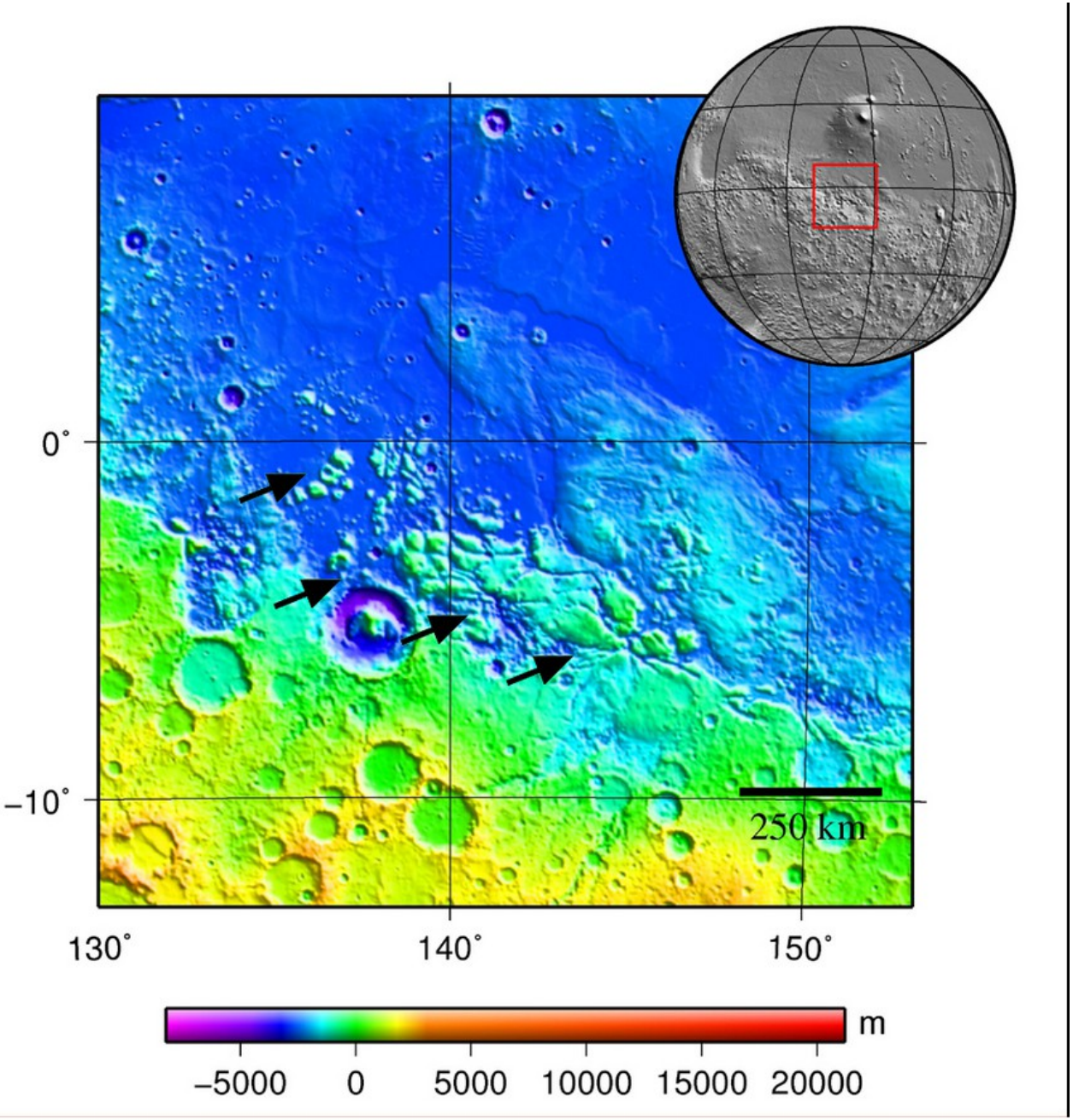

Aeolis Mensae 3S 220W

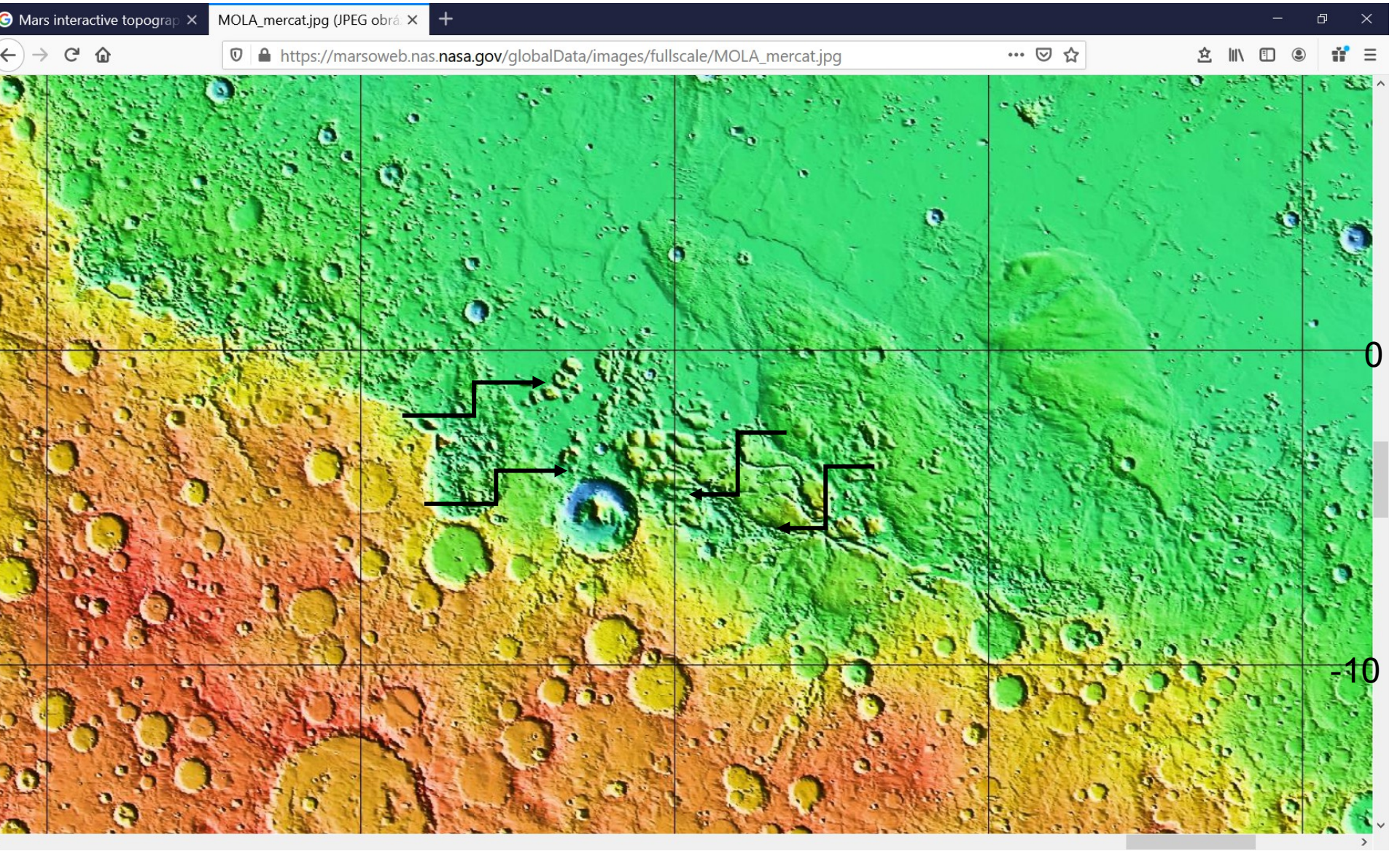

220W

Nilosyrtis Mensae is an area of Mars in the Casius quadrangle. It is centered on the coordinates of 36.87° N and 67.9° E. Its western and eastern longitudes are 51.1° E and 74.4° E. North and south latitudes are 36.87° N and 29.61° N.[2] Nilosyrtis Mensae is just to the east of Protonilus Mensae and both lie along the Martian dichotomy boundary

36.87°N 67.9°E
Coordinates of centre

Perseverance landing site (18N, 70E), Lake Crater, wet and dry zone

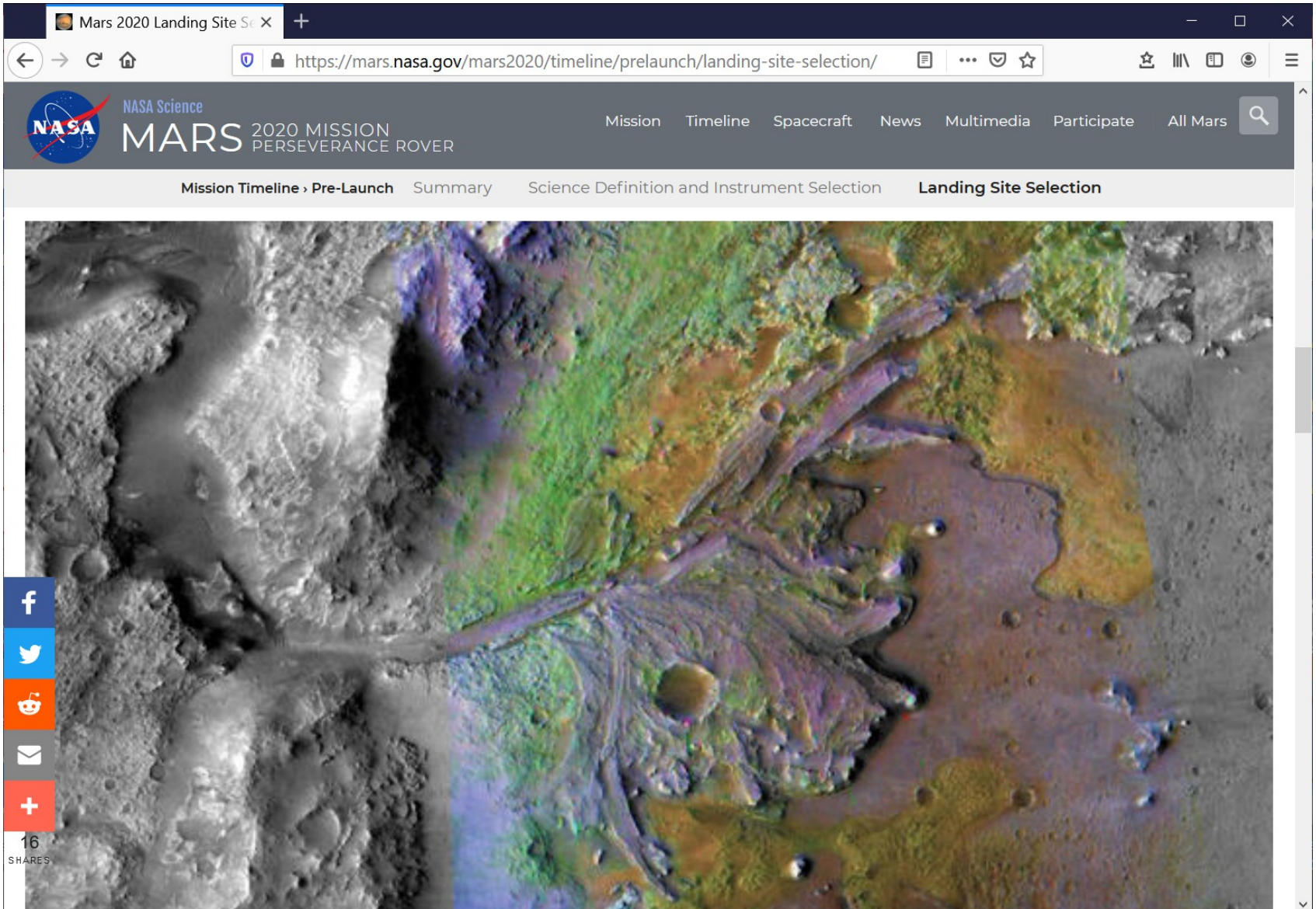

Our main results

Northern paleoocean

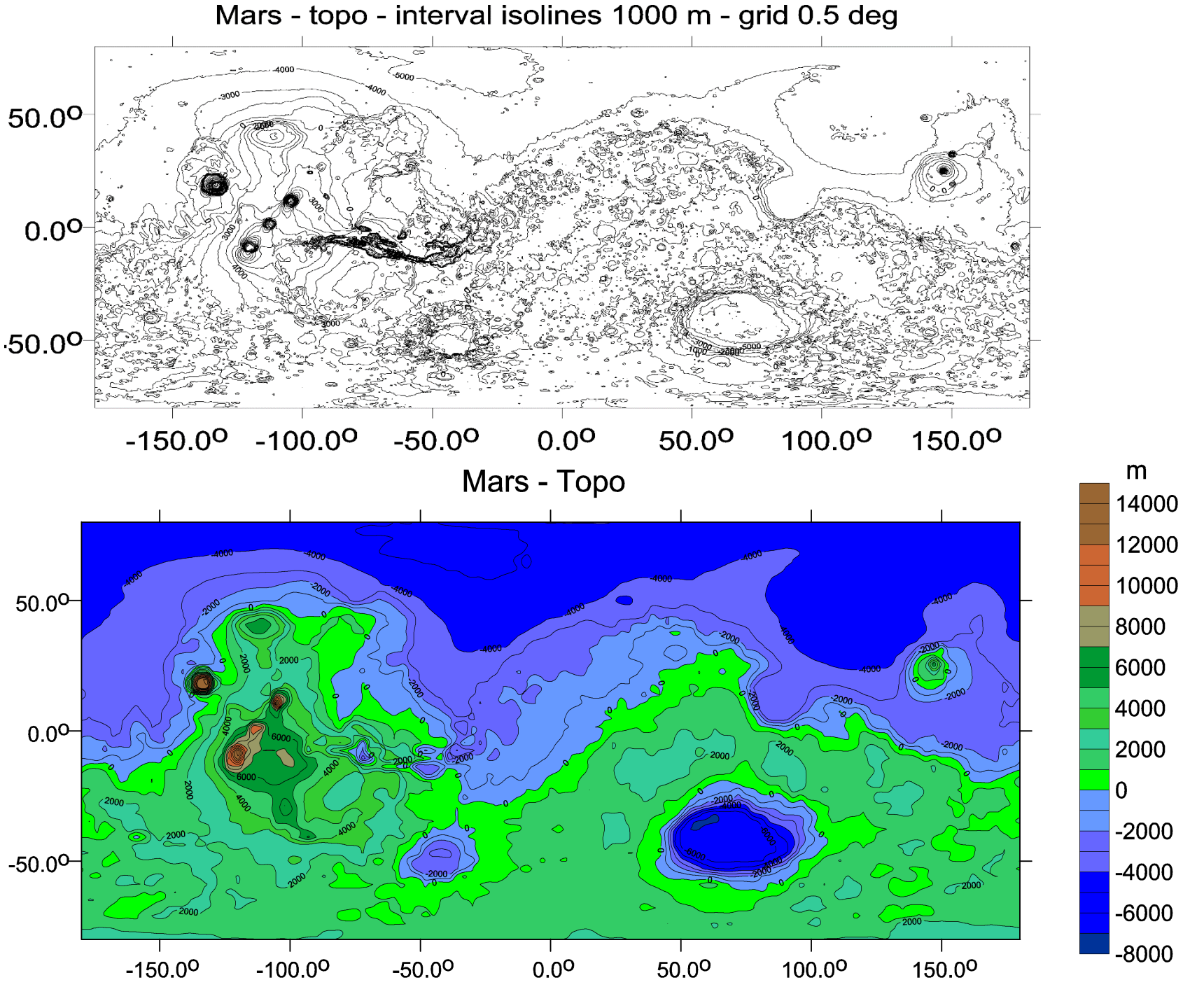
Mars - topo - interval isolines 1000 m - grid 0.5 deg
50.0°
0.0°
-50.0°
-150.0°
-100.0°
-50.0°
0.0°
50.0°
100.0°
150.0°
Mars - Topo
m
14000
12000
10000
8000
6000
4000
2000
0
-2000
-4000
-6000
-8000

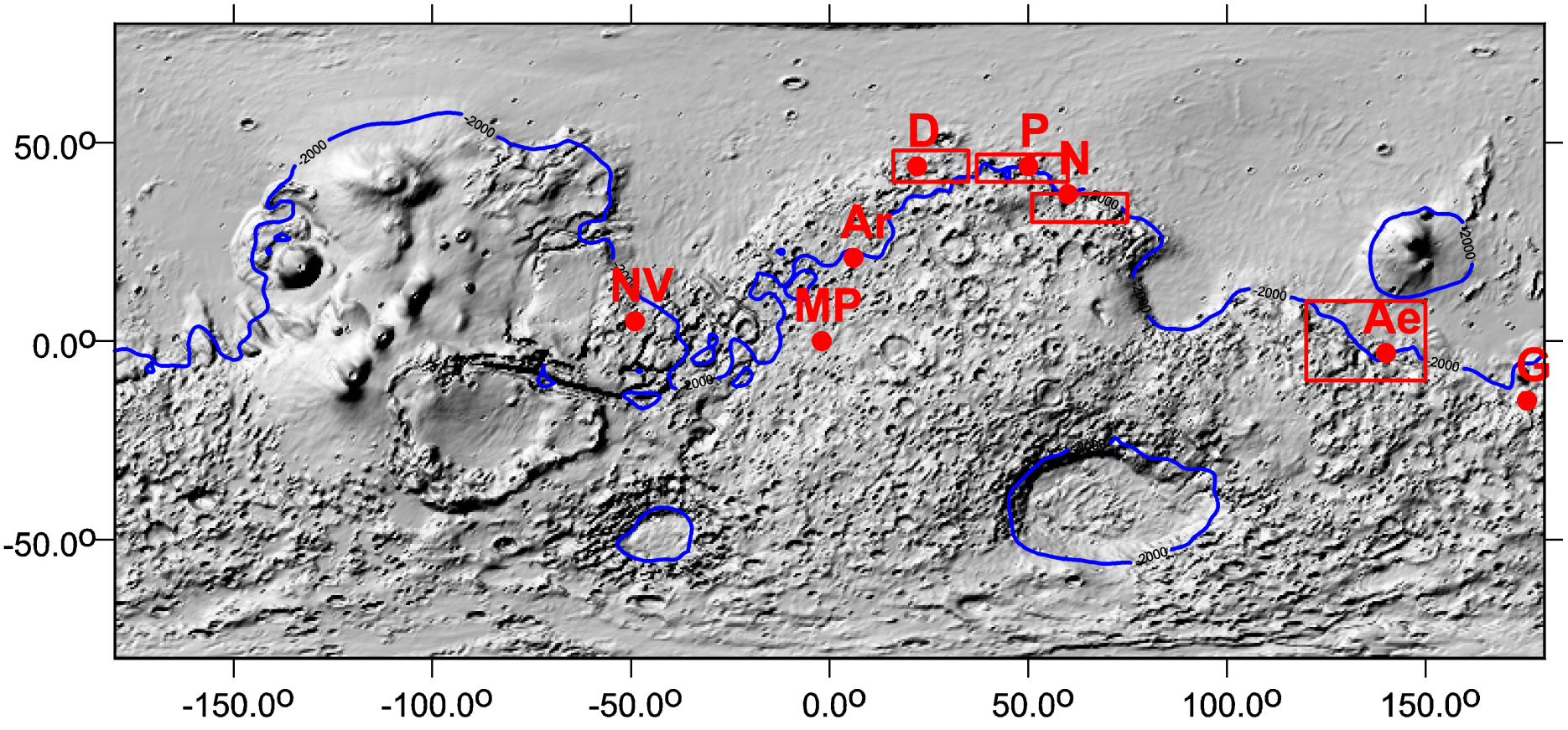
Mars - Topo + oblasti
50.0°
0.0°
-50.0°
-150.0°
-100.0°
-50.0°
0.0°
50.0°
100.0°
150.0°
D
P
N
Ar
NV
MP
Ae
G
-2000

Strike angles with the comb factor to emphasize highly combed areas / potential water

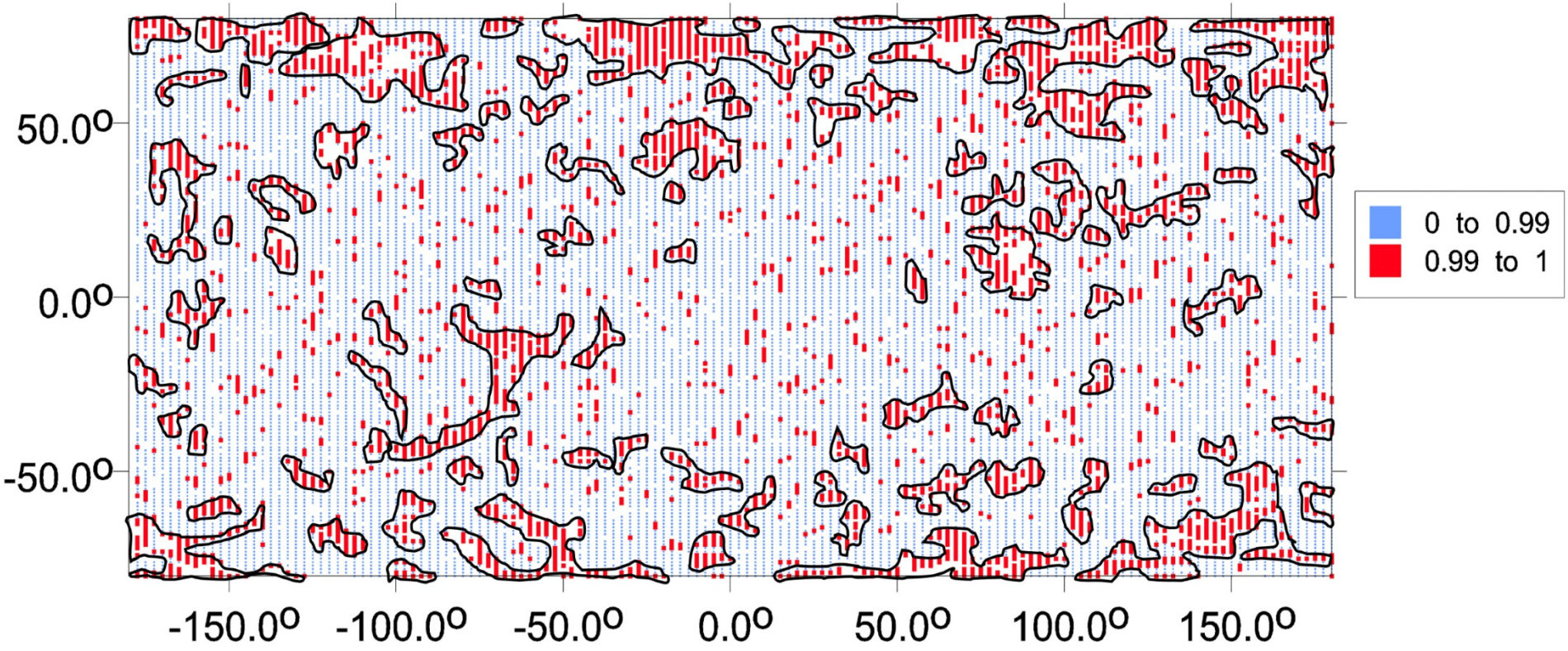

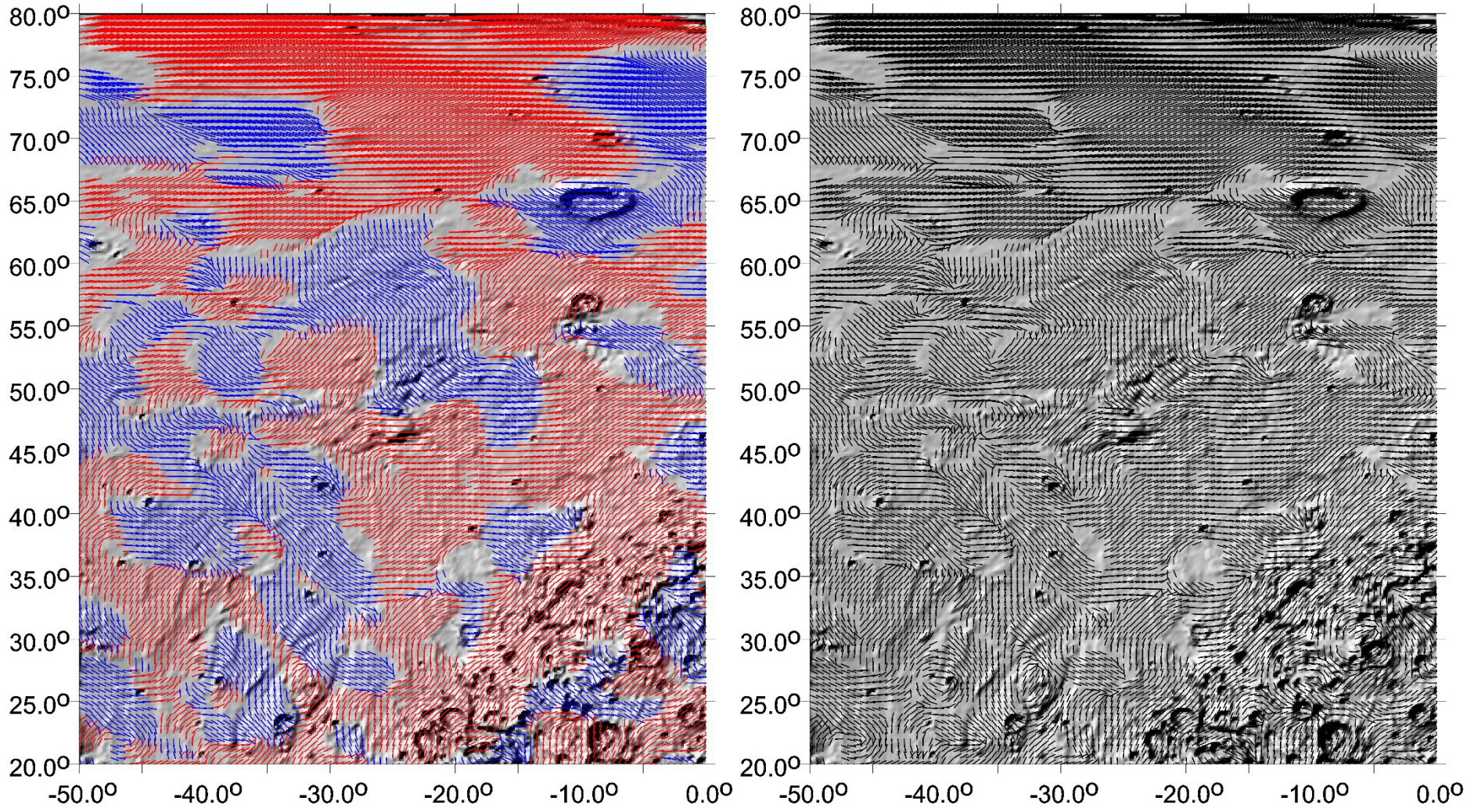
80.0°
75.0°
70.0°
65.0°
60.0°
55.0°
50.0°
45.0°
40.0°
35.0°
30.0°
25.0°
20.0°
-50.0°
-40.0°
-30.0°
-20.0°
-10.0°
0.0°

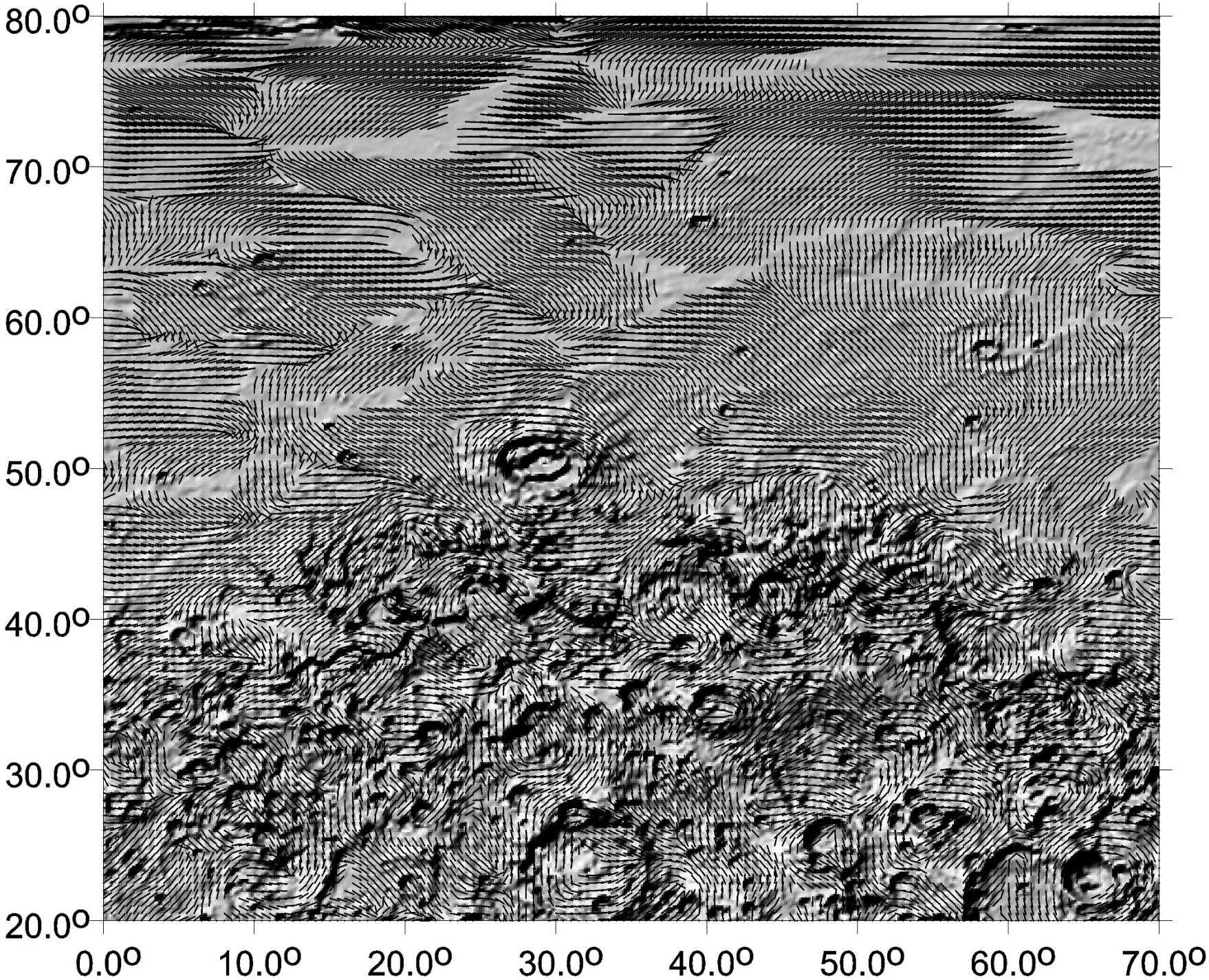
80.0°
70.0°
60.0°
50.0°
40.0°
30.0°
20.0°
0.0°
10.0°
20.0°
30.0°
40.0°
50.0°
60.0°
70.0°

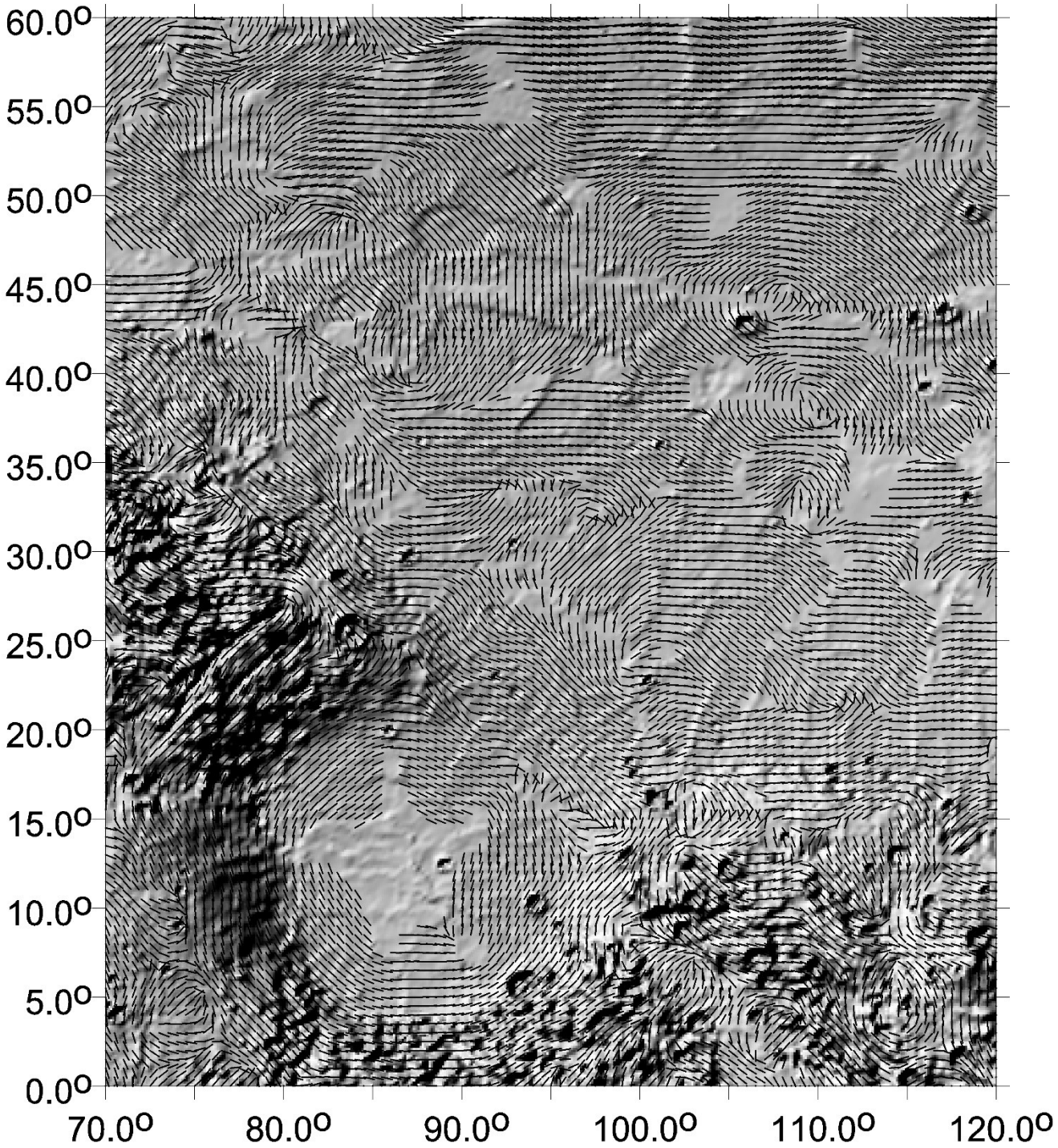
60.0°
55.0°
50.0°
45.0°
40.0°
35.0°
30.0°
25.0°
20.0°
15.0°
10.0°
5.0°
0.0°
70.0°
80.0°
90.0°
100.0°
110.0°
120.0°

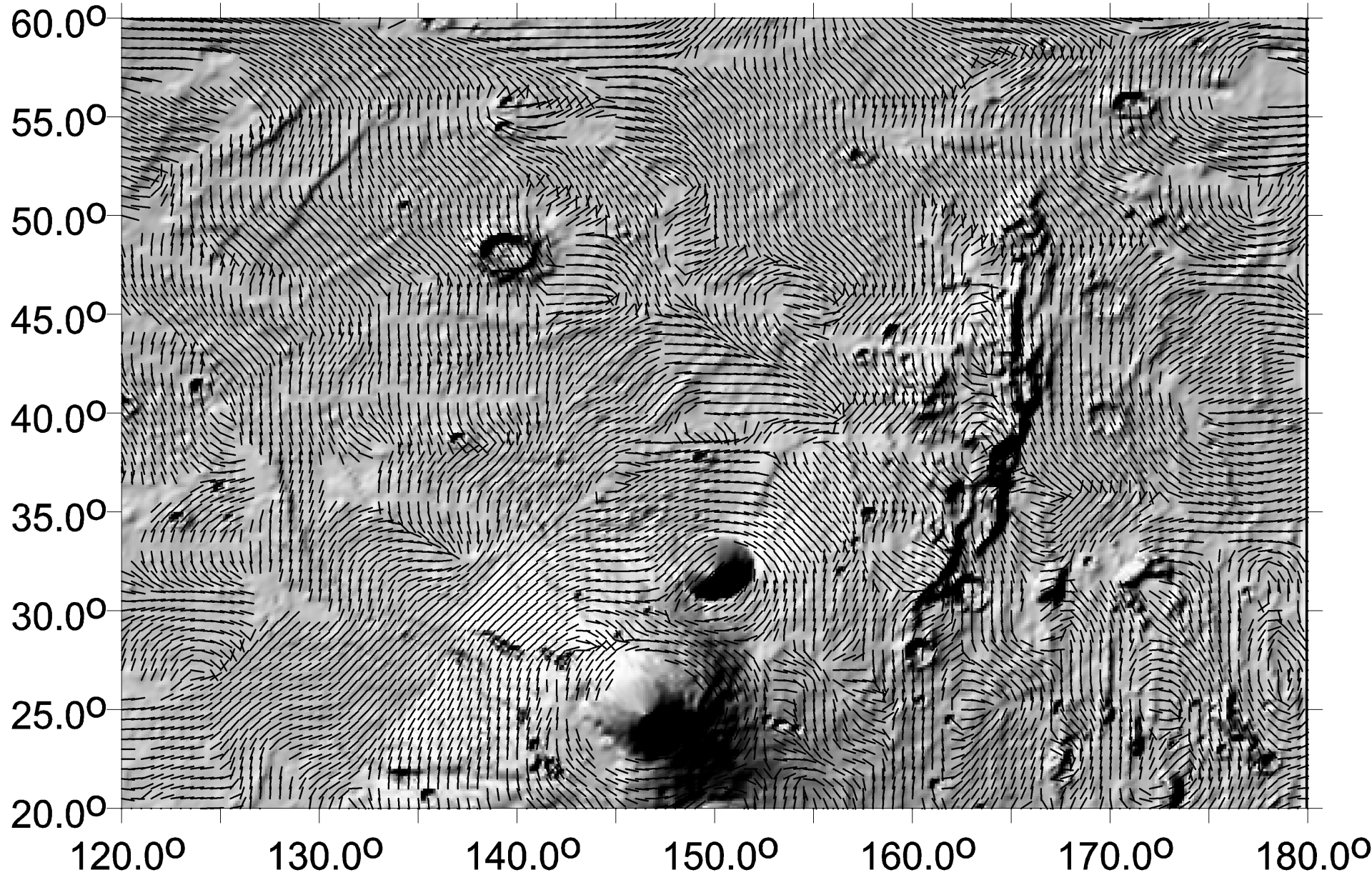
60.0°
55.0°
50.0°
45.0°
40.0°
35.0°
30.0°
25.0°
20.0°
120.0°
130.0°
140.0°
150.0°
160.0°
170.0°
180.0°

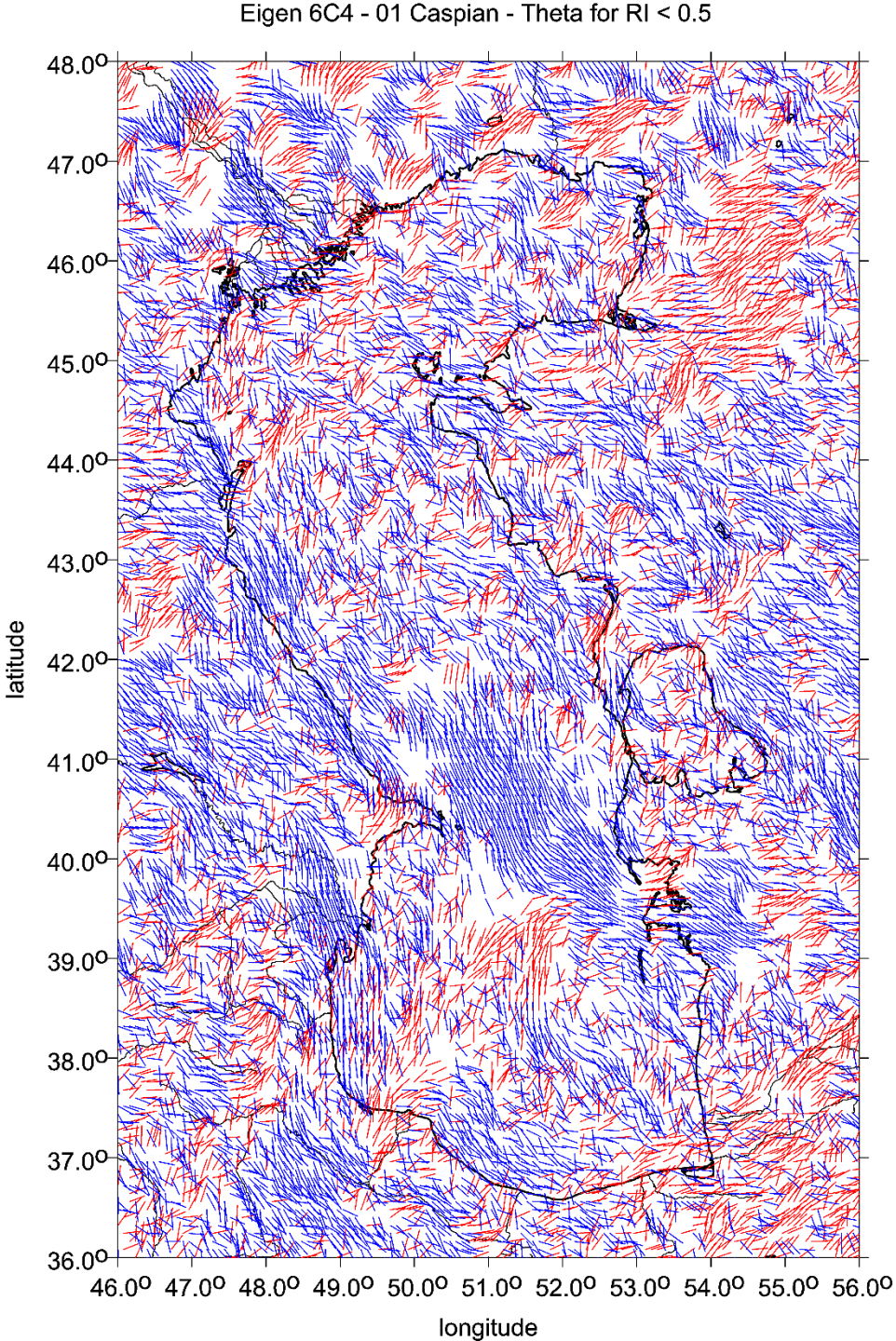
Eigen 6C4 - 01 Caspian - Theta for RI < 0.5
48.0°
47.0°
46.0°
45.0°
44.0°
43.0°
42.0°
41.0°
40.0°
39.0°
38.0°
37.0°
36.0°
latitude
46.0° 47.0° 48.0° 49.0° 50.0° 51.0° 52.0° 53.0° 54.0° 55.0° 56.0°
longitude

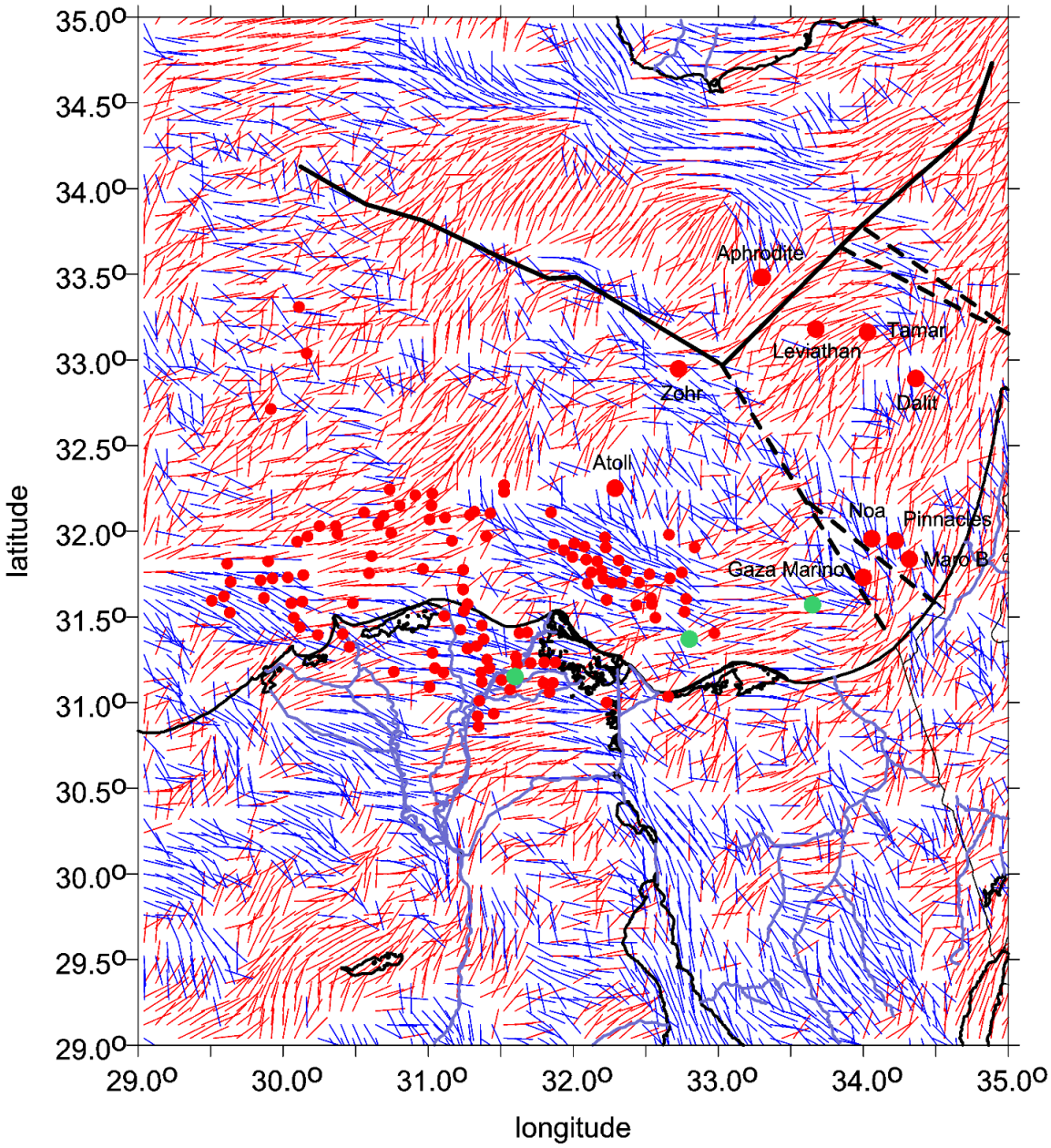
Eigen 6C4 - Egypt - Theta for RI < 0.9 - opr
and sources of GAS and Oil
Aphrodite
Tamar
Leviathan
Zohr
Dalit
Atoll
Noa
Pinnacles
Mary B
Gaza Marine
35.0°
34.5°
34.0°
33.5°
33.0°
32.5°
32.0°
31.5°
31.0°
30.5°
30.0°
29.5°
29.0°
latitude
29.0°
30.0°
31.0°
32.0°
33.0°
34.0°
35.0°
longitude

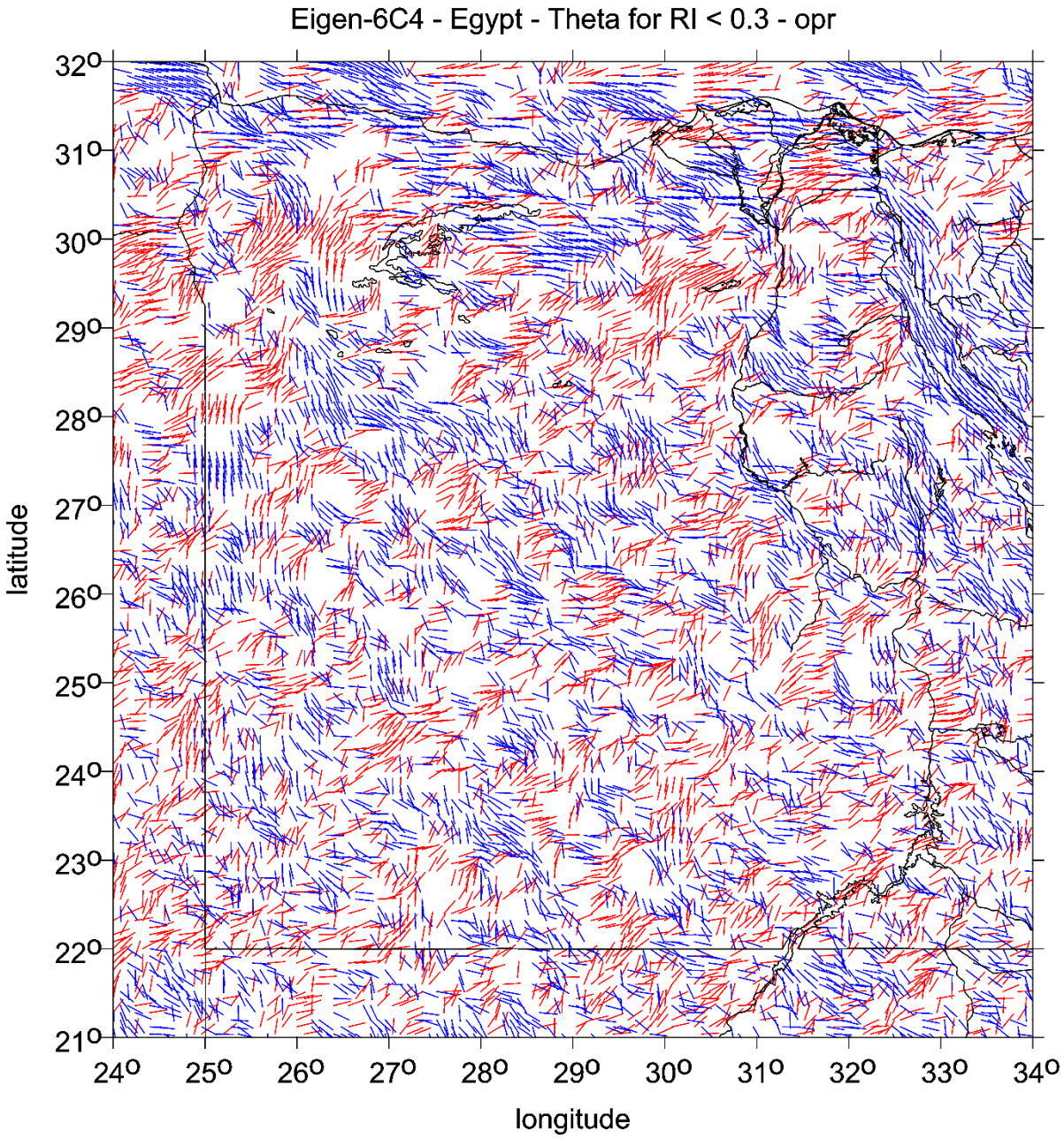
Eigen-6C4 - Egypt - Theta for RI < 0.3 - opr
32°
31°
30°
29°
28°
27°
26°
25°
24°
23°
22°
21°
latitude
24°
25°
26°
27°
28°
29°
30°
31°
32°
33°
34°
longitude

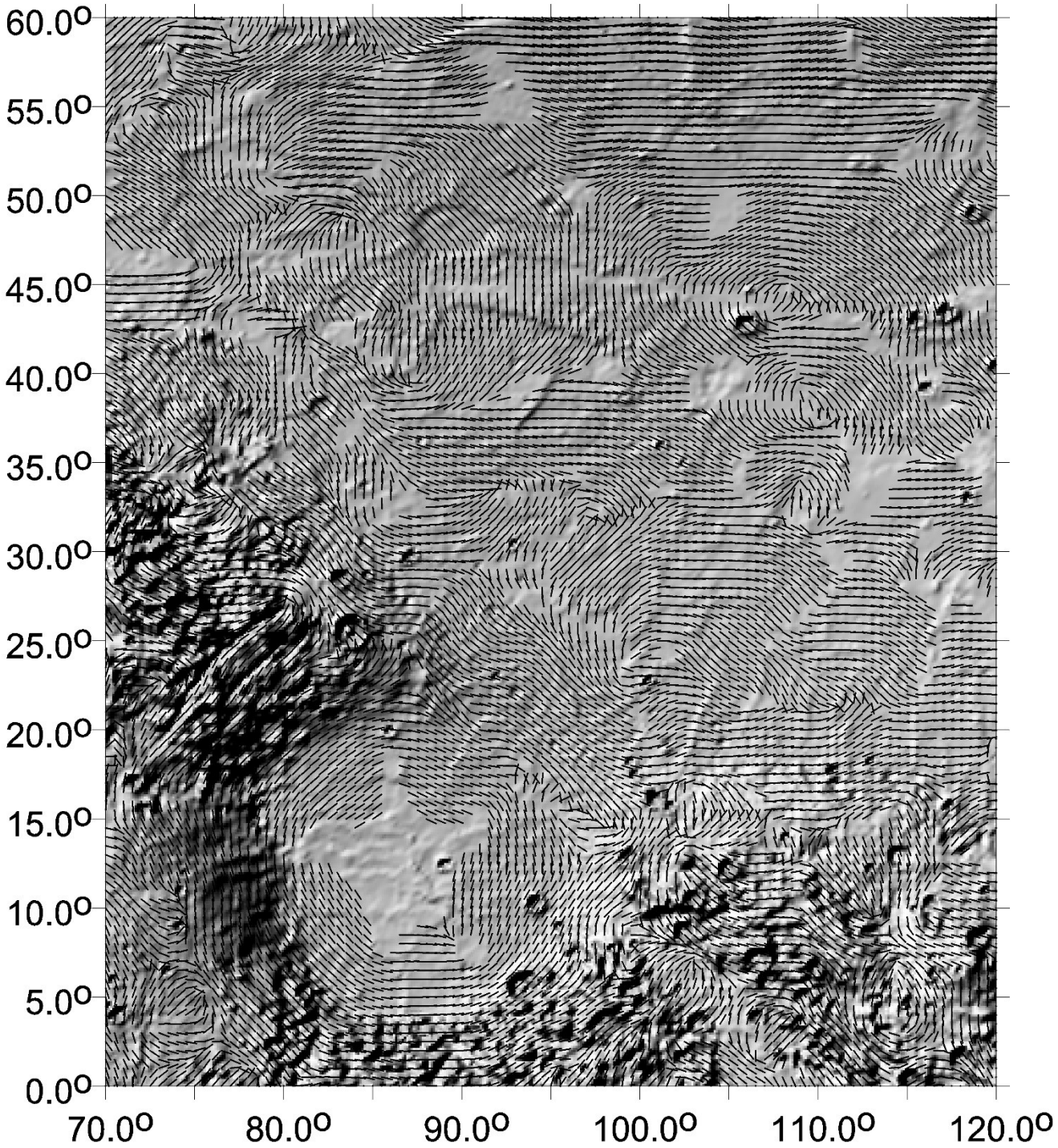
60.0°
55.0°
50.0°
45.0°
40.0°
35.0°
30.0°
25.0°
20.0°
15.0°
10.0°
5.0°
0.0°
70.0°
80.0°
90.0°
100.0°
110.0°
120.0°

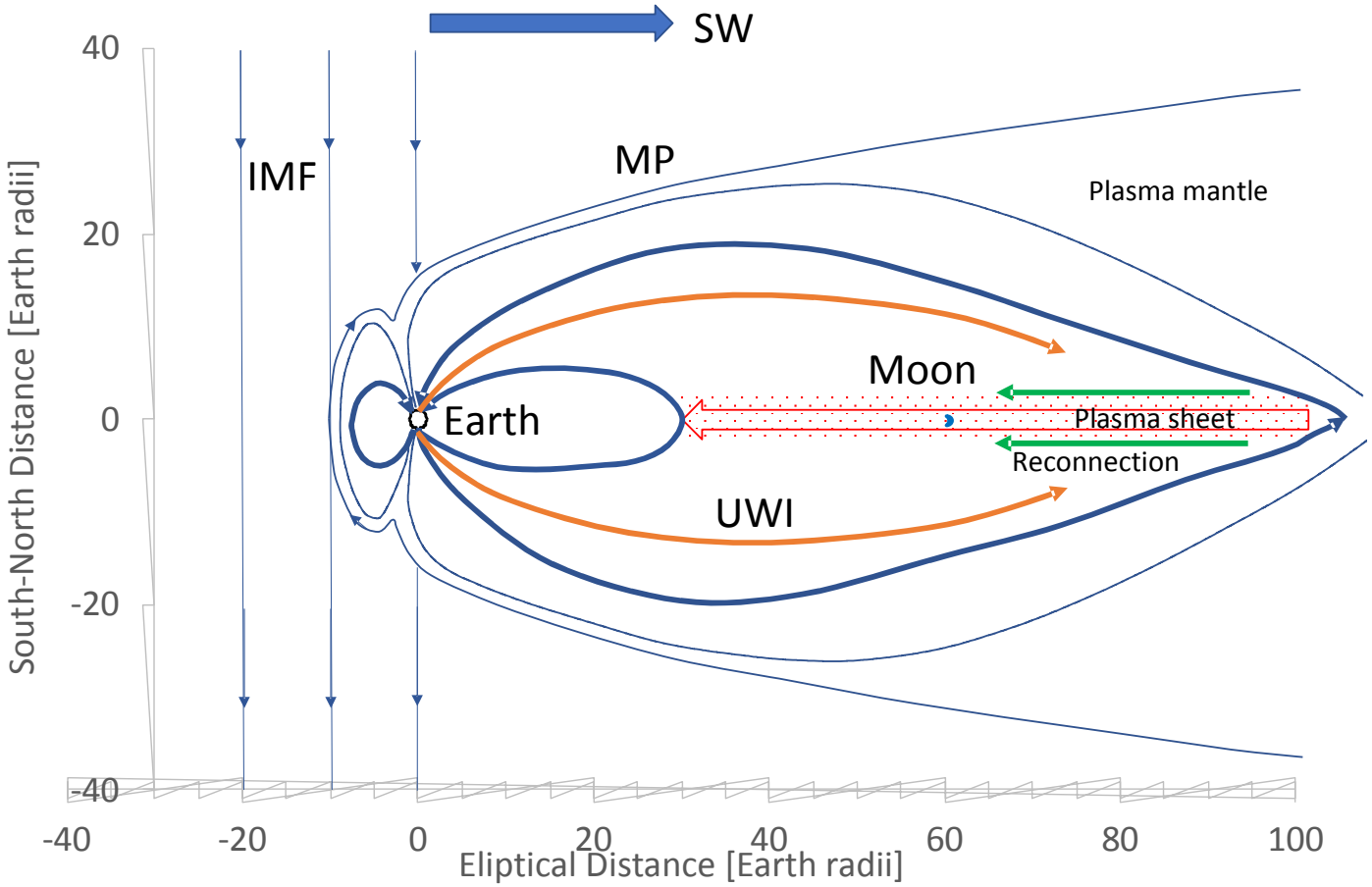

Tvar zemské magnetosféry. Rovina oběžné dráhy Měsíce kolem Země je skoro totožná s rovinou oběžné dráhy Země kolem Slunce. Magnetosféra Země směrem od Země sahá daleko za oběžnou dráhu Měsíce kolem Země. Měsíc prolétá zemskou magnetosférou každý měsíc kolem úplňku po dobu asi pěti dnů. Z ionosféry se ionty dostávají do magnetosféry a pohybují se podél oranžových šipek. Zelené šipky ukazují na pohyb iontů díky tzv. "rekonekci" (přepojení siločar magnetického pole, což způsobí urychlení iontů v magnetosféře směrem k Zemi). IMF meziplanetární magnetické pole se slunečním větrem SW, MP magnetopauza, UWI ionty ze Země, které se mohou dostat na Měsíc.

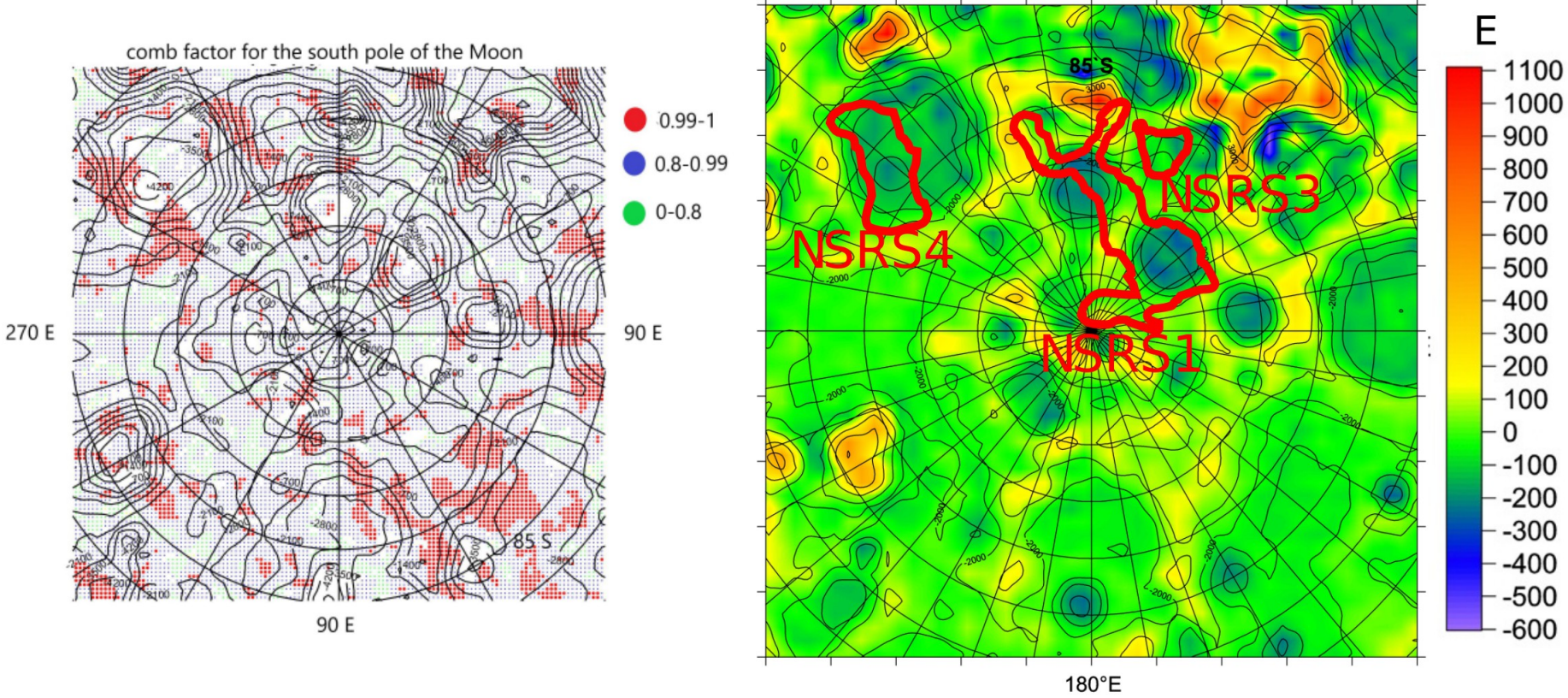

Oblast kolem jižního pólu Měsíce, vlevo úhly napětí (největší učesanost červeně), vpravo druhé radiální derivace poruchového potenciálu (v jednotkách Eötvös) z nejnovějšího modelu gravitačního pole Měsíce z měsíčních družic (lunárních orbiterů), spolu s topografií měsíčního povrchu z laserového altimetru LOLA (vrstevnice). Tři oblasti označené červeně NSR S1, NSR S3 a NSR S4 s potenciálně na vodu bohatým permafrostem (regolitem) z nezávislých měření. Obrázky J. Kostelecký, G. Kletetschka, K. Karimi z [1].

Citace [1] Kletetschka G, Klokočník J, Hasson N, Kostelecký J, Bezděk A, Karimi K. 2022, Distribution of water phase near the poles of the Moon from gravity aspects . *Scientific Reports* (Springer-Nature), Mar 16;12(1): 4501; doi: 10.1038/s41598-022-08305-x.

Více info o našich pracech tohoto typu na, www.asu.cas.cz, /jklokocn

Astronomický ústav AV ČR

Astronomical Institute of the Czech Academy of Sciences